EPITAXIAL GROWTH AND SOME MAGNETIC PROPERTIES OF FERROMAGNETIC FILMS

by

M.S. ZAFAR.

A thesis submitted for the degree of Master of Science in the University of London.

Department of Physics,
Royal Holloway College.

December 1963.

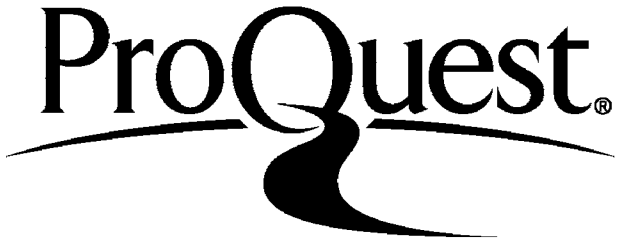

Acknowledgements

I wish to express my sincere thanks to Drs. O.S. Heavens and R.F. Miller, for guidance, help and encouragement throughout this work. I am also indebted to the Colombo Plan Authorities for financial support throughout my stay here.

M.S.Z.

ABSTRACT.

A review of the existing theories of epitaxy is given and it is emphasised that the temperature at which epitaxy occurs is a function of conditions under which the film is deposited.

A series of iron films were deposited on cleaved NaCl, NaBr, KCl and polished (100), (110) NaCl faces. A study of the conditions underwhich single crystal films can be grown was made. KCl and NaCl are the substrates on which iron films of single orientation can be prepared. Iron films were continuous at a thickness of 400Å.

A comparison of growth of films on surfaces cleaved in air and also on those cleaved in vacuum was made. Decoration and replication techniques were employed. The decoration features were observed on air-cleaved surfaces and on those cleaved in vacuum and exposed to air. No decoration was observed on vacuum cleaved surfaces not exposed to air. The decoration features in the case of iron persisted upto 100Å instead of $<$ 20Å in the case of gold. This difference is explained in terms of the lower mobility of iron as compared to gold.

Nickel films were grown on freshly epitaxed copper on sodium chloride and the azimuthal anisotropy in Faraday Rotation on (100) and (110) films was investigated.

CONTENTS.

CHAPTER 1.

I. Introduction.

Since thin films have become an important tool of Solid State research, a shift in emphasis regarding film structure can be noticed. To-day, research concentrates on lattice defects pinpointing their various forms and individual sites. It probes into the influence of substrates and stresses on the growth mechanism and the resulting defect concentration, and attempts to correlate real structure and physical properties using the latest advances of Solid State theory.

This progress has been made possible by a considerable refinement of experimental techniques. Electron-microscopy has reached, in a steady development, the resolution almost of the lattice periodicity and enables individual dislocations to be observed. Electron-diffraction has been developed, to use a remark by Professor Trillat, "to a chemical microlaboratory" permitting the continuous recording of Solid State and surface reactions as well as phase transitions.

Despite the progress in experimental methods of observation, only recently has emphasis laid on the cleanliness of the substrate surface and vacuum conditions. With the inception of vacuum cleaving of the Crystal, some doubt has been cast on the previous results. It seems necessary that work should be done under ultrahigh

vacuum conditions for it would then be possible to have a unifying quantitative theory of film growth and of the interrelationship between deposition parameters, film structure and physical properties. A review of the theories of epitaxy to date is given in Chapter 2.

Chapter 3 reviews the methods of preparing thin films and explains why the method of electron bombardment of a pendant drop was finally selected. This leads on to a description of the vacuum system and evaporation chamber. The choice of the Substrate and the preparation of its surface are then described, and it is shown in detail how an optically smooth substrate surface may be obtained. There follows an account of the deposition of the film, either directly on halide or on to an intermediate epitaxially grown metallic layer. The Chapter closes with the description of the vacuum cleaving system and measurement of film thickness.

Chapter 4 is confined to the results of the study of the iron films in the electron-microscope. It reveals the nature of such films deposited directly on halides and a comparison is made of the films deposited on vacuum and air-cleaved potassium iodide crystals. Decorations features on differently treated surfaces were studied and an explanation of the existence of decorations upto $\approx 100\text{A}^{\circ}$ thickness is given.

Chapter 5 deals with the results for nickel grown on freshly epitaxial copper on NaCl and Chapter 6 gives the results of some Faraday Rotation measurements on (100) and (110) films.

Finally, in Chapter 7, there is a brief summary of the kind of investigations that, it is hoped, might be stimulated by the work described in this thesis.

CHAPTER 2

EPITAXY

2.1. Introduction

The term Epitaxy ('arrangement on') was coined by Royer in 1928 to designate the oriented overgrowth of one crystalline substance on another, although it was first observed in natural crystals in 1817; comprehensive lists of early examples have been given by Wallerant[69] (1902) and by Mugge[44] (1903).

Such observations led to variety of experiments designed to bring about oriented growth in the laboratory; Frankenhein[26] (1836) grew a salt from its aqueous solution onto a single crystal of a different salt; Aminoff and Broom[1,2] (1936,38), Wilman[71] (1940) obtained thin films by chemical attack; Cochrane[12] (1936); Finch and Sun[21] (1936) electrodeposited metal films and Bruck[10] (1936) condensed metal films on a substrate from the vapour phase. These films were found to be oriented in some cases. Optical microscopy, X-ray and electron diffraction have been widely used to study epitaxy and the results so obtained are found in comprehensive reviews (Van der Merwe[68] 1949; Seifert[55] 1953; Pashley[48] 1956). Later Pashley[49] (1959); Bassett and Pashley[8] (1959) and Reimer[53] (1959) extended the field of observation by examining the films with electron-microscopy which has certain advantages over the other

methods, e.g. i) the resolution attainable is very large ii) the deposit can be examined directly and considerable details of the internal structure are revealed. However, it provides only limited information about the relative geometry of the substrate and the overgrowth.

Barker[3,4,5] (1906,07,08) was the first to study epitaxy systematically and later Royer [54] (1928) repeated much of his work, extending it to cover many other examples of growth from solution, and put forward three rules for epitaxy. These are:

i) that oriented growth occurs only when it involves the parallelism of two lattice planes which have networks of identical or quasi-identical form, and of closely similar spacings. This implies a minimisation of the degree of misfit between the parallel lattice spacings. Percentage misfit is defined as :

$$100\ (b-a)\ /a.$$

where a and b are the corresponding lattice network spacings in the substrate and overgrowth respectively. Royer's results suggested a maximum possible misfit of 15%.

ii) that the deposit ions, which take positions that substrate ions would have taken had the substrate continued to grow, should have the same polarity that the substrate ions would have had.

iii) that the type of binding between elements of the deposit should be identical with that between elements of the substrate.

TABLE 1.

METAL		ORIENTATION		MISFIT %
		METAL	ROCK SALT	
Fe b.c.c.	(i)	(001) <100>	(001) <100>	- 49.1
	(ii)	(001) <110>	(001) <100>	- 28.1
Co f.c.c.	(i)	(001) <100>	(001) <100>	- 36.8
	(ii)	(001) <100>	(001) <110>	- 10.7
Ni f.c.c.	(i)	(100) <100>	(100) <100>	- 37.6
	(ii)	(100) <100>	(100) <110>	- 11.5

Since then, Sloat and Menzies[64](1931) found orientation of ammonium bromide and of cesium chloride deposited from aqueous solution onto a single crystal of silver. Johnson[33] (1950) found epitaxy between sodium chloride deposited from solution onto oriented silver. Many more examples of epitaxy between ionic and metallic crystals can be found (Brück[10] 1936). All these examples indicate that Royer's third rule is not valid at all. Also epitaxial films are not always formed on heated rocksalt as predicted by Royer's rule (1); observations of Brück[10] (1936), Shirai[56,57]. (1937,38). and of Collins and Heavens[13] (1957) are listed in table 1.

According to table 1, case no. (ii) for the above elements would be the obvious possibility, but, in nature case (i) seems to be more stable.

The well defined limits of misfit (-13% to + 9% for a KCl substrate) set by Royer [50](1928) and Sloat and Menzies[64] (1931) for epitaxy from solution, are not applicable in vapour phase condensation. (Schulz[53] (1951) and Lüdemann[38] (1954)).

Similarly, doubt has recently been cast on the minimum temperatures observed by Brück[10] (1936) for the epitaxial growth of vapour-deposited metals on alkali halides. Sloope and Tiller[65] (1961) investigated Ag films on NaCl and found that the minimum deposition temperature for the formation of single-crystal films is rate-dependent and that an epitaxial temperature does not exist.

Germer etal[28] (1961) studied the (110) nickel surface with the help of low energy electron diffraction and concluded that when the surface is clean and free from foreign atoms, the surface (110) plane of atoms has the normal arrangement expected for such a plane. Very slight contamination by oxygen and perhaps other atoms results, in some cases, in an arrangement of the topmost layer of atoms in which nickel and oxygen (or another atom) alternate along each 100 line and also along each 110 line. If this is the case, naturally any surface cleaved in air, is not clean enough and the conditions for epitaxy will definitely be affected by it. Hence Trillat and Sella[67] (1963), to avoid adsorption on cleaved surface of rocksalt, carried out the cleavage in vacuum and found that the epitaxial temperature for gold is 200°C instead of the usual 400°C. The epitaxial growth of iron occurs at a lower temperature on a vacuum-cleaved surface of KI as compared to the air-cleaved surface as will be seen in Chapter 4. The above examples definitely show that epitaxial temperature for a metal is not a fixed quantity, but depends upon the conditions underwhich the film is grown.

Now before proceeding any further, it seems necessary to give an account of the oriented metallic films grown by vacuum deposition and to discuss the correlation with existing theories of epitaxy.

2.2. Epitaxy of metallic layers.

A considerable amount of information has been obtained by means of electron diffraction and electron microscopy, concerning the epitaxy of metal films on single crystal surfaces. The method of vacuum evaporation is the cleanest and most controllable means of deposition and has been widely used for the preparation of films on alkali halides, and on metals.

i) The growth of metals on non-metals.

The substrate which has been most frequently used is the cleavage face of single crystal rock salt. When metal vapours are condensed on a cold face of a rocksalt crystal, a polycrystalline film is obtained with random orientation, or a degree of textured orientation depending on the direction of incidence of the vapour beam. On the other hand, condensation on the surface of a rock salt single crystal heated to a suitable temperature leads to the formation of a highly oriented layer consisting of large crystals and acquiring the structure of a mosaic single crystal, accurately oriented with respect to the rock salt crystal. Analogous phenomena are observed during the crystallisation of metal vapours on heated surfaces of mica, calcite, ~~flouride~~ fluoride and mineral sulphides (Rudiger[55] 1937). Bruck[10] (1936) investigated the orientation of films of Ag, Au, Al, Cu, Ni, Pd, Co, Fe and Cr, deposited from the vapour on heated rocksalt. A minimum 'epitaxial temperature' was observed for each - a phenomenon

which may be dependent upon conditions of deposition (Sloope[65] and Tiller 1961). Transmission electron diffraction of detached films also revealed epitaxial growth.

a) in some cases, the orientation of a deposit improves as it builds up, (Rudiger[55] 1937; Pashley[48] 1956) but in view of the uncertainties involved the majority of evidence concerning orientation improvements with thickness is not decisive. Even where the improvement is established as being a genuine effect of an increase in the thickness of the deposit, it is usually not possible to decide whether this has resulted from some kind of preferential growth on to the better oriented nuclei, or whether a complete recrystallisation of the film has occurred at a certain stage of the deposition. More experiments on this aspect of the oriented growth are necessary before any further conclusions can be drawn.

b) irrational reflections were present in the diffraction patterns. These have since been shown to be caused mainly by repeated twinning on (111) type planes (Menzer[41,42] 1938, Reimer[53] 1959, Burbank and Heidenreich[72] 1960).

c) differences exist between the orientation of face-centred cubic metals and body centred metals on face-centred substrates. In the case of face-centred deposits the orientation of the film is usually parallel to the (100) plane of the substrate and along the <100> direction. In the case of the body-centred deposit, the orientation is parallel to the (100) face of the substrate, but with a mixture of

orientations with the <100> direction of the deposit along the <100> and <110> directions in the (100) plane of rocksalt. Other orientations of body centred cubic metals may exist at different temperatures, (Shirai - see Pinsker 1953).

Growth of metals on polycrystalline substrates, even at high temperatures produces only polycrystalline films with no regular azimuthal orientation.

From the work of Bassett[6](1958) and others (Bassett [8] and Pashley 1959), it is evident that three-dimensional nuclei are initially formed when a metallic vapour is condensed on rocksalt. Electron micrographs of gold nuclei of 10°A in size show that nucleation takes place preferentially along cleavage steps on the rocksalt surface, the distribution in between them being random. Further deposition results in an absorption of other nuclei, until the substrate is completely covered at a thickness of about 1000°A. A high density of crystal faults e.g. 10" dislocations /cm^2., are observed by the diffraction contrast and Moirétechniques of Bollman [9] (1956) and of Pashley[50], Menter and Bassett (1957). Pashley has made a cine-film of gold growing epitaxially by evaporation on to molybdenum disulphide, in the transmission electron microscope. This film shows an initial distribution of three dimensional nuclei, with some nuclei growing at the expense of others, until a mosaic of oriented crystallites

is formed, with empty channels in between. Diffraction contrast shows the nuclei to be crystallographically ordered, yet a transfer of atoms between one nucleus and another appears to be possible, the larger of two neighbouring nuclei increasing in size while the other diminishes. The channels between crystallites are also filled in by a process similar to the joining together of liquid drops, in spite of the fact that the main bulk of each gives rise to typical crystalline diffraction contrast features. Moiré pictures also reveal that, during growth, crystallites appear to be able to alter their orientation with respect to the substrate by the order of a degree of arc, and still preserve their crystalline order. (Bassett[7] 1960). While it must be borne in mind that the films grown under such conditions are subjected to bombardment by the electron beam, and that the usual contamination by cracked pump oil is bound to be present, the experiments certainly indicate that a high degree of mobility exists among the nuclei in the early stages of film growth, and that the relationship between the arriving deposit atoms, the substrate, and the other nuclei already present, is a dynamic one likely to involve surface forces of a complex nature.

ii) The growth of metals on metals.

The earliest investigations into metal films grown epitaxially on metallic surfaces were made on electolytic deposits. Cochrane[12] (1936) used etched (111) and (110) faces of single crystal copper as

substrates for Ni, Cu, Zn, Cd, Ag, Cr and Co. For the face-centred cubic metals, there was found to be an upper limit to the current density for the production of oriented deposits, as detected by reflection electron diffraction. Irrational reflections observed were associated with twinning. Zn and Cd showed no orientation. Studies of electrodeposits on iron and copper were also made by Finch, Wilman & Yang[22] (1947).

Brück[10] (1936) deposited silver and gold on each other from the vapour phase, the substrates being oriented metallic films formed by deposition on rocksalt. Oriented growth occurred when the substrate was heated above a certain temperature. Bassett and Pashley[8] (1959) have examined the initial stages in the growth of gold on thick, epitaxial, single crystal silver deposited on mica. The mode of growth is found to differ from that of gold on rocksalt. Three-dimensional nuclei are still formed, but the gold spreads more easily over the silver surface and produces a continuous layer at about 100°A thickness. Similarly, better spreading for a lower misfit has been observed by Schulz for the growth of alkali halides on each other - see Gomer & Smith 1953. Heavens etal[31] (1961) grew Ni & Ni-Fe alloy on thick single crystal films of Cu and found that the nuclei also spread easily. This case of spreading metal on metal and halides on halides as compared to metals on halides may be due to difference in the binding forces and the smaller lattice misfit.

2.3 Theories of Epitaxy.

To explain the experimental observations various theories of the epitaxial growth have been put forward in recent years; most of them are based on the concept of a geometrical fitting between the lattices of the substrate and the overgrowth. This should be the obvious line of thought for explaining the mean features of a film obtained by electron diffraction.

2.4 Small misfit theories.

One of the earliest theoretical treatments of epitaxy is that of Dixit[15] (1933) for amorphous substrates. This was later [16](1957) extended to include growth on cleaved surfaces. He considers that the atoms in the first layer behave like a two dimensional gas; the substrate behaves not only as a support but there is also interaction between the ions of the substrate and the arriving atoms. From this he concludes that the epitaxy depends upon the lattice constant and the orientation of the substrate and also that the epitaxial temperature depends upon the plane. It is predicted that $T_{111} > T_{100} > T_{110}$ where T_{hkl} is the epitaxial temperature for the corresponding (hkl) plane. This may point to the simple conditions for epitaxy but does not take into account the rate of deposition of the deposit material.

Dankov[14] (1946, see Pinsker 1953 page 220) has attempted to establish the condition for the growth of an oriented crystal nucleus,

strained to fit the substrate, by considering the energy of deformation which results from the misfit. However, this calculation cannot be carried out in most cases, because of the absence of the necessary lattice data.

Some attempts at explanation of the occurrence of large misfits have been based upon the idea that an oriented layer corresponding to a good fit occurs during the initial stages of growth and that subsequent growth gives rise to different orientation. Menzer[40,41,42] (1938) considered the growth of nickel and silver on rocksalt, in the light of the data of Brück[10] (1936), which showed that silver and nickel films of several hundred Angstroms thickness grown by evaporation, in vacuo, on the cleaved rock salt, were prominently twinned on their (111) planes. Since the twinned lattices have their (221) planes parallel to the (001) rocksalt surface, Menzer suggested that the initial nuclei grow with their (221) planes parallel to the rocksalt, the misfit being less than that for (001) planes parallel to the substrate. Considerable doubt is thrown on this hypothesis by later electron diffraction investigations of the initial stages of growth ($<20^{\circ}A^{\circ}$) of metals on rocksalt. Kehoe[34] (1957) observed no twinning in silver nuclei on rocksalt for thickness below $10^{\circ}A^{\circ}$. Also, the results of Collins and Heavens[13] (1957) indicate the normal lattice dimensions and no twinning, in nickel layers of $20A^{\circ}$ thickness on rocksalt. Matthews and

Allison[39] (1963) observed that in the face-centred cubic metal films twins do not occur in films of thickness less than 20 Å. It is suggested that these twins are formed when two nuclei, which happen to be approximately twins of one another, coalesce and rotate into precisely twin relationships as seen by Bassett[7] (1960).

Engel[18,19] (1952,53) has considered the growth of metal deposits on rocksalt on the assumption that the deposit metal is ionised and the binding to the surface is predominantly electrostatic. If the appropriate ionisation state of the metal is assumed, then the epitaxial temperature is found to increase linearly with ionization potential. The correct orientation is predicted for Ag on NaCl, assuming a monolayer of the deposit-metal salt to exist at the interface. Examination of results in the light of this treatment is difficult on two grounds: (i) it is impossible to decide which ionization state to assume for the added metal, (ii) values of the higher ionisation potentials are in many cases not available. In view of the observations of Kehoe[34] (1957), Sloope & Tiller[65] (1961), Heavens etal[31] (1961) and the results given in Chapter 4, on iron that good orientation occurs at temperatures appreciably lower than Brück's epitaxial temperature, this theory appears to be inadequate.

Frank and Van der Merwe[23] (1949) put forward a theory in which it is assumed that the initial stage of growth of an oriented deposit

is an immobile two dimensional monolayer of regular atomic pattern. In order to fit on to the substrate, this monolayer is homogeneously deformed so as to have the same spacing, i.e. to form a pseudomorphic first layer. The conditions for stability of such a system are examined when it is subjected to a periodic force due to the substrate atoms, assuming the overgrowth to cohere under the action of a linear force law. This system is shown to be unstable for misfits greater than 9%, with a possible metastable configuration having up to 14% misfit at low temperatures. Once this oriented layer has formed, a macroscopically thick layer can be formed by a repetition of the process. Further layers are subjected to successively less deformation until the strain-free bulk deposit is obtained. Smollet and Blackman[66] (1951) have criticised the theory on the grounds that it predicts constrained monolayers which would not necessarily be stable. Two dimensional arrays of atoms were considered, with the configuration of the lattice planes of various alkali halides. Several pairs of alkali halides were considered between which epitaxy is known to occur and it is shown that, for many cases, the strain required to produce a monolayer of the deposit material to fit with the substrate would lead to instability. Conversely, it is shown that, in certain cases where a strained monolayer would be stable, epitaxy does not occur. It was therefore concluded that the orientation observed experimentally does not arise from a pseudomorphic layer.

The evidence for and against the existence of a strained monolayer is conflicting and gives little support to the theory of Frank and Van der Merwe[23,24](1949) that oriented monolayers are constrained to fit the substrate lattice. Finch and Quarrell[20](1933) introduced the term 'Basal plane pseudomorphism' in an explanation of the results which they obtained for the growth of ZnO and Zn, in which certain reflection electron diffraction rings were interpreted as arising from a modified oxide structure caused by the constraining influence of the Zinc substrate. Further observations of modified spacings were also interpreted as arising from a modified oxide structure caused by the constraining influence of the zinc substrate. Further, observations of modified spacings were also interpreted as the effects of pseudomorphic growth by Cochrane[12](1936) Miyake (1938) and Clark, Pish and Weeg[11](1944). Pashley[48](1956) has made a reexamination of these results in the light of more recent work,(Raether[52]-1950, Lucas[37]-1951, Newman[45]-1956), and has shown that in fact there is no justification for their interpretation as proof of pseudomorphism as a mechanism in epitaxy. Further Shishkov[58,59](1952,57) has reported Pt in thin layers with a lattice constant 1.5% larger than that of the bulk material and Fe, in the initial stages of deposition on mica, with a lattice constant 5% greater than normal but this conclusion can barely be supported by the limited accuracy of the measurements. Nevertheless, lead and thallium (Newman[46] 1957) deposits had their own characteristic lattice constants in the earliest stage of their growth.

The spacings found were somewhat modified from those of the bulk metal i.e. 4% lower than that of the x-ray determination, but there was no evidence to support the theory of Frank and Van der Merwe[23,24] (1949) which predicts that oriented monolayers are constrained to fit the substrate lattice.

The electron diffraction evidence concerning the growth of films (especially metals) during the first few Ångstroms certainly indicates that in general the formation of a monolayer (Grunbaum[30] 1958) is an exception rather than the rule. (Schulz[57] 1952, Newman & Pashley[47] 1955). Investigations made on films deposited under the relatively controlled conditions of vacuum evaporation, show that nucleation occurs, resulting in the formation of three-dimensional crystallites distributed across the substrate surface (Bassett[6]1958). Similar results are obtained for growth from the solution (Newman and Pashley[47] 1955) and by chemical action (Lisgarton [36] 1954). In such cases, the Frank and Van der Merwe theory would not hold, since it is based on an initial mechanism which is not applicable.

The problem of stability of thin deposits has been examined by Drabble[17] (1949), in terms of the co-ordination conditions of the deposited atoms, and it is shown that the observed orientation is frequently governed by a tendency to continue the substrate structure across the boundry (Royer's second rule) so that the normal co-ordination

of the atoms at the interface is preserved. Some evidence in support of this was found by Collins and Heavens[13] (1957).

It is clear that all theories which predict that orientation occurs provided there is a small misfit cannot have any general application, and the reason that they breakdown is that very little is known about the initial stages of growth of an oriented film. The theories are almost certainly based upon unrealistic models for the mode of nucleation of a deposit film.

2.5. Nucleation Theory.

The earliest observable stage of growth of a film produced by condensation on to a substrate is the formation of discrete nuclei. The form of the deposit nuclei varies considerably from case to case and tends to approximate closer to a monatomic island the smaller the misfit. There is no direct evidence how the initial nucleation occurs. According to the classic theory of Frenkel[27] (1923), when atoms arrive on the substrate surface they are free to move over the surface and have a finite life-time there before they re-evaporate. If, during this finite lifetime, collisions with other atom occur, aggregates of adsorbed atoms form. Aggregates should be more stable toward re-evaporation than single adsorbed atoms since they are bound to each other by the condensation energy. However, as long as the aggregates are very small, their surface to volume ratio is also very high. The resulting high

surface energy tends to dissociate them again. The sum of these two counteracting effects determines the net stability of the aggregates:

$$\Delta F = a_1 \sigma_1 + a_2 \sigma_2 + V \Delta F_v$$

where a_1 and σ_1 are the surface area and the surface energy (positive) of that portion of the aggregate which is not bound to the substrate, respectively; a_2 and σ_2 are the surface area and the surface energy (positive or negative) of that portion of the aggregate which is bound to the substrate, V is the volume of the aggregate, ΔF_v is the free energy of condensation of the film material per unit volume in the bulk.

As the size of the aggregate increases, the free energy goes through a maximum at which point the aggregate has reached a critical size. If an additional atom is added to an aggregate of this size (called a critical nucleus) it becomes stable, and will, on the average, not dissociate again into single atoms but will grow to form a larger island. If, on the other hand, an atom is taken away from the nucleus, it dissociates again. It is therefore clear that in order to condense at all, aggregates of critical size or larger have to be created. Walton[70] (1962) using statistical mechanics and kinetic theory, tried to evaluate the size of the critical nucleus in the formation of metal deposits from the vapour and found it to be containing 10 atoms or less, which agrees well with the Pound[51] etal (1954) results. The main drawback in Walton's argument is that he

completely ignores the influence of the substrate on the arriving atoms.

The rate of film nucleation will now be given by the rate at which material can be added to the critical nuclei which are in equilibrium with the adsorbed atoms which in turn are in equilibrium with the impinging atoms from the gas phase. The resulting rate equation (Pound[51] etal 1954) is an exponential involving, among other things, the supersaturation ratio and the free energy of the critical nucleus, ΔF^{*} (positive

$$I \propto \left(\frac{N\downarrow}{N\uparrow(0)} \right)^{2} \exp \left(-\Delta \frac{F^{*}}{KT} \right) \text{nuclei/cm}^{-2}\text{/sec}^{-1} \quad .1$$

where T is the substrate temperature, $N\downarrow$; the impingement rate of film atoms on the substrate from the gas phase, $N\uparrow(0)$ the evaporation rate of the film material. Although I will be positive for all values of the supersaturation ratio $N\downarrow/N\uparrow(0)$ larger than unity, this ratio must exceed a critical value before a perceptible condensation rate will be achieved.

The necessity of obtaining perceptible condensation rates thus explains the need for high supersaturation ratios and impingement rates to achieve film condensation. Of course, once enough stable nuclei exist, condensation will continue for any value of $N\downarrow/N\uparrow(0) > 1$.

2.6. Effect of Nucleation on Film Structure

The following predictions can be made from nucleation theory about film structure:

(1) If the activation energy of desorption i.e. $\Delta H_{ad} \gg KT$ there is no nucleation barrier to film condensation, i.e., the critical nucleus consists of one atom or less, and condensation can occur at even very low impingement rates.

(2) If $\Delta H_{ad} \ll KT$, there is a nucleation barrier, and the impingement rate has to exceed a critical value before film condensation becomes perceptible.

(3) If there is a nucleation barrier the film must have an island structure in the initial stages of growth. Even if there is no nucleation barrier, however, island formation is possible, since there may be surface diffusion which allows aggregates to form even though they are not a prerequisite for film condensation.

(4) There is a critical size which nuclei must reach before they are stable and this initial size is increased by: an increase in substrate temperature, a decrease in impingement rate, a decrease in the free energy of condensation ΔF_v, and a decrease in the free energy of binding ΔF_{ad} between film atoms and substrate. Since ΔF_v increases with the boiling point of metals, films of high boiling metals will have smaller initial nuclei than films of low boiling

metals, at the same substrate temperature. There is some experimental support for this conclusion (Leomstein[35] 1949). Further, it follows from Eq (1) that high impingement rates or low substrate temperatures tend to give a high density of nuclei, while low rates or high temperatures tend to give a low density of nuclei. This means that films made at high rates or low temperatures will have a smaller grain size and become continuous at a much lower coverage than films made at low rates or high temperatures.

(5) By first "seeding" the substrate with critical nuclei, either of the same or a different metal, it is possible to achieve film condensation at even low impingement rates.

All these predictions are observed in the electron-microscopic studies of the thin films.

In the limiting case of very small coverage, where there is no interaction between the adsorbed film atoms, each atom will reside in some potential energy well and, if there is sufficient mobility, will find the deepest well, corresponding to tightest binding, and spend most of its lifetime on the surface on it. Such a "film" would be perfectly ordered with respect to the substrate.

In practice the interaction between adsorbed atoms cannot be ignored, and will lead to the formation of metal islands, as seen above. The positions that the atoms in the bottom layer of the

island take with respect to the substrate are now determined by the loci of minimum potential energy resulting from the overlap of the potential energy contours of both substrate and film. Thus the stability of the binding between the island and the substrate will be determined by how frequently sites of tight binding are encountered between the two. If the lattice parameters of the substrate surface and the metal islands do not match, only a relatively small fraction of the metal atoms can actually reside exactly in the deepest well on the substrate without distortions that are energetically expensive and thus unlikely. Since, therefore exact matching is improbable, the island must find its position of lowest energy by orienting so that a maximum number of sites of at least partial overlap of potential minima is encountered between film and substrate. On a single crystal substrate tight binding sites are encountered with the greatest frequency in the low-index cystallographic direction along which they occur with certain periodicity. Hence the film islands will encounter positions of tight binding and greatest stability when they orient with respect to the substrate along the low index directions, even for a large lattice misfit. It is possible that the lowest energy orientation of a very small island, consisting of only a few atoms, is different from the lowest energy orientation after it has grown to contain many atoms. If the substrate temperature is high enough, however, such an

island will be able to reorient itself to find its new, more stable position unless, of course, it is too big. Such a reorientation of islands has indeed been observed in the electron microscope by Bassett[7] (1960).

In order that the adsorbed metal atoms find the positions of tightest binding they must possess enough mobility, and this means that the substrate temperature must be sufficiently high. This is why epitaxial growth of single crystal film is observed at higher temperatures dependent on the rate of deposition and materials involved.

At present it is necessary to carry out experiments to find out the critical size of the nucleus for different metals and single crystal substrates as a function of the rate of deposition and the temperature of the substrate. As we know from the results of Schlier and Farnsworth [56](1958) and of Germer etal[28,29] (1961,1962), the surfaces of the crystals are not normally clean. Ideally the crystals should be cleaved in a vacuum of 10^{-9} torr. and immediately the film should be deposited and studied. This will definitely improve the understanding of epitaxy.

REFERENCES

1 Aminoff and Broome, 1936, Nature, Lond. 137,995.

2 Aminoff and Broome, 1938, Kunge, Sevenska Vetensk, Hanb.,16,7.

3 Barker, 1906, J. Chem. Soc. Trans., 89, 1120.

4 Barker, 1907, Mineral Mag., 14, 235.

5 Barker, 1908, Z. Kristallogr., 45, 1.

6 Bassett, 1958, Phil. Mag., 3, 1042.

7 Bassett, 1960, Proc. European Regional Conference on Electron Microscopy, Delft. Vol.1.

8 Bassett and Pashley, 1959, J. Inst. Metals. 87, 449.

9 Bollman, 1956, Phys. Rev., 103, 1588.

10 Brück, 1936, An.. Phys., 26, 233.

11 Clark, Pish and Weeg., 1944, J. Appl. Phys., 15,193.

12 Cochrane, 1936, Proc. Phys. Soc., 48, 723.

13 Collins and Heavens, 1957, Proc. Phys. Soc., B, 70, 265.

14 Dankov, 1946, Zhur. Fiz. Khim, 20, 853.(see Pinsker "Electron Microscopy")

15 Dixit, 1933, Phil. Mag., 16, 1049.

16 Dixit, 1957, Indian J. of Phys., 30, Presidential Address Indian Physical Soc., Calcutta.

17 Drabble, 1949, Ph.D. Thesis, University of London.

18 Engel, 1952, J. Chem. Phy., 20, 1174.

19 Engel, 1953, J. Res.Nat. Bur. Stand. Wash., 50,249.

20 Finch and Quarrell, 1933, Proc. Roy. Soc. A, 141,398.

21 Finch and Sun, 1936, Trans. Faraday Soc., 32, 852.

22 Finch, Wilman and Yang, 1947, Disc. Faraday Soc., A, 43,144.

23 Frank and Van der Merwe, 1949, Proc. Roy.Soc.A, 198, 205.

24 Frank and Van der Merwe, 1949, Ibid, 198, 216.

25 Frank and Van der Merwe, 1949, Ibid, 200, 125.

26 Frankenheim, 1836, Ann. Phys., 37, 516.

27 Frenkel, 1923, Z. Phys., 26, 117.

28 Germer, MacRae and Hartman, 1961, J. Appl. Phys., 32, 2432.

29 Germer and MacRae, 1962, Proc. of the National Academy of Sciences, 48, 997.

30 Grunbaum, 1958, Proc. Phys. Soc., B, 62, 459.

31 Heavens, Miller, Moss & Anderson, 1961, Proc.Phys. Soc., 78, 33.

32 Heidenreich, Nesbitt and Burbank, 1959, J. Appl., Phys., 30,995.

33 Johnson, 1950, J. Appl. Phys., 21, 449.

34 Kehoe, 1957, Phil. Mag., 2, 455.

35 Levinstein, 1949, J. Appl. Phys., 20, 306.

36 Lisgarton, 1954, Trans. Faraday Soc., 50, 684.

37 Lucas, 1951, Proc. Phys. Soc., A; 64, 943.

38 Ludemann, 1954, Z. Naturforsch, 8a, 252.

39 Matthews and Allison, 1963, Phil. Mag., 8, 92, 1283.

40 Menzer, 1938, Naturwiss., 26, 385.

41 Menzer, 1938, Z. Kristallogr., 99, 378.

42 Menzer, 1938, Ibid, 99, 410.

43 Miyake, 1938, Sci. Pap. Inst. Phys. Chem. Res. Japan, 34, 565.

44 Mugge, 1903, Neues Jarbuch Fur Mineralogie, Beilage-Band, 16,335.

45 Newman, 1956, Proc. Phys. Soc., B, 69, 432.

46 Newman, 1957, Phil. Mag., 2, 1.

47 Newman and Pashley, 1955, Phil. Mag., 46, 927.

48 Pashley, 1956, Advances in Physics, 5, 173.

49 Pashley, 1959, Phil. Mag., 4, 324.

50 Pashley, Menter & Bassett, 1957 , Nature, 179, 752.

51 Pound, Simnad and Young, 1954, J. Chem. Phys., 22, 1215.

52 Raether, 1950, J. Phys. Radium, 11, 11.

53 Reimer, 1959, Optik, 16, 30.

54 Royer, 1928, Bull. Soc. Franc. Mineral, 51, 7.

55 Rudiger, 1937, Ann. Phys., 30, 505.

56 Schlier and Farnsworth, 1958, J. Chem. Phys., 6, 271.

57 Schulz, 1951, Acta Crysta., 4, 483.

58 Schulz, 1952, Ibid, 5, 130.

59 Seifert, 1953, (See Gomer and Smith 1953; pp. 218-72).

60 Shirai, 1937, Proc. Phys. Math. Soc. Japan, 19, 937.

61 Shirai, 1938, Ibid, 20, 855.

62 Shishkov, 1952, Zh. Eksper, Teor. Fiz., 22,241 (Pashley, 1956).

63 Shishkov, 1957, Fiz. Metallovi Metallovedince, 169.

64 Sloat and Menzies, 1931, J. Phys. Chem., 35, 2005.

65 Sloope and Tiller, 1961, J. Appl. Phys., 32, 1331.

66 Smollett and Blackman, 1951, Proc. Phys. Soc., A, 64, 683.

67 Trillat and Sella, 1963, Conference on single crystal films - Blue Bell - Pennysylvania.

68 Van der Merwe, 1949, Disc. Faraday, Soc., 5, 201.

69 Wallerant, 1902, Bull. Soc. France Mineral, 25, 180.

70 Walton, 1962, J. Chem. Phys., 37, 2182.

71 Wilman, 1940, Proc. Phys. Soc., 52, 323.

72 Burbank and Heinderich, 1960, Phil. Mag., 5, 373.

CHAPTER 3.

The Preparation of Thin Films and Thickness measurements.

3.1. Introduction.

There are various methods for producing thin films and they can be grouped into four classes.

a) Electrolysis

b) Thermal decomposition from vapour

c) Sputtering

d) Thermal Evaporation in vacuo

The electrolysis and sputtering methods are liable to introduce contamination in thin films, while vacuum evaporation produces "clean films" (Holland[9] 1958). Besides this, it is known that ferromagnetic materials (Collins[5] and Heavens 1957) are grown epitaxially when condensed from vapour phase on crystalline substrate in vacuum, so this method is preferred.

3.2. Vapour Source.

For producing a continuous vapour source, it is necessary to support the molten material to keep the temperature of the evaporant constant in order to maintain a constant rate of evaporation. It is also essential that the support material and the charge should not react chemically or alloy. The merits and drawbacks of the various sources, used for evaporating ferromagnetic materials, are discussed in the following paragraphs.

a) Evaporation from a Ceramic Crucible.

Olsen[13] etal (1945) have made an extensive survey of the effectiveness of alumina and beryllia crucibles for evaporating metals including Co, Fe and Ni. However, no chemical analysis of the material was made, and there is the possibility of contamination, since a slag is usually formed on the surface of the molten charge. Behrndt and Jones[3] (1958) observed that part of the slag consisted of metal oxides, a large proportion of which consisted of crucible material. The amount of slag varied from crucible to crucible and from melt to melt; its presence definitely influenced the evaporation rate. Behrndt[2] (1959) found upto 2% of silicon in nickel-iron films evaporated from silica crucibles. In view of the above experience it was decided not to use this method.

b) Evaporation from a refractory filament.

The substances which can be used for filament heaters are those which have a high melting point, low volatility and which do not alloy with the charge. The usual materials are tungsten (M.P. 3382°C), tantalum (M.P. 2996°C) and molybdenum (M.P. 2622°C). Reference to the phase-diagrams (Smithells[15] 1955) for the system under discussion shows that iron at concentration upto 30% forms solid phases with tungsten, tantalum and molybdenum for temperatures less than 1600°C. Nickel forms partial liquid phases for all

concentrations above 1500°C. Consequently nickel should more readily dissolve a tungsten or tantalum filament than iron even at low evaporant concentrations, and in this respect it is noted that nickel is more difficult to evaporate than iron. It may be possible to prevent a tungsten tantalum and molybdenum heater from being attacked by iron by maintaining an evaporation temperature lower than 1600°C, i.e. limiting the evaporation rate, whereas for nickel rapid evaporation at high temperatures may be the only protection against undue alloy attack since no solid phase exists at the evaporation temperature. These aspects require further investigation.

Heavens[6] (1952) studied the contamination in evaporated films by the material of the source support. Microchemical and radioactive tracer techniques were used to detect contamination in evaporated films of silver and germanium by the boats and filaments of tungsten or molybdenum. Heavens concluded that the rate of transfer of boat material to the target depends directly on the pressure of the system and also on the temperature of the ~~boat~~ source support.

Although the filament or boat evaporation gives a wide range of evaporation rates, and the geometry can be selected to give a uniform and parallel-sided film, the following disadvantages outweigh the advantages.

i) the possibility of alloying of the charge and the support at higher temperature, hence increased risk of contamination.

ii) uncontrollable heating of the substrate by radiation from the source. Careful substrate temperature control is essential for epitaxial growth.

iii) the appearance of holes in the film (Miller[10] 1962).

c) Evaporation by sublimation from a filament material.

The great advantage of obtaining films by sublimation from a filament material is that there is no possibility of contamination from its support; and the shape of the filament can be varied to get a uniform film. But the real disadvantage is that of the limited rate of evaporation. If the rate of deposition is increased by reducing the source and substrate distance, the result is undue heating of the substrate, and, on the other hand, if the rate of deposition is increased by increasing the temperature, the wire melts.

d) Evaporation by Electron Bombardment of Pendant drop.

Kelly[10] (1959) and Heavens[7] (1959) have described the above method and used it for epitaxial growth of several metals. It is an ingenious method, in which there is no danger of contamination of the film by the support. This method is used for growing epitaxial films discussed in this thesis.

Fig (3.1, 3.2) show schematically the arrangement of the electron-bombardment system. The 'spec-pure' material rod R is set coaxially

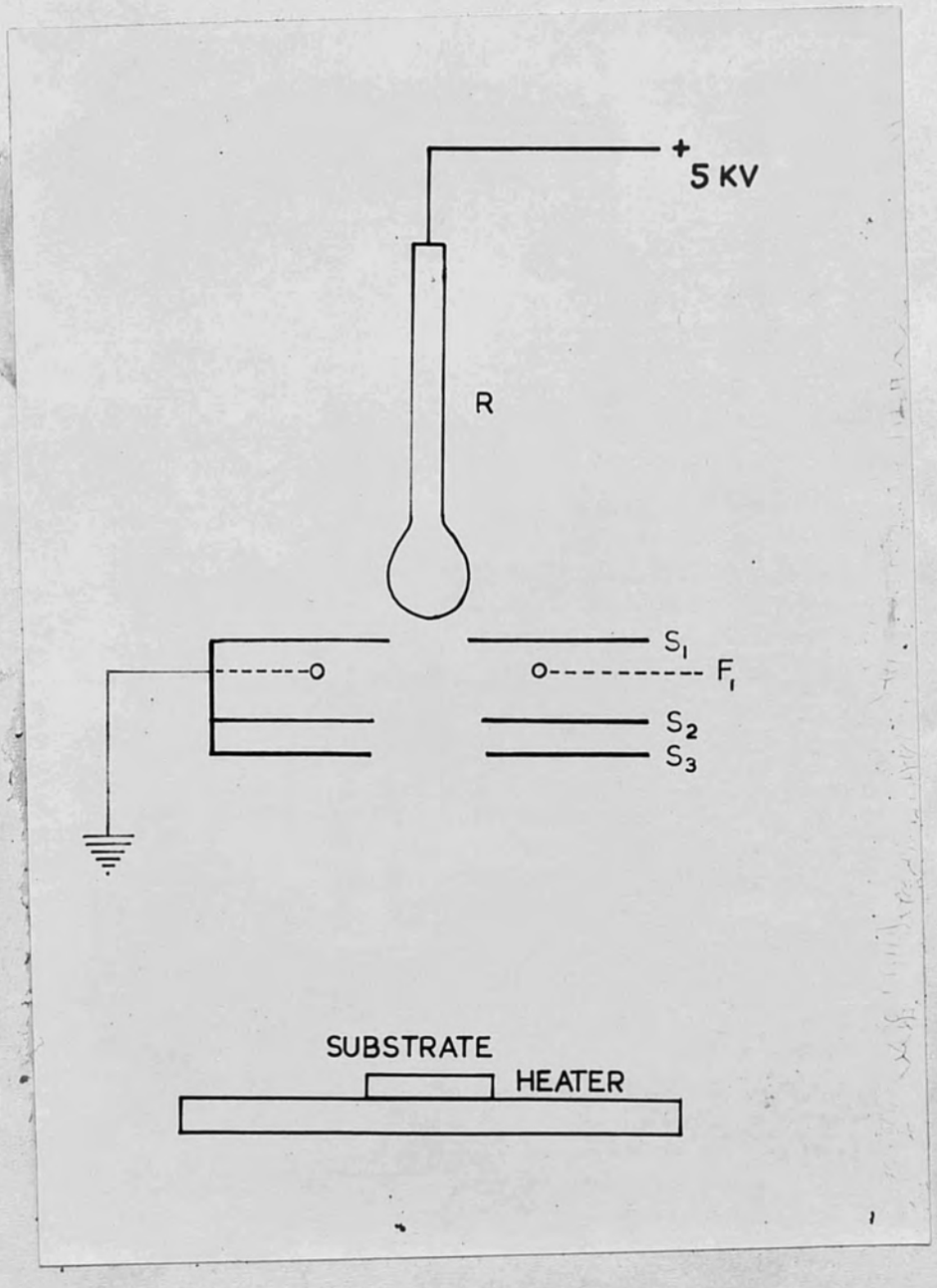

Fig 3.1. Schematic diagram of electron bombardment apparatus.

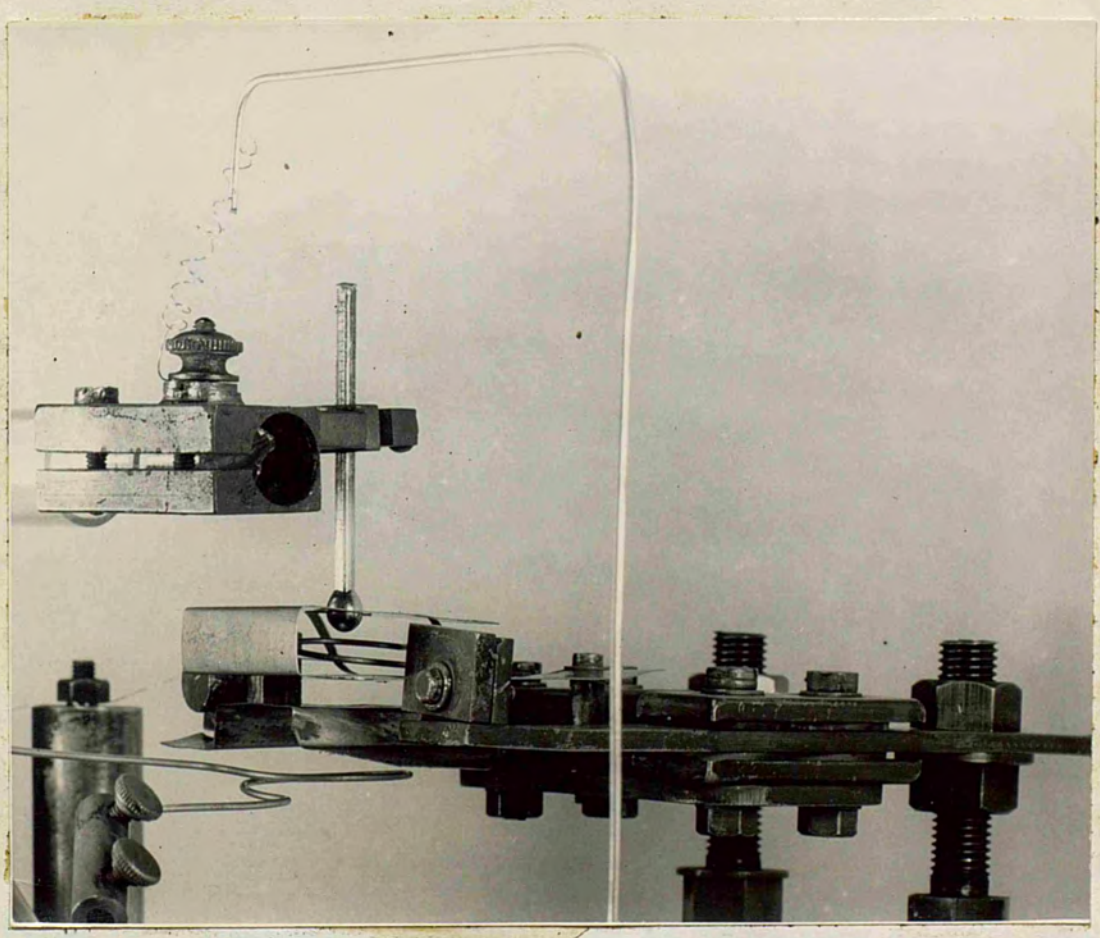

Fig 3.2. Photograph of electron bombardment apparatus.

with respect to a single turn tungsten filament F, through which an alternating current upto about 50 amps. is passed from a transformer regulated by a 'Variac'. Electrons are emitted by the filament and are accelerated to the end of the rod by maintaining it at +5KV with respect to the filament. S_1 is a thin molybdenum shield with a 1cm. diameter hole which serves to focus the electrons on the end of the rod and also to protect it from contamination by material evaporated from the filament. It is achieved by arranging the filament so that it could not see the rod. A similar molybdenum sheet S_2 is kept below the filament F to avoid any contamination reaching the substrate. S_3 protects the substrate from any impurities coming from the lower surface of S_2 which becomes red hot during evaporation. S_1, S_2 and S_3 are all earthed. An electron bombardment current of 20-25 m.a. is sufficient to melt the ferromagnetic rod of diameter 3m.m. and form a pendant drop of diameter 5-6 m.m.

When the rod is melted for the first time to form a pendant drop, spitting and outgassing occurs. It is necessary to melt the drop completely and thus outgas it thoroughly. Afterwards the bombardment current is reduced, until the surface separating the liquid and the solid phase is just above the middle of the drop fig. 3.3. This ensures that there will be no further outgassing. The distance between the filament and the drop is kept constant with a vertical movement controllable from outside the vacuum system.

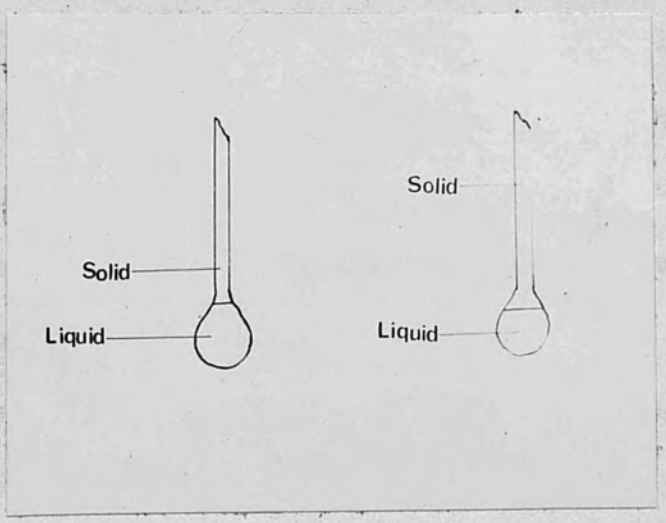

Fig 3.3. Positions of liquid and solid phases in the pendant drop.

a) while outgassing
b) while evaporating

The temperature of the drop is very close to the melting point of the metal, so there is little possibility of variation of rate of evaporation for a given size of the drop. The rate of evaporation may be varied by using rods of different diameters (2.5 m.m. to 4 m.m.), resulting in different sizes of the drop. For rods of small diameter, spitting and oscillation occurs and sometimes amplitude of oscillation is so large that the pendant drop comes into contact with the filament or the shield S_1. This is why rods of diameter less than 2.5 m.m. are not used.

The rate of deposition of the nickel can be varied, by varying the source-substrate distance, from 60 Å min^{-1} to 250 Å min^{-1}. For iron, the range 80 Å min^{-1} to 300 Å min^{-1} is attained. A source to substrate distance of 7 c.m. was adopted, as a compromise between uniformity of film thickness and contamination by residual gas.

3.3. Choice of the substrate.

The choice of the substrate for an oriented film depends upon the following factors.

i) Fe and Ni should not react with the substrate.

ii) Epitaxy must occur on the substrate.

iii) Since the film structure is studied by transmission electron-microscopy, it must be possible to remove the film from the substrate. This will release any stress developed due to differential contraction.

iv) It should have low vapour pressure at the temperature of deposition.

It is rather difficult to get all the above mentioned qualities in one substrate. Heavens[8] etal (1961) grew epitaxial films of Ni & Ni-Fe on all the principal faces of NaCl; Collins and Heavens[5] (1957) obtained epitaxial films of Ni, Fe & Co on NaCl and Shirai[14] (1937) that of Fe and Mo on cleaved faces of NaCl, KBr, KCl and KI. Epitaxial growth on these four substrates have been investigated.

As is evident from the following table, the melting points are substantially higher than the temperatures required for epitaxy.

Substrate	Melting Point °C
NaCl	801
KBr	730
KCl	776
KI	723

The crystals can be easily dissolved in water, so that the speciment prepared can be studied with the help of transmission microscopy. These substances do not react chemically or form alloy with Ni and Fe.

3.4. Preparation of the Substrate Surface.

i) Air-cleaved halides.

All the above mentioned halides are artificially grown and cleaved into $\frac{1}{2}$" cubes. These halides have a cubic structure and cleave easily along (100) planes. Examination of the cleavage faces by multiple-beam interferometry (Tolansky[17] 1948) reveals numerous steps as high as 1000°A fig 3.4. As is evident from the Fizeau fringes on the KI crystal, fig 3.4, C, silver is attacked, so the (110) and (111) surfaces of the crystals were not studied. This silver attack occurs only when the surface is exposed to atmosphere. Cleaved pieces 3 - 4 m.m. thick are produced by a guillotine and placed in the vacuum chamber as quickly as possible, without undue handling to minimise contamination and atmospheric attack.

ii) Vacuum cleaved halides.

A cleaved crystal of size 6 x 3 x 5 m.m.^{3} is held in a holder as shown in the fig. 3.5. It is held in position by a horizontal bar, screwed into the holder. If one piece of a crystal is used, the shield is removed but on the other hand if two pieces of a crystal are used, the shield covers one. The two pieces of the crystal are cleaved simultaneously to ensure that the stresses developed in the two pieces are the same, thus giving a fair comparison of the film developed on air - and vacuum-cleaved surfaces. The crystal holder is made of heavy brass bar which rests on the heater. The crystal holder is again attached to a brass rod which rests against the

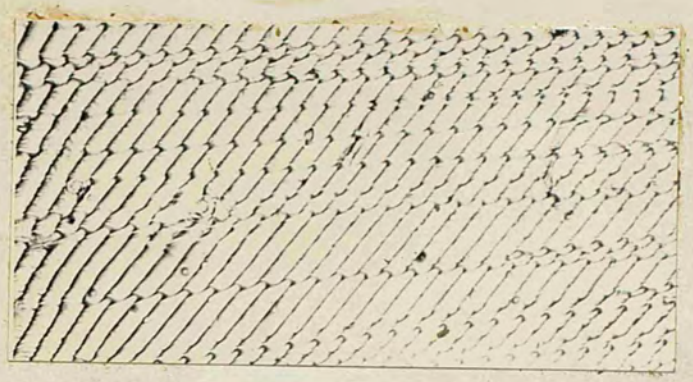

a) NaCl, reflection (X50)

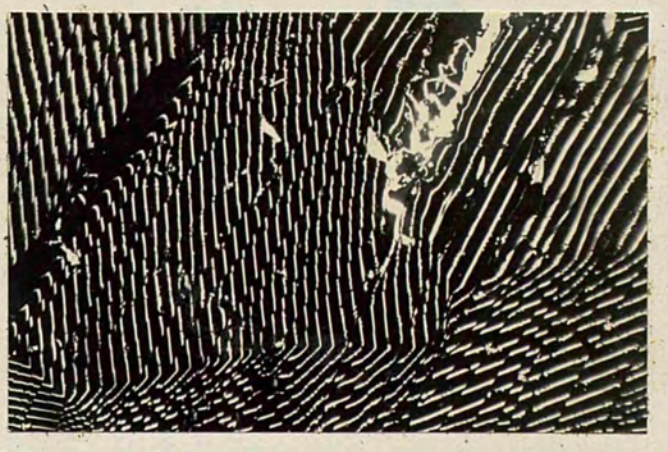

b) KBr, transmission (X40)

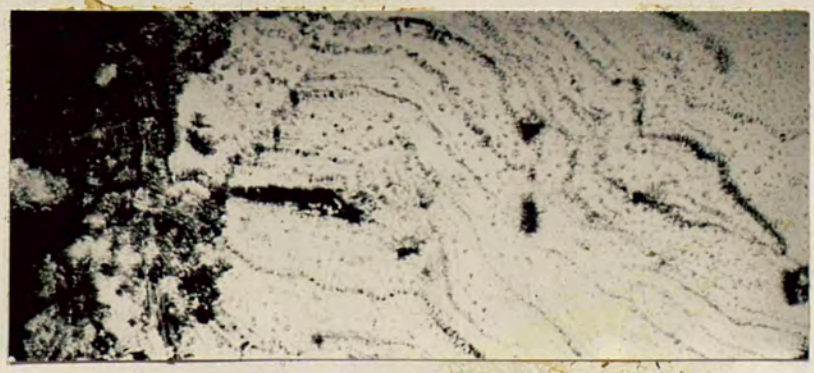

c) KI, reflection (X40)

Fig 3.4. Multiple-beam interferogram of a cleavage face of a crystal.
(λ = 5461A°)

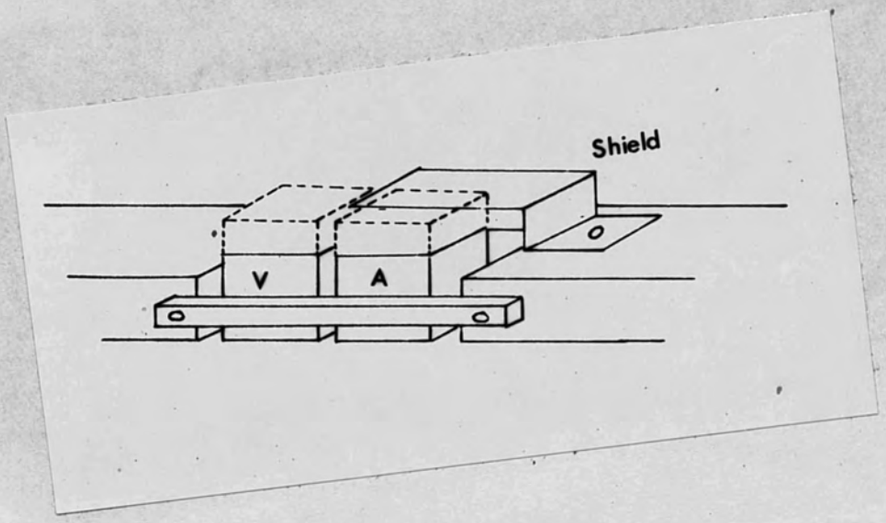

Fig. 3.5. Crystal Clamping System for cleaving in vacuum.

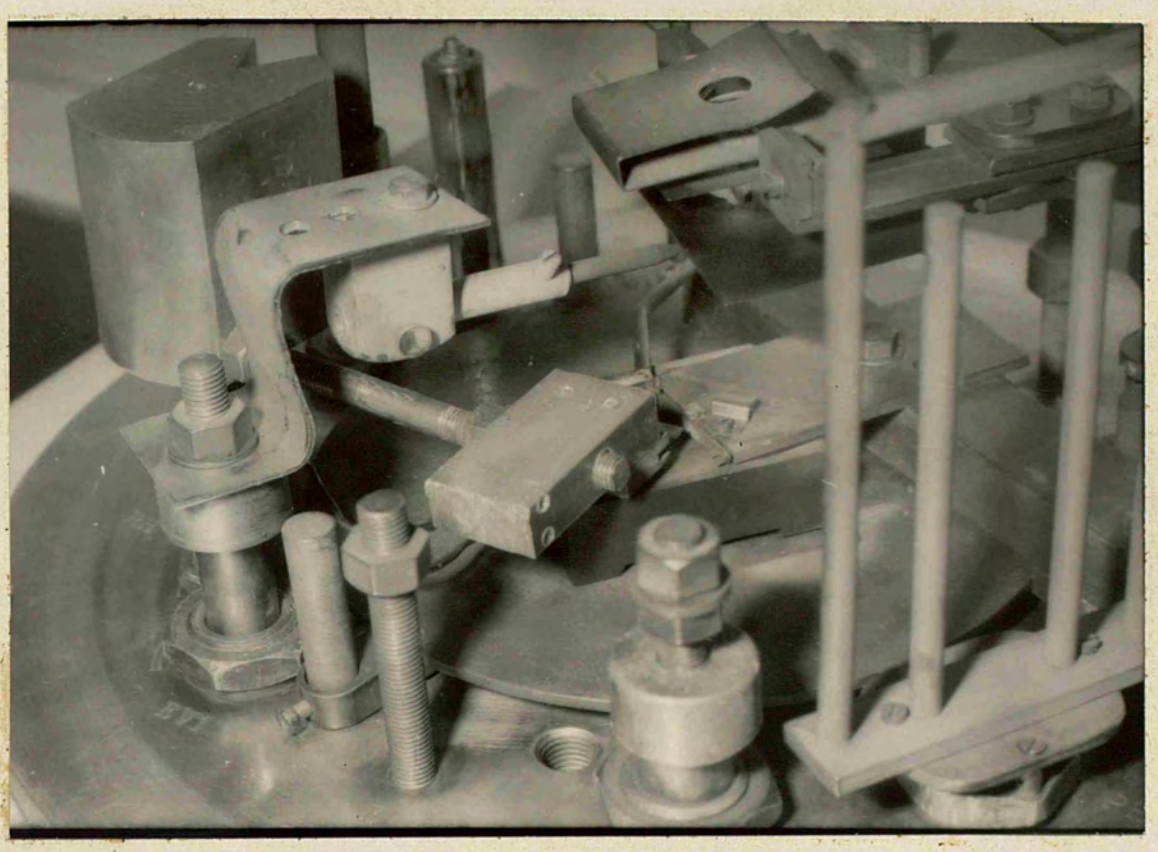

Fig. 3.6.

Photograph of the vacuum cleaving system.

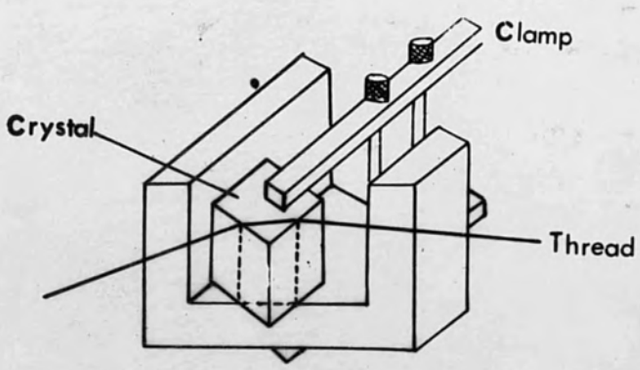

Fig. 3.7.
Jig used for cutting (110) faces of cubic crystals.

earthed electrodes. This is done only to ensure that there is no movement of the crystal from its position directly under the pendant drop.

As shown in the fig. 3.6, the cleaver is attached to a small brass rod. Which in turn is attached horizontally to a rotating system. This can be operated from outside. The height of the cleaver can be altered by raising or lowering the rotating system. The cleaved portion is pushed aside by a small nail attached just above the blade.

iii) Polished Halides

For studies of the anisotropy in Ni-films, it is essential to have a parallel sided film of 1 c.m. diameter. Although, on a cleaved crystals steps are flat (Bassett[1] 1958), this results into discontinuties of the same order as the thickness of the film. Besides this, it is necessary to treat all the faces of the crystal similarly.

(100) face is obtained as mentioned above, (110) and (111) planes are obtained by holding the crystal in especially designed jigs (e.g. fig 3.7.) and cutting it with a wet thread "saw". The surfaces so obtained have steps and bumps. These are removed by rough polishing them on a wet filter paper. A Multiple-beam interferograms on NaCl and KBr crystals are shown in the fig. 3.8. This gives a contour map of the topography of the surface, showing a large variation on the

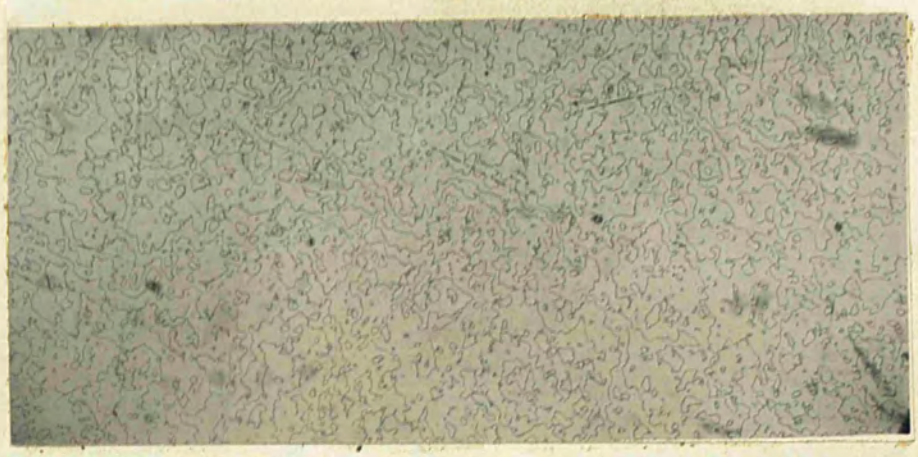

a) NaCl crystal (X50)

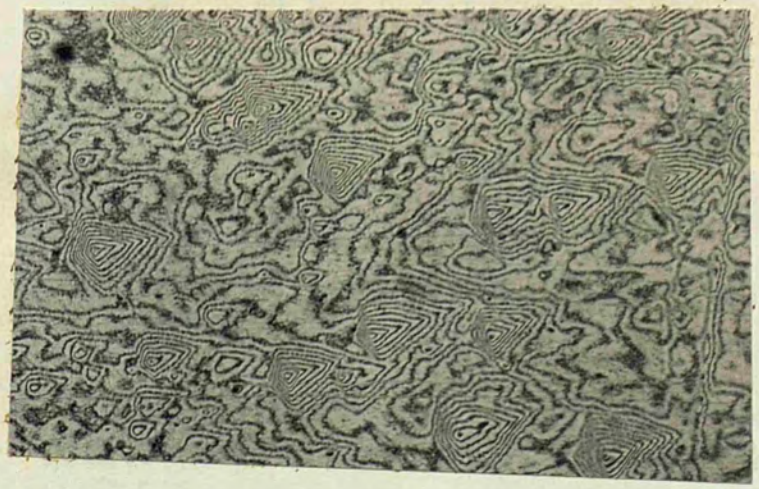

b) KBr crystal (X50)

Fig. 3.8. Multiple beam interferogram of (110) face of the substrate after polishing on wet filter paper.

(X50 λ = 5461A°)

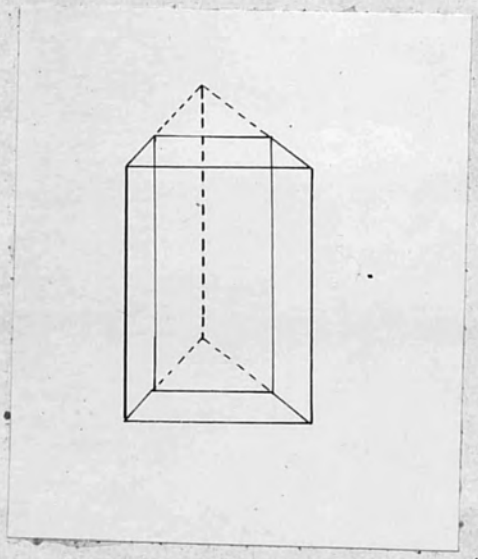

Fig 3.9. Portion of the crystal to be removed to make it parallel sided.

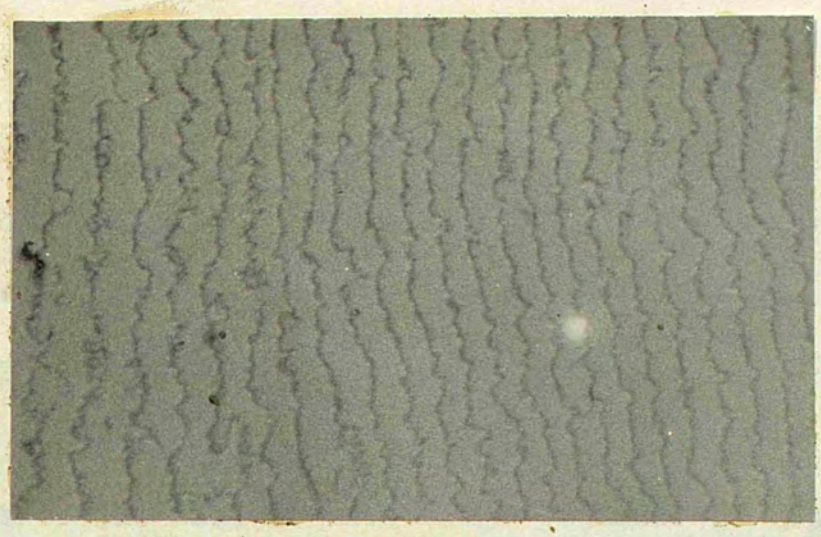

a) NaCl crystal
Reflection X50.

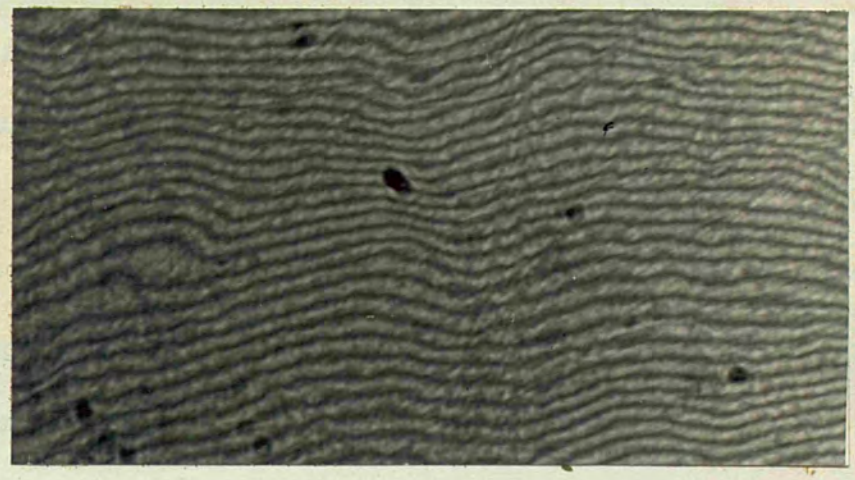

b) KBr crystal
Reflection X50.

Fig 3.10. Multiple-beam interferogram of a (110) face crystal after complete polishing treatment.
(X50, λ = 5461A°)

surface. This variation in height and projection of faces on microscopic scale produce disorientation; and local sagging occurs when the film is removed from the substrate.

The portion of the crystal shown in the Fig 3.9 is removed to obtain a parallel sided slab of thickness 3.5 - 4 m.m. The other side of the slab is also rough polished to improve the thermal contact with the heater.

The rough polished surfaces (100) and (110) of the crystal are polished on a rotating flat surface pitch-beeswax lap prepared as described by Strong[16] (1938). The polishing medium is putty powder in saturated solution of the corresponding halide. This solution acts as a lubricant without any danger of etching the crystal. The polishing process is continued until the lap is completely dry. The surface is then polished on 'sylvyt' cloth wetwith isopropyl alcohol and lastly on dry 'sylvyt' cloth, thus removing any traces of putty powder. To avoid etching by water vapour it is transferred directly either to the vacuum chamber or to the desiccator. Multiple-beam interferograms, Fig 3.10, show that the gross irregularities are removed.

iv) Intermediate Epitaxial layer.

As is known from the work of Heavens etal (1961) Ni and Ni-Fe films grow epitaxially on an intermediate epitaxial layer of Cu,

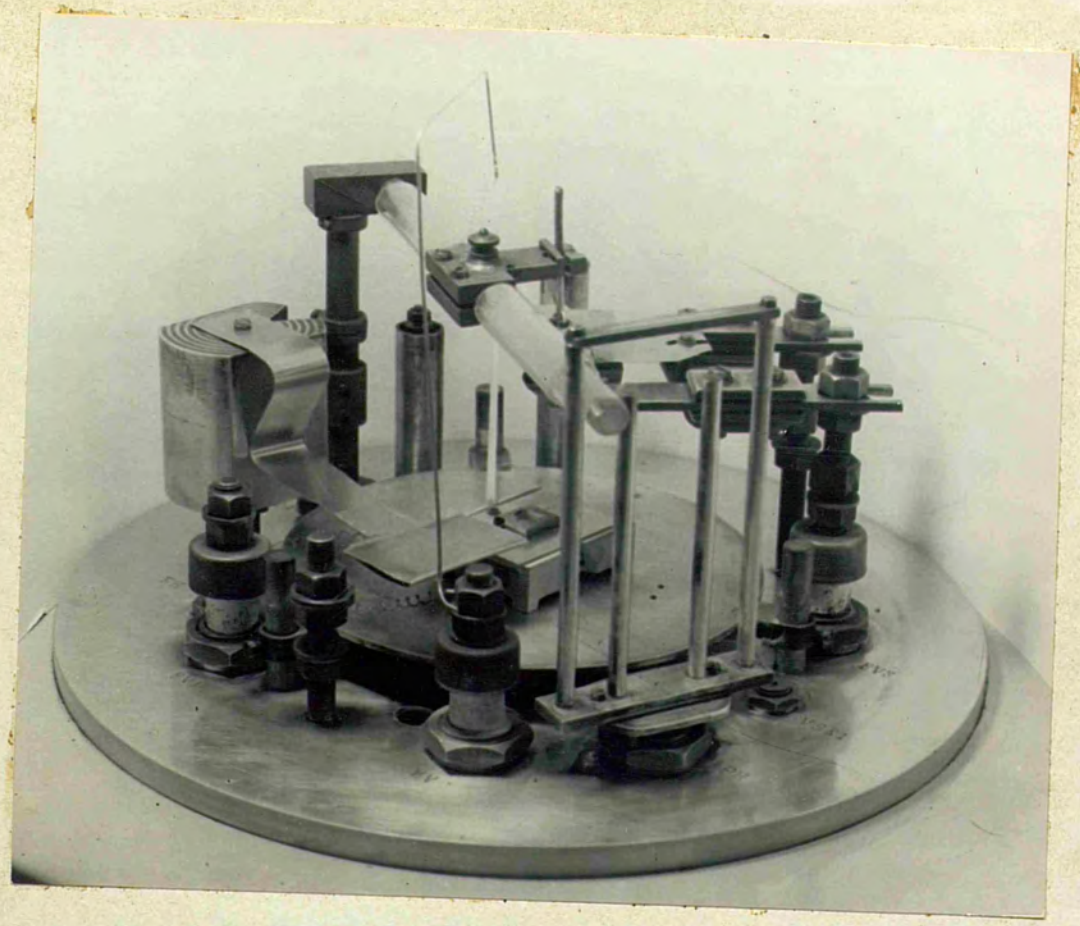

Fig. 3.11. Photograph of evaporation gear: F_2 and the upper shutter are removed for clarity.

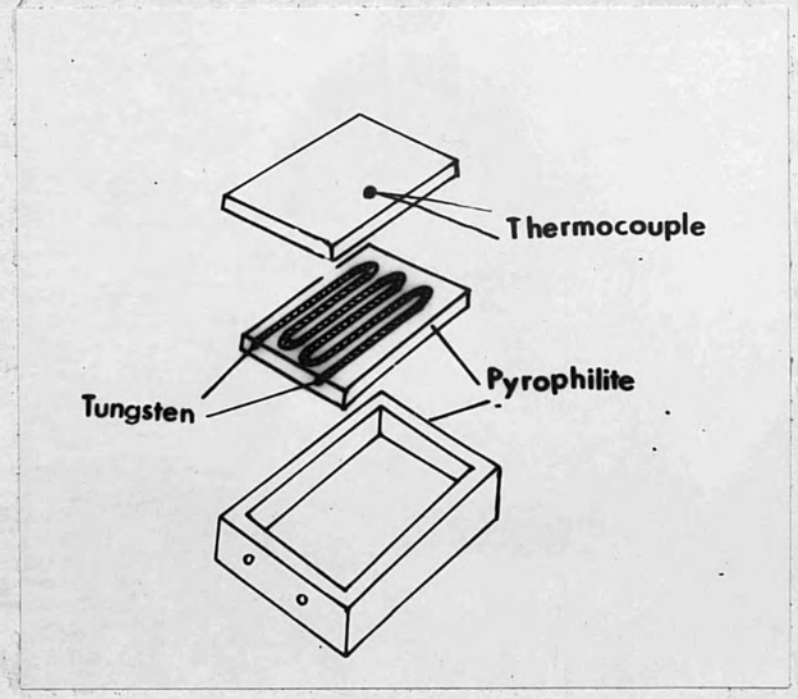

Fig. 3.12. The Specimen Heater.

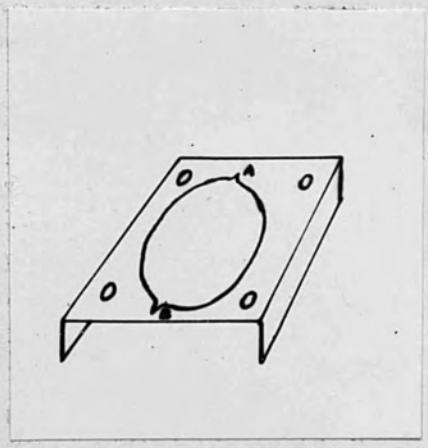

Fig. 3.13. The Specimen Mask.

so this substrate is used to grow Ni films for anisotropy studies. The copper, in the form of 'spec-pure' wire, is evaporated by electrical heating from a circular loop of vacuum-cleaned tungsten wire. Since tungsten shows no sign of attack, there is little likelihood of contamination by this method of evaporation. A continuous monocrystalline surface of Cu is formed by depositing sufficient Cu on polished rocksalt surface.

3.5 The deposition of the films.

i) The Vacuum System.

An Edward Coating Unit Model 12EA/204 is used. The pumping system is conventional, consisting of a three stage oil diffusion pump, backed by a rotary pump, with a P_2O_5 trap in between. The operative pressure attainable is $2\text{-}5 \times 10^{-5}$ m.m. Hg. The main constituents of the residual gases in such a system is O_2 (Caswell[4] 1961). Mitchell[12] (1959) showed that polycrystalline films, grown under such vacuum conditions, are oxidized only to the extent of a few atomic layers. Some oxidation in the films is therefore to be expected in these experiments.

ii) The Deposition Chamber.

Fig 3.11 shows the general lay out of the deposition chamber. The 12 in. bell jar accommodates all the apparatus for evaporation by electron-bombardment. The filament F_2, from which copper is evaporated, is arranged below screen S_3, Fig 3.1. The substrate

is put on an electrically heated stainless steel plate of the heater consisting of tungsten filament, supported on a baked pyrophillite base fig 3.12; the temperature of the heater plate is measured by a T_1, T_2 thermocouple.

Only in the case of Ni-films a mask is used. This consists of a molybdenum sheet with a punched circular hole of 3/8" diameter fig 3.13, with marks A and B across a diameter to indicate the relative position of the crystallographic axes.

The time of deposition of the film is controlled by a shutter of molybdenum sheet between S_3 and the substrate. This is rotated in a horizontal plane from outside. This shutter prevents the pendant drop and the lower surface of S_3 from contamination by the evaporated halide during its annealing. It is very important to clean the lower side of the shutter after every evaporation and the lower sides of the shields S_2 and S_3 after every two evaporations. Failing this, contamination of the surface of the substrate ensues, resulting in fragile and poorly oriented films.

In the case of vacuum cleaved halide, the apparatus is altered slightly, as is evident by the comparison of the figs. 3.6 and 3.11. The shutter attached to the rotating system is replaced by the cleaving system. In the system are incorporated a pair of carbon rods, placed about 30° from the normal to the substrate, so that carbon could be deposited, soon after cooling of the film and prior to exposing it to atmosphere.

iii) The temperature of the substrate surface.

The surface temperature of the substrate and that of the heater plate will in general differ. The procedure of Miller[11] (1962) is therefore adopted to establish the temperature of the surface of substrate. Instead of putting a thermocouple wire on the surface of the substrate, thus producing local cooling, the surface temperature of substrates of uniform thickness, is calibrated by putting small quantities of materials which do not react with the halides used, and observing their melting from a telescope. All this is carried out in vacuum system. In this way the surface temperature of the crystal is calibrated in terms of the surface temperature of the heater plate within $\pm 10^{\circ}C$, as shown in the fig 3.14.

Hence all the temperatures mentioned are the true surface temperature as derived from the graph.

iv) Evaporation procedure.

Freshly cleaved or polished crystal is put on slightly warm heater surface to avoid any attack by atmospheric moisture. In the case of nickel films prepared for Faraday Rotation measurements, the mask is placed on the substrate so that the line joining A and B is parallel to a particular axis on the rocksalt. The chamber is evacuated until the pressure is 2×10^{-5} m.m.Hg. The temperature of the rocksalt is raised to $400^{\circ}C$, KBr to $370^{\circ}C$ and KI to $320^{\circ}C$ in small steps. At about this temperature, the crystal is annealed for an hour.

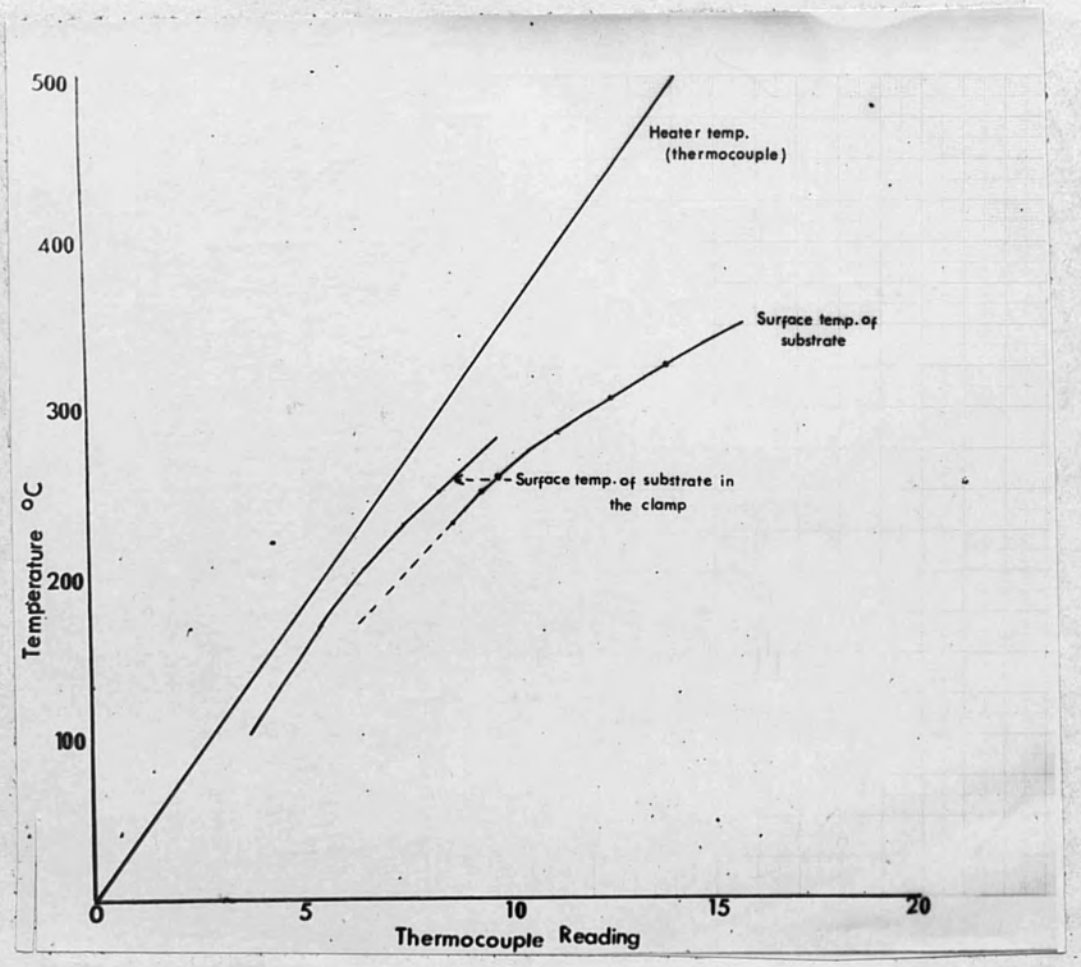

Fig 3.14. Calibration curve for the substrate heater.

After this, the temperature of the crystal is lowered to the desired value and during this time the pendant drop is formed and outgassed. When, again the pressure 2×10^{-5} m.m.Hg. is achieved, the surface separating the liquid and the solid state is brought to half the height of the drop. The shutter is removed for a desired time and a film of desired thickness is formed. The film is allowed to cool under vacuum. The time to cool to room temperature is about $1\frac{1}{2}$ hours. On removal from vacuum system, it is stored in a desiccator.

For a vacuum cleaved surface, the crystal is heated to the desired temperature, the pendant drop is melted and the system is outgassed. When the system has attained the desired conditions, the crystal is cleaved and the film is immediately deposited for the necessary time. Afterwards it is allowed to cool to the room temperature, and is kept covered till after the carbon arc is started and kept going for a few minutes. The film is then exposed to deposit a carbon film of thickness $\sim 100 A^{\circ}$. Afterwards the crystal is stored in a desiccator.

b) Copper Substrate.

As described in this chapter, copper is evaporated on rock salt substrate which is kept at $330^{\circ}C$ to produce a thick copper film with parallel orientation with a substrate (see Chapter 5). Afterwards nickel is deposited at the same temperature, producing a monocrystalline Ni film.

3.6. Removal of the films from the substrate.

Films deposited on either rock-salt or copper substrate are detached from them for study by transmission electron microscopy. In the case of nickel films for Faraday Rotation studies, it is necessary to relieve the films from compressive stresses due to the difference in the thermal expansion coefficients of nickel and the substrate. Different techniques are used for different substrates. On very thin films, which usually break up when drying on the grid, a carbon film of about 100A° thick is deposited.

i) Removal from halide.

The substrate, with the film, is gently lowered into a shallow dish of distilled water to which a few drops of isopropyl alcohol are added, to reduce the surface tension. The substrate is kept horizontal and the water allowed to dissolve the substrate. The film floats off gently. It is picked up by a clean glass plate and is floated off twice in two different dishes full of distilled water. This action washes away any remaining halide from the film.

ii) Removal from copper.

Following the technique of Miller (1962), a solution of 10gm of rocksalt in 300 m.l. of water is prepared. The composite film is left floating overnight, and the remaining unattacked Ni film is washed thrice in distilled water. For Faraday rotation study, the

film is picked upon a quartz slip; while small pieces are picked up on microscope grids. These are also washed thrice.

3.7. Thickness measurements.

Thickness measurements are carried out by Fizeau fringes techniques. The film is deposited on the cleaved or polished surface at the required temperature with its surface partly covered by a razor blade to get a sharp edge. After cooling the film, it is floated off the substrate, mounted on a glass flat, and then dried in the desiccator. After silvering it, the Fizeau fringes are observed in the usual way. The shape of the fringes is as shown in the Fig 3.15 and the thickness is calculated from the formula,

$$t = \frac{a}{b} \times \frac{\lambda}{2}$$

which is self explanatory from the Fig 3.16.

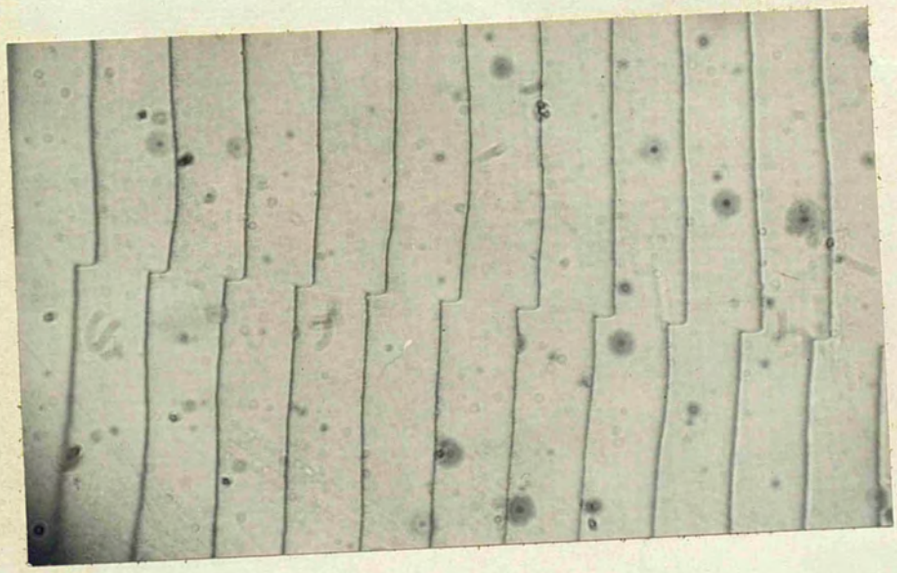

Fig. 3.15. Example of a Fizeau Fringe.
(X50, λ = 5461Å)

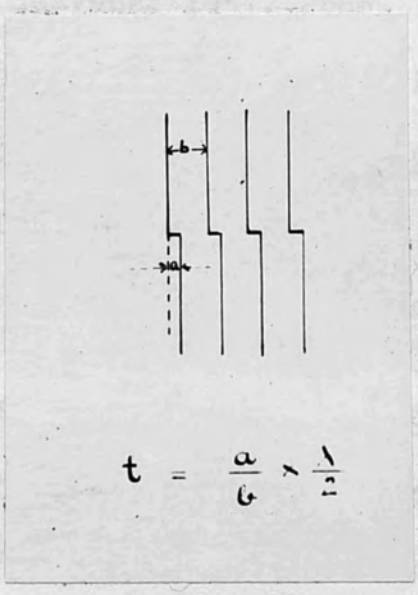

Fig. 3.16. Appearance of the Fringes.

REFERENCES

1 Bassett, 1958, Phil. Mag., 3, 1042.

2 Behrndt, 1959, I.B.M. Eng.Rep. 1M-410, Kingston, N.Y.

3 Behrndt and Jones, 1958, Fifth National Symposium on Vacuum Technology Transactions, (London: Pergmon), 217.

4 Caswell, 1961, Symposium on the Electric and Magnetic Properties of Thin Metallic Layers, (Louvain)

5 Collins and Heavens, 1957, Proc. Phys. Soc., B, 70, 165.

6 Heavens, 1952, Proc. Phys. Soc., B, 65, 788.

7 Heavens, 1959, J. Sci.Instrum., 36, 95.

8 Heavens, Miller, Moss & Anderson, 1961, Proc. Phys. Soc., 78,33.

9 Holland, 1958, Vacuum Deposition of Thin Films, (London: Chapman and Hall).

10 Kelley, 1959, J. Sci. Instrum., 36,89.

11 Miller, 1962, Ph.D. Thesis, London University.

12 Mitchell, 1959, Structure and Properties of Thin Films. (New York: Wiley), 258.

13 Oslen, Smith and Crittenden, 1945, J. Appl. Phys., 16,245.

14 Shirai, 1937, Proc. Phys. Math. Soc. Japan, 19, 937.

15 Smithells, 1955, Metals Reference Book (London: Butterworths Scientific Publications).

16 Strong, 1938, Modern Physical Laboratory Practice, Chapter 2. (London; Blackie).

17 Tolansky, 1948, Multiple Beam Interferometry (Oxford: Clarendon)

Chapter 4.

Epitaxial Growth of Iron.

4.1. Introduction:

The epitaxial growth of iron on cleaved rock salt has been observed by Brück[2] (1936), Shirai[9,10] (1937, 1938) and Collins and Heavens[3] (1957). Shirai[9] (1937) also grew iron epitaxially on cleaved faces of KCl, ~~and~~ KBr and KI. Only Collins and Heavens grew it epitaxially on polished (110) and (111) faces of rock salt.

Brück[2] (1936) and Shirai[9,10] (1937, 1938) observed the following orientations on the (100) faces of rock salt.

(a) Fe (001) $\langle 100 \rangle$ || NaCl (001) $\langle 100 \rangle$

(b) Fe (001) $\langle 110 \rangle$ || NaCl (001) $\langle 100 \rangle$

In the case of cleaved KBr and KCl crystals type (a) orientation is weaker than that of type (b) (Shirai ~~l.c.~~) Besides these orientations of Fe on (100) face of rock salt, Collins and Heavens noted two more orientations.

i) Fe (111) $\langle 11\bar{2} \rangle$ || NaCl (001) $\langle \bar{1}10 \rangle$

ii) Fe (210) $\langle 112 \rangle$ || NaCl (001) $\langle 100 \rangle$

In films grown on (110) face of rock salt a mixture of the following orientations were observed

i) Fe (110) $\langle 001 \rangle$ || NaCl (110) $\langle 001 \rangle$

ii) Fe (111) $\langle \bar{1}10 \rangle$ || NaCl (110) $\langle 001 \rangle$

whilst in the case of (111) rock salt, the epitaxial film of iron gave a mixture of sharp spots and broader arcs. The sharp spots were due to (111) Fe and broad arcs were due to Fe (110) $\langle 100 \rangle$ || NaCl (111) $\langle \bar{1}10 \rangle$. A third, weaker, orientation was also present, namely Fe (111) $\langle \bar{2}11 \rangle$ || NaCl (111) $\langle \bar{1}10 \rangle$.

4.2. Iron films grown on cleaved (100) KBr, KCl and NaCl.

i) Influence of Substrate temperature on orientation.

Iron films were prepared on several cleaved halide crystal (KBr, KCl and NaCl) substrates at temperatures ranging from 20°C to 300°C. Fig. 4.1 shows the typical diffraction patterns of the films for temperatures in the range 20°C to 300°C. The films were of thickness 500A° and grown at 200A°/minute. Iron, deposited at room temperature shows diffraction rings characteristic of the body-centred form, stable at temperatures below 900°C. As the temperature of the Substrate is raised, the intensity of the rings increases and spots start to appear on the otherwise uniform rings.

Films deposited at 200°C showed even better orientation with an increase in the intensity and number of reflections, with two orientations present. Substantially complete orientation is obtained for the different substrates at the temperatures shown in the following table.

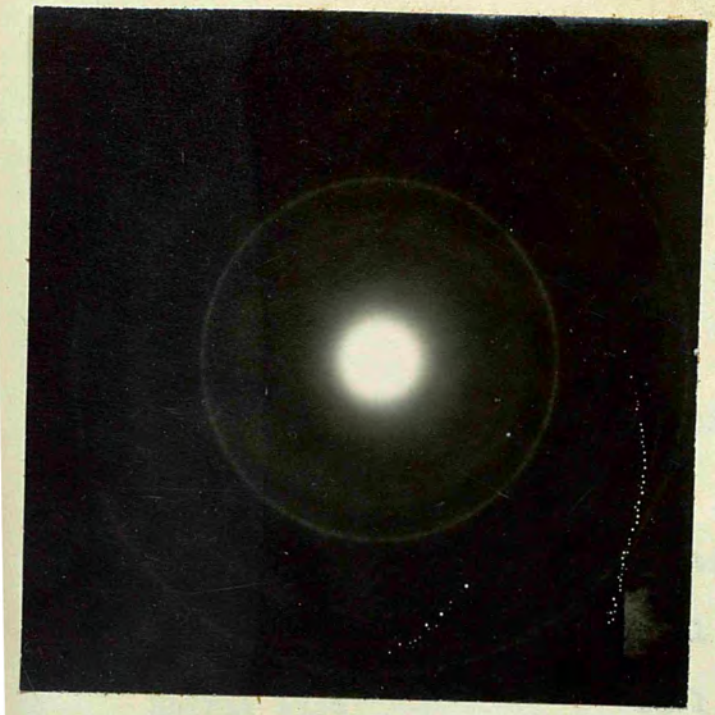

20°c

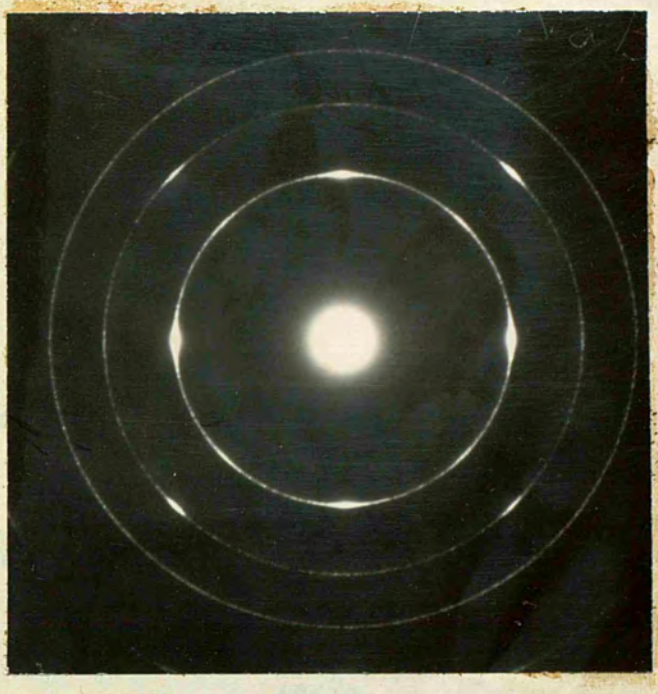

150°c

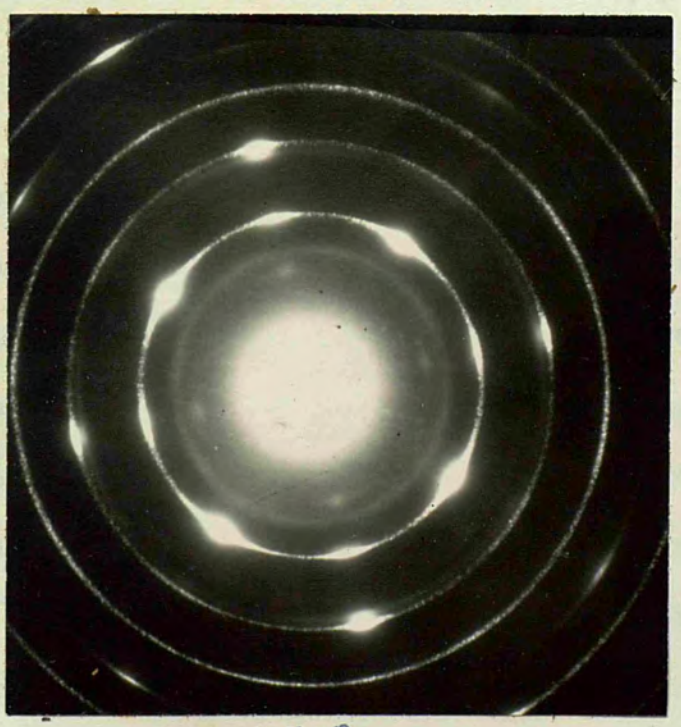

250°c

Fig 4.1.

Diffraction Patterns at different temperature.

Substrate	Temperature
NaCl	300°C
KCl	320°C
KBr	320°C

This optimum temperature for epitaxy is lower than that previously reported.

Reference	Substrate	Epitaxial temperature
Collins and Heavens[3] 1957	NaCl	470°C
Shirai[4] 1936	NaCl	486°C
	KCl	520°C
	KBr	510°C
	KI	440°C
Brück[2] 1936	NaCl	> 520°C

Collins and Heavens, Shirai, measured the temperature of the Substrate heater in contact with the Substrate. This is bound to be higher than that of the surface temperature of the heater. The deposition of the film at higher temperatures produces sometimes only single orientation but at 350°C the films are heavily oxidized.

ii) Influence of film thickness on orientation.

By moving a shutter in discrete steps across the substrate surface during deposition a series of regions varying in thickness from 20 A° to 500 A° are obtained with the substrate at the epitaxial temperature. The diffraction patterns of the films of thickness up to about 60 A° show rings, although the thicker films are well oriented.

This is probably due to the stripping which results into misalignment of the crystallites. Double orientation is more marked in the case of thicker films.

iii) Influence of the rate of deposition on orientation.

As discussed in Chapter 3, the optimum deposition rate from consideration of apparatus geometry was estimated to be 300 A°/minute. This can be increased by reducing the source and substrate distance but this results into the oxidation of the iron film. Low evaporation rates ($< 50\ A^{\circ}$ per minute) produce poor orientation. This may be attributed to poor vacuum conditions ($\approx 10^{-5}$ m.m. of Hg) and high vapour pressures of the substrates. Thus we note that for Substrates such as mica, having a low vapour pressure, deposition rates of 2 or 3 A° per minute favour orientation.

iv) Structure of the iron films grown on halides.

a) Influence of the Substrate temperature on the microstructure of the films.

Iron films of 300 A° thickness were deposited on different substrates at various temperatures in the range 20°C to 300°C. The crystallite size at 20°C is very small. As the temperature of the substrate rises, the crystallite size also increases. At the optimum temperature for epitaxy, the crystallites seem to coalesce, so that large continuous regions are formed, separated by channels.

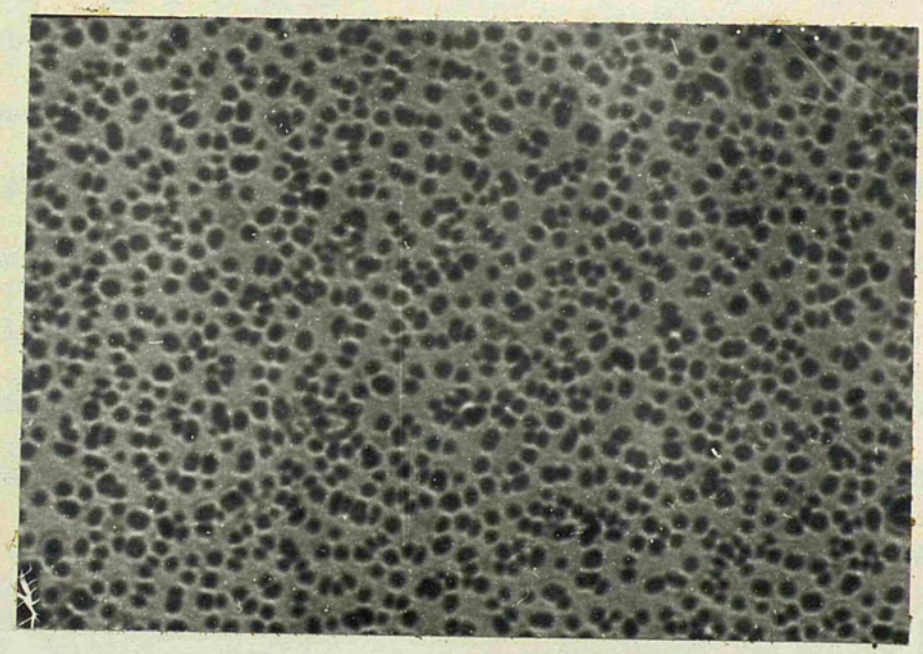

X 32 000

Fig 4.2.

Distribution of Initial nuclei.

The greater crystalline order and larger crystallites are associated with a higher surface mobility at the higher temperature.

b) Variation of Microstructure with thickness in oriented films.

A 'stepped' film was prepared, as in section (ii), with the substrate at 300°C, so that a range of thickness from 50A° to 600 A° was obtained. Fig 4.2. shows that initial nuclei are randomly disposed on the surface but there is a tendency for the nuclei to form preferentially at the steps on the substrate. The density of the nuclei between the steps is 2.5 x 10"/cm^2 at a thickness of 50 A°. The dimensions of the nuclei are ≈ 200A° in diameter. As the thickness increases, the nuclei also increase in size by receiving new deposit atoms. As the nuclei grow in size, existing nuclei join together and develop very irregular shapes. They appear to flow together, as shown in Fig. 4.3. The crystallites which join together are either at right angles or at 45° to each other. It is also possible to find square and rectangular shaped crystallites in the channels.

In studies of the epitaxial growth of Nickel on Sodium chloride, Miller (1962) found that the nickel nuclei join together and form a lace-work pattern upto 500 A°thickness. Miller suggested that the linking of the nuclei serves to reduce the 'free ends' in a slightly ferromagnetic material (Ni-Epitaxial temperature 330°C, Curie Point 358°C). No such linking of free ends or the formation of 'lacework'

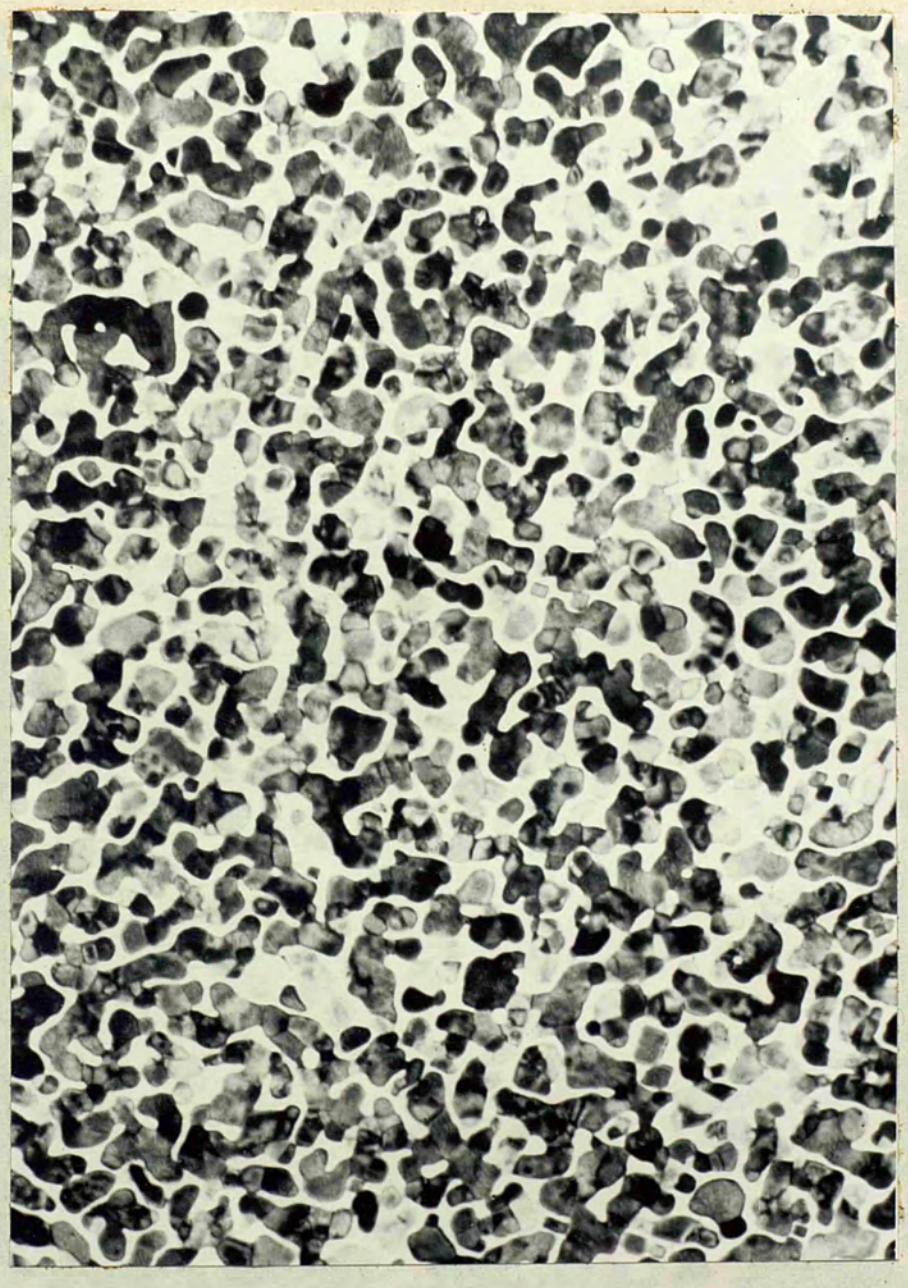

Fig. 4.3
X32000

'Flow Structure' of an Epitaxial Iron film, 150 A° thick.

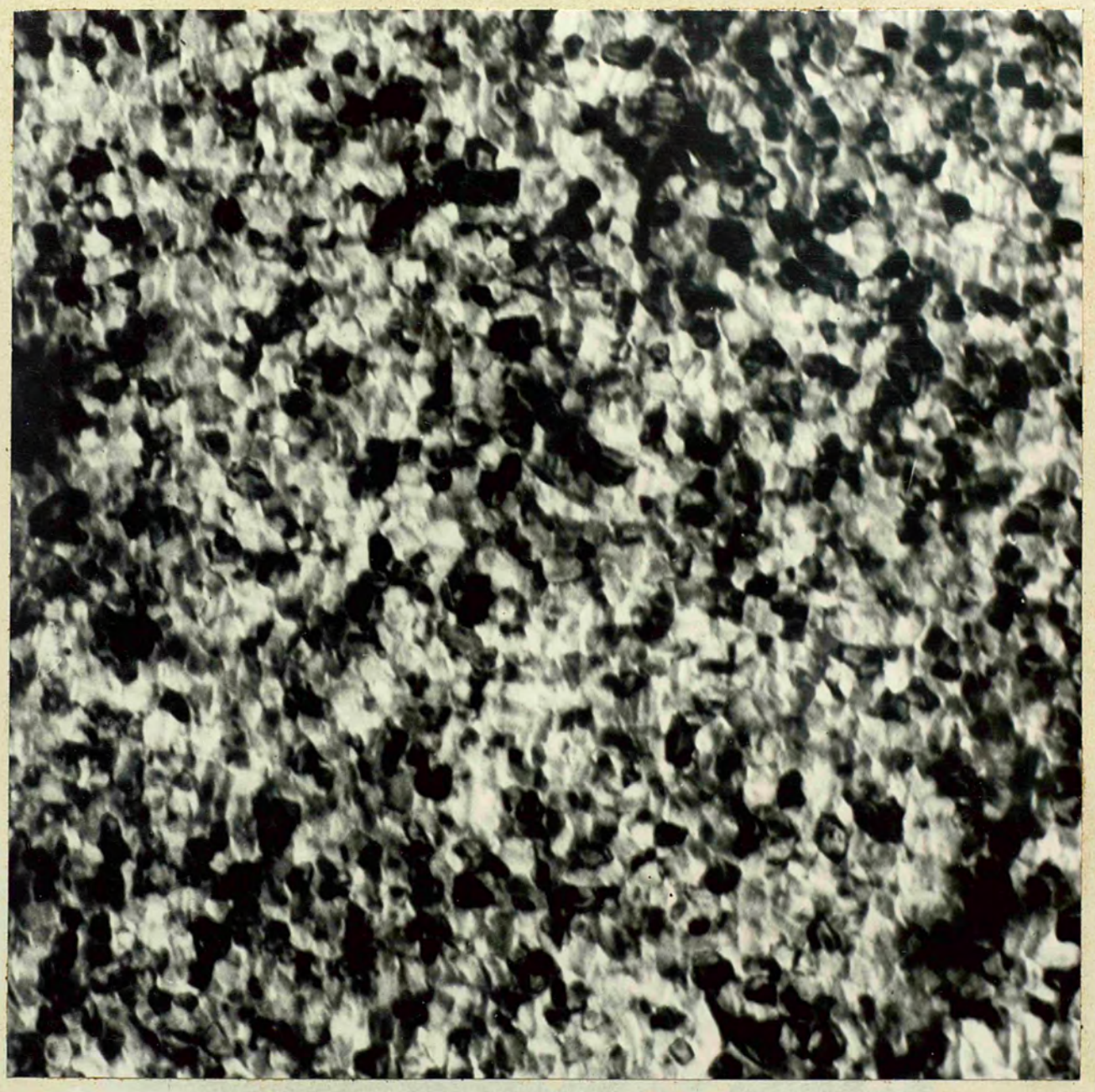

Fig. 4.4
X60,000

Electron-micrograph of a continuous film 400 A° thick.

Fig 4.5
X10,000

Impression of crystallites
on carbon film.

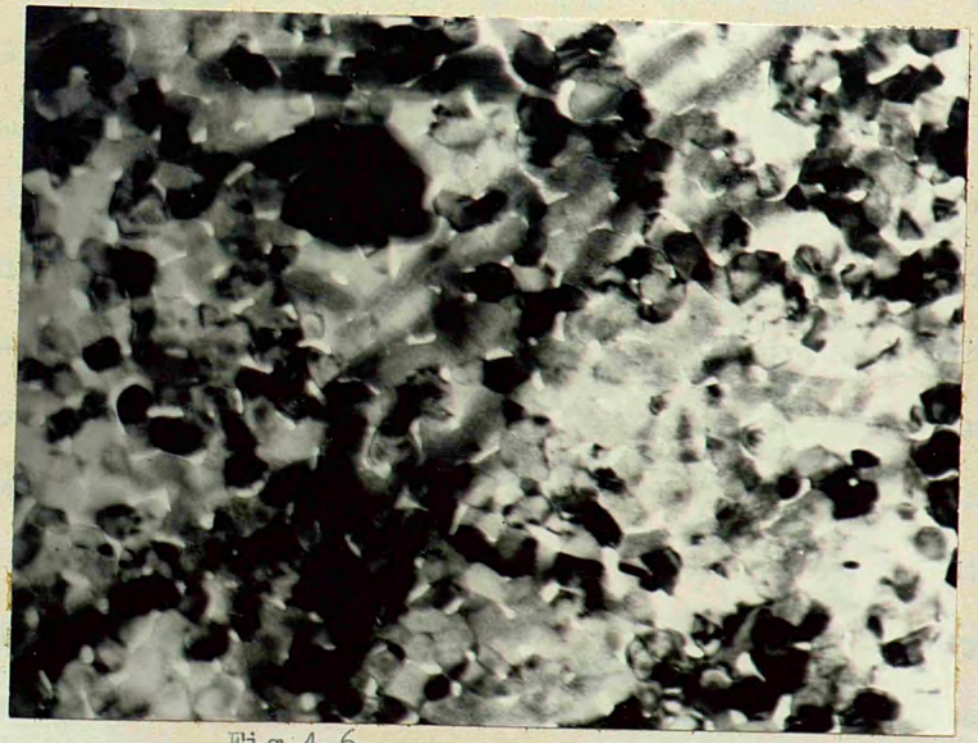

Fig 4.6
X32,000

Electron micrograph of (111)
iron on (110) face of rock salt.

was observed in the case of iron (Epitaxial temperature $\sim 300^{\circ}C$, Curie point $770^{\circ}C$). The mobility of iron and nickel nuclei is nearly the same (Umanski and Krylov[11] 1936) and so this effect should be more pronounced in the case of iron, being more ferromagnetic than nickel under the above conditions.

Fig. 4.4. shows the electron-micrograph of a 400 A° doubly oriented iron film. The shape of the crystallites is quite different from that of the face-centred cubic material. All the crystallites are oriented either along $\langle 001 \rangle$; $\langle 010 \rangle$ or $\langle 011 \rangle$ directions. Some join together to form angular shaped crystals.

Fig. 4.5. shows a micro-graph of an oriented film. The iron crystallites have failed to leave the substrate with the carbon. In the figure, the impression of the crystallites are quite marked.

v) Structure of the iron films grown on (110) face of NaCl.

Fig. 4.6. is a micrograph of a 300 A° thick film deposited on (110) face of rock salt. It is obvious that the film is not continuous. Fig. 4.7. shows the micrograph of an iron film on the (110) face of rock salt. These crystallites are elongated in the $\langle 001 \rangle$ direction as seen by Miller[6] (1962) in the case of nickel. This effect persists until the lateral dimensions of the crystallites is several thousands of Angstroms, and continuity is approached.

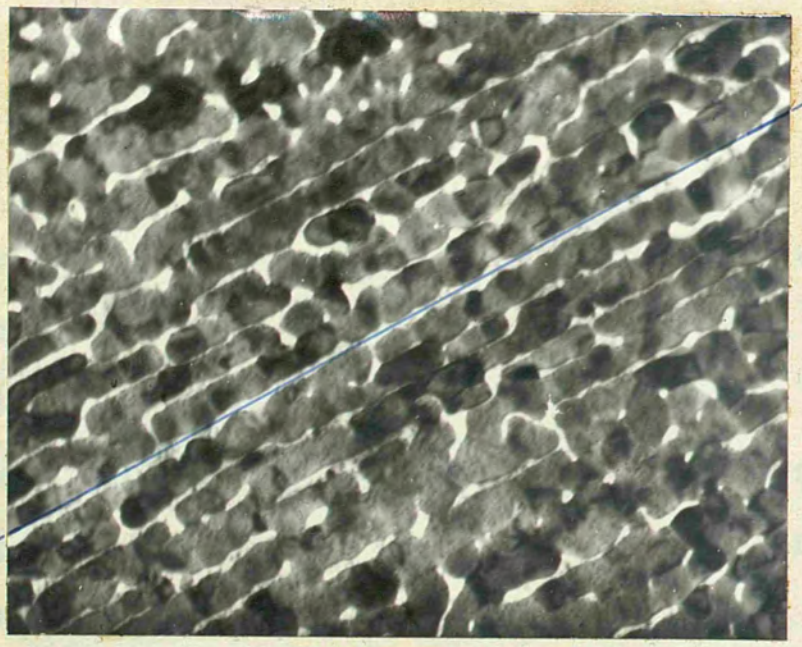

Fig 4.7
X32,000

Elongation of the iron crystallites on (110) face of rock salt.

Fig 4.8
X32,000

Annealing of (100) Fe film under electron beam.

The origin of the elongation of the crystallites cannot be attributed to the self shadowing as the vapour-beam was normal to the substrate. Polish marks on the surface are an unlikely origin, because of the regularity and small scale of the effect. Miller, while exploring its origin in the magnetic effect of the nickel film, ruled out the possibility, as this effect persisted below and above the Curie point (358°C) of the nickel. Since, iron at such a low pressure (10^{-5} m.m.) oxidizes heavily above 350°C, no attempt was made to deposit the film above its Curie point (770°C).

It seems possible that the elongation could be caused by the formation of minute prisms on the surface of the (110) rock salt surface by projecting (100) and (010) cleavage planes (Miller[6] 1962). Such prisms might, in pairs, form channels with prefered nucleation sites along the $\langle 001 \rangle$ direction or, singly, present ridges where nucleation is unfavorable. This effect might be masked by the higher mobility and larger crystallite size of the iron at the higher substrate temperature.

Observations have been made recently by Germer etal (1961) on the positions of impurity atoms, e.g. oxygen, on the (110) face of nickel crystals, and these indicate a further possibility. Impurity atoms sometimes tend to occupy consecutive sites on the (110) surface, forming rows along $\langle 001 \rangle$ directions. While it is difficult to predict what effect they would have on arriving atoms from a beam of

vapour, the orientation of these rows might be of significance, especially in vacua of the order of 10^{-5} m.m. of Hg.

vi) Effects of annealing on iron films.

Annealing experiments were performed on films detached from the substrates and freely supported on microscope grids. Fig 4.8. shows the result of heating the film under the electron beam for about five minutes. The crystallites, instead of having an irregular shape, tend to form a "globule" feature. Some times the film is contaminated by the accumulation of the cracked hydrocarbons.

4.3. Analysis of Diffraction Patterns.

i) Introduction.

Iron is a body-centred cubic metal and its reciprocal lattice is represented by a face-centred cube. For measuring the lattice constant, calibration is done by evaporating NaCl on the film and the relation between the Bravis Lattices of the iron and the substrate is obtained by putting the film in a particular fashion with respect to the grid Fig 4.9 and getting the diffraction patterns along with the photograph of the grid.

ii) Iron on cleaved NaCl (100) face.

Fig 4.10 shows the diffraction pattern of a film 400 A^{0} thick deposited on NaCl (001) face at 300°C with a rate of deposition 200 A^{0} per minute. This is a mixture of two orientations, namely:

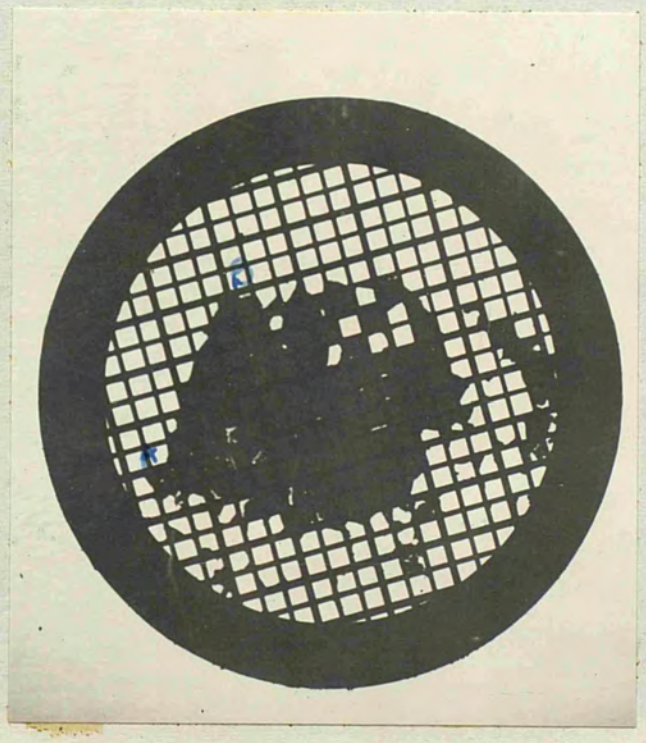

Fig. 4.9

Iron film placed on the grid, with a sharp edge along AB. AB is parallel to $\langle 001 \rangle$ direction of the substrate.

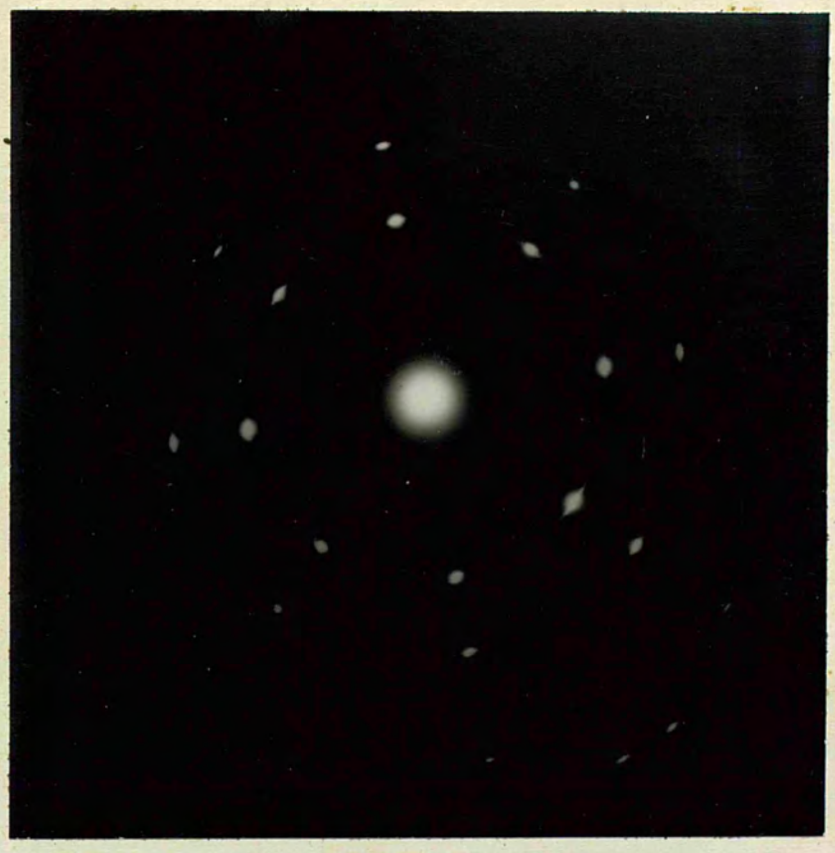

Fig 4.10

Double orientation of iron on (001)
NaCl face.

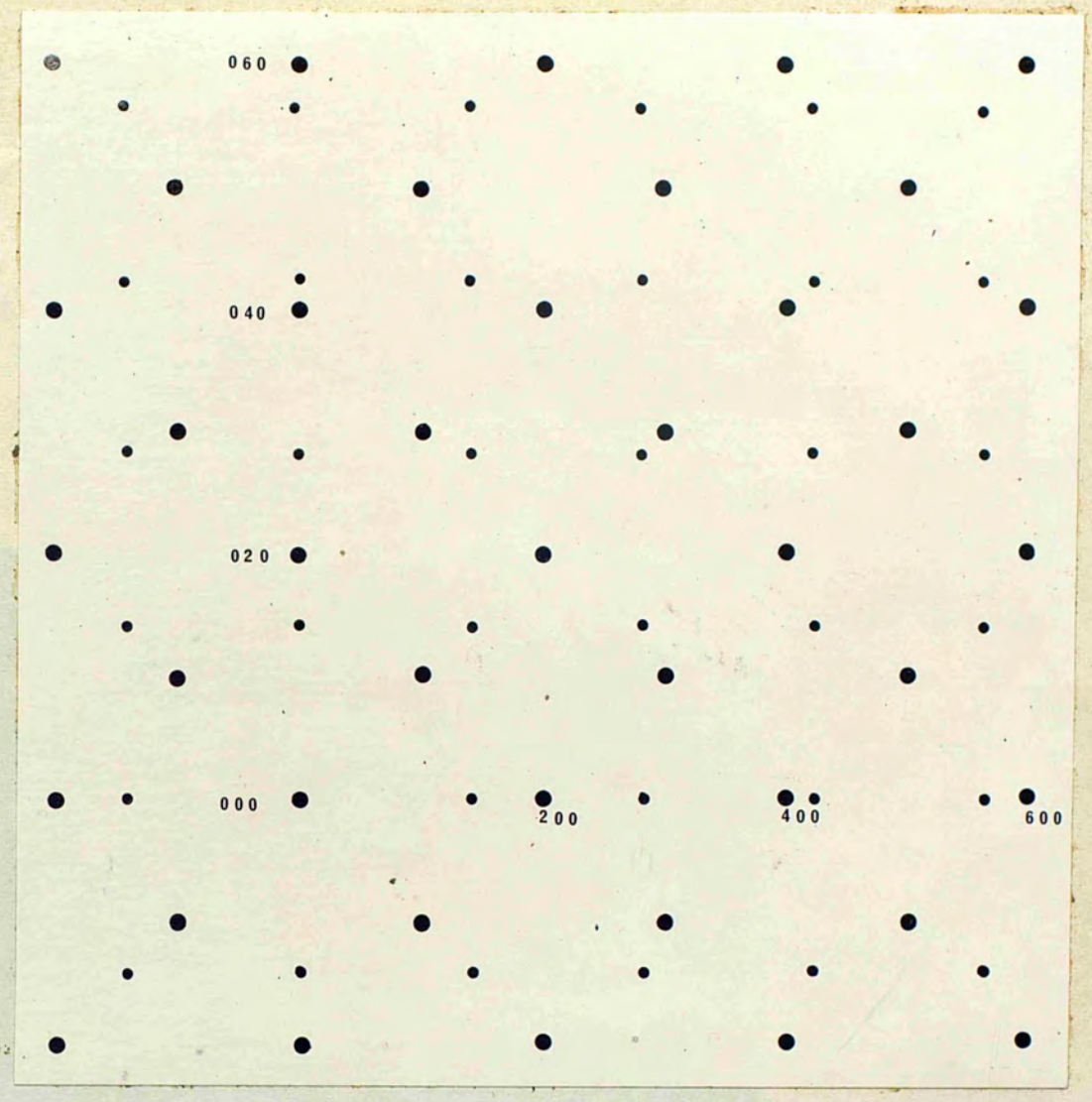

Fe (001) <100> || NaCl (001) < 100 >

Fe (001) < 110 > || NaCl (001) <100 >

Fig. 4.11

Reciprocal lattice of Fe with the double orientation.

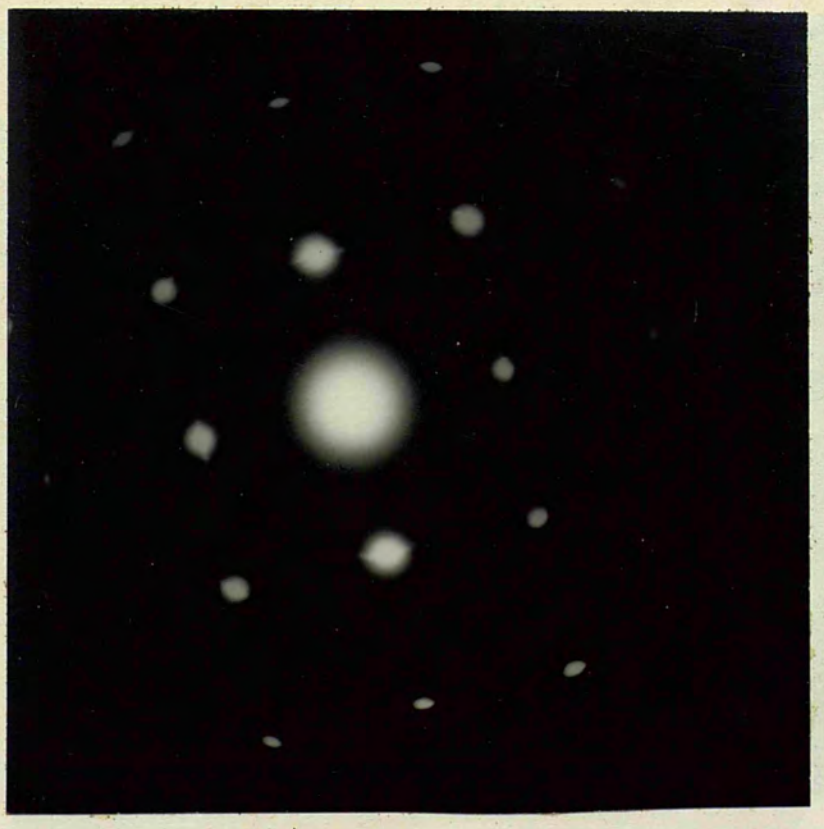

Fig 4.12

Diffraction pattern of a 300 A^{o} thick single crystal iron film.

Fig 4.13

Double diffraction and
(211) and (231) rings.

1) Fe (001) <100> || NaCl (001) <100>

2) Fe (001) <110> || NaCl (001) <100>

Besides these orientations, there exists very faint (211) and (231) type rings. These do not come out well in the print. The reciprocal lattice of the double orientations is shown in Fig 4.11. Even if the temperature is raised, the presence of (211) and (231) rings persists but their intensity decreases.

An attempt was made to separate the two orientations by varying the rate of deposition and the temperature of the substrate. It was found that to some extent, a film of iron is of single orientation when it is deposited at 320°C and at a rate of deposition 300 A° per minute. Fig 4.12 shows the diffraction pattern of such a film of thickness 400 A°. Fig 4.13 shows the diffraction pattern of another film of thickness 600 A° in which secondary diffraction occurs of the beams from the following planes (110); $(\bar{1}10)$; $(\bar{1}\bar{1}0)$; $(1\bar{1}0)$; (200); (020); $(\bar{2}00)$ and $(0\bar{2}0)$. In both the diffraction patterns rings due to (211) and (231) type planes are also quite visible.

Fig 4.14 shows the diffraction pattern of a film which is slightly oxidized. The fact that the intensity of the main diffraction spots is not uniform, suggests that the film is buckled. The main spots are due to the film with (001) plane parallel to the (001) plane of the rock salt and <100> direction of Fe parallel to that of <100>

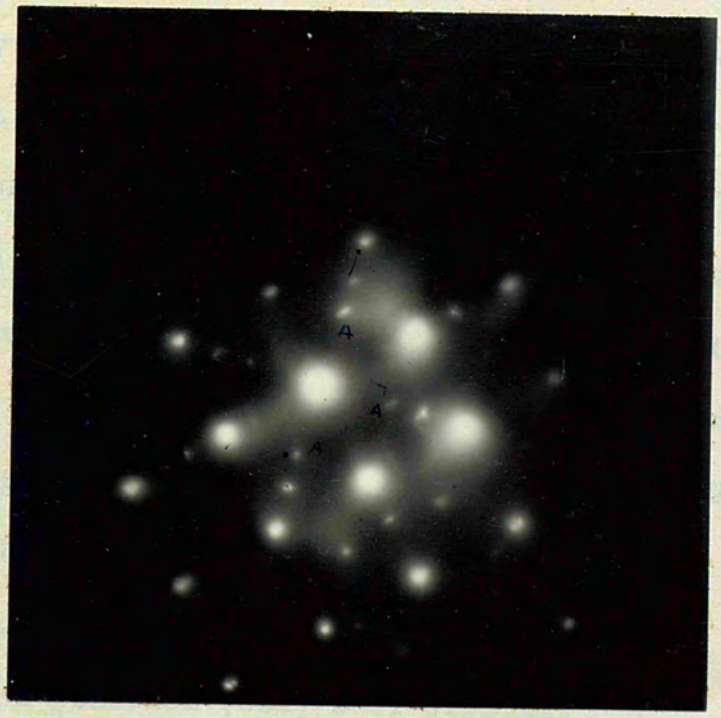

Fig. 4.14

Diffraction Pattern of Fe film
with Feo.

of the rock salt. The other spots can be explained on the basis of the double orientation with Fe (001) $\langle 110 \rangle \parallel$ to NaCl (001) $\langle 100 \rangle$. The spots marked A do not correspond to possible reflection from Fe. They are probably due to a thin film of FeO grown epitaxially on a single crystal iron film. Since the number of diffraction spots of FeO is very limited, hence it is very difficult to say in what stage the oxidation process is. It is possible that the film is in transition stage from body-centered of Fe crystal to the face-centered of FeO. Also, it is known that FeO (001) $\langle 110 \rangle$ grows epitaxially on Fe (001) $\langle 100 \rangle$ which is the right direction indicated by the spots. If these spots are indexed as (002) type and taking Fe as the caliberating standard, the lattice spacing of FeO comes out to be 4.1 ± 0.2 A°. X-ray value is 4.33A°.

iii) Iron on polished (001) NaCl crystal.

In the case of films deposited on polished and annealed (001) surfaces of the NaCl crystal, the diffraction spots follow the same pattern as that on the cleaved surface except that complete orientation occurs at 330°C and at a rate of deposition 300 A° per minute.

The films deposited on cleaved or polished (001) faces of rock salt, show strong diffraction spots parallel to the (001) plane and the $\langle 100 \rangle$ direction of the substrate. These films become free of the orientation (001) $\langle 110 \rangle$ Fe $\parallel$ (001) $\langle 100 \rangle$ NaCl at 330°C. The

spacing of iron deduced from this pattemis 2.86 $\pm$ 0.02 A° compared with X-ray value of 2.86 A°.

iv) Iron on cleaved NaBr (100).

Although the most usual form of orientation on NaBr (100) face is the same as that on other halides Fig 4.16 shows the diffraction pattern of a 200 A° thick film deposited at 320°C. It consists of the usual orientations:-

i) Fe (100) $\langle 001 \rangle$ // NaBr (100) $\langle 001 \rangle$.

ii) Fe (100) $\langle 011 \rangle$ // NaBr (100) $\langle 001 \rangle$.

together with

iii) Fe (110) $\langle 001 \rangle$ // NaBr (100) $\langle 001 \rangle$.

iv) Fe (110) $\langle \bar{1}10 \rangle$ // NaBr (100) $\langle 001 \rangle$.

The four orientations are superimposed in the appropriate directions in Fig 4.17, giving the possible diffraction spots in such a mixture of orientations.

v) Iron on cleaved KBr (100).

Fig 4.18 shows a typical diffraction pattern of iron on the (100) KBr face. The strong diffraction patterns are due to the Fe (001) $\langle 110 \rangle$ // KBr (001) $\langle 100 \rangle$. The thickness of the film was 240 A° and it was grown at 330°C. Usually there is no marked change in the diffraction pattern with the change in the temperature of the substrate and the rate of deposition.

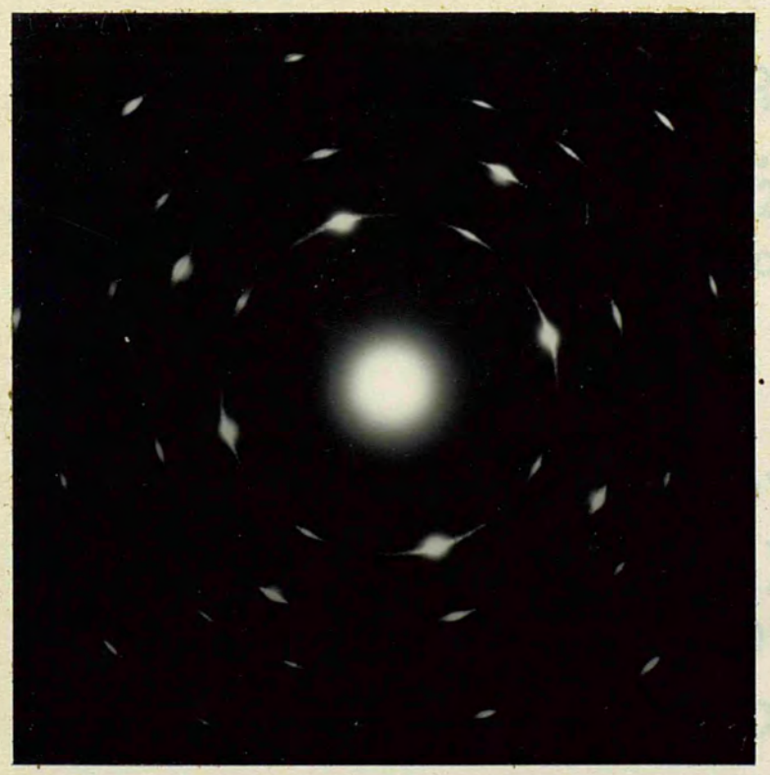

Fig. 4.16

Diffraction Pattern of Fe on (100) NaBr.

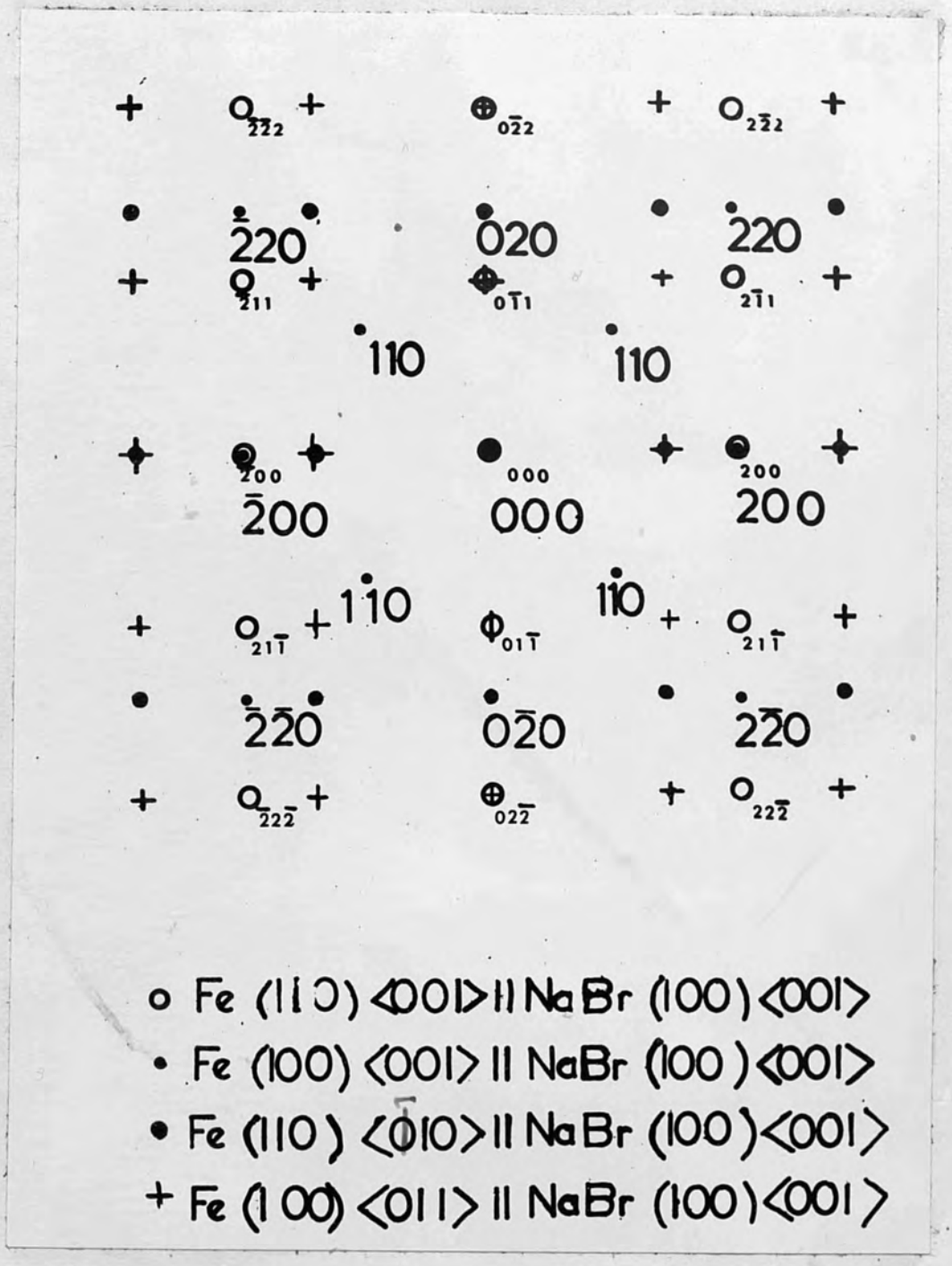

Fig. 4.17

Indexing of the spots of Fig (16) along with the other possible spots.

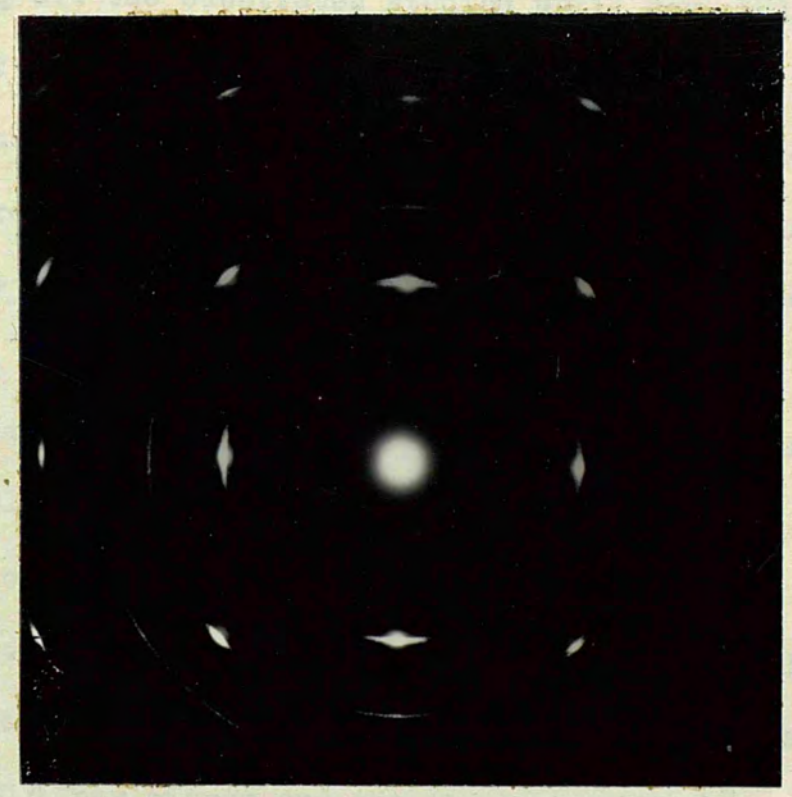

Fig 4.18

Diffraction pattern of (001) Fe on (100)KBr.

Fig 4.19 shows another diffraction pattern of (001) Fe on (001) KBr. Usually the double orientations are inclined to each other at 45° but in this case they are inclined at 30° to each other.

vi) Iron on cleaved KCl (001).

Among all the substrates studied uptil now, KCl is the most promising for obtaining a single orientation film. The film grown at 300°C and at a rate of 200 A° per minute, was single crystal with a slight presence of a second orientation. On raising the temperature of the substrate to 330°C and rate of deposition to 300 A° per minute, the films obtained were completely single crystal (Fig 4.20). The orientation of the film with respect to the substrate is (001) Fe $\langle 110 \rangle \| (001)$ KCl $\langle 100 \rangle$.

vii) Iron on (110) face of NaCl.

Fig 4.21 shows the diffraction pattern of Fe film deposited on (110) polished face of NaCl at 320°C. The rate of deposition of the film was 300 A° per minute and the thickness 400 A°. It is interesting to note that Fe (111) $\langle \bar{1}10 \rangle$ is parallel to NaCl (110) $\langle 001 \rangle$ (Collins and Heavens L.C.).

viii) Conclusion.

Films of iron have been epitaxially grown on cleavage faces of NaCl, KBr, KCl and NaBr and on polished (100) and (110) faces of rock salt. Separated nuclei are formed in the early stages of growth and complete continuity is not achieved until 400 A° mean thickness is reached. The films are thus not strictly 'single crystal' below this

Fig. 4.19

Diffraction pattern of (001) Fe on (001) KBr.

Fig 4.20

(001) Fe <110> || (001) KCl <100>

Fig 4.21

(111) Fe on (011) NaCl.

thickness and the crystallite size in the intermediate stages can vary considerably even for films of equal thickness grown under apparently identical conditions. The crystallite shape in discontinuous (110) films also displays a characteristic elongation.

NaCl and KCl are the substrates on which films of single orientations can be achieved. In the case of NaCl, the <001> direction of the iron film is parallel to <001> NaCl. Whereas in the case of KCl, <001> Fe is parallel to <110> KCl.

4.4. Comparison of Air- and Vacuum- cleaved surfaces.

i) Introduction.

Among the important factors in the epitaxial growth of metals on cleaved surfaces of ionic crystals, cleanliness of surface and surface features play an important part. The orientation of the initial nuclei on the surface depends largely on the features of the surface and on the surface mobility of the initial nuclei. The mobility may be affected by adsorbed gases on the surface. The following cases are considered:

1) Air cleaved surfaces
2) Vacuum cleaved followed by exposure to air
3) Vacuum cleaved surfaces

ii) Air-cleaved Surfaces.

The surface features depend on stresses produced in a crystal. All crystals are cleaved in the same way as described in Chapter 3.

Although the various specimens exhibit the same general features, there are some differences of detail.

Fig 4.22 shows the phase contrast micrograph of KI air-cleaved crystal. The cleaved steps flow unidirectionally in a parallel fashion. Since KI absorbs moisture very readily, the appearance of etch figures is quite prominent along these cleaved lines. Etching sometimes makes the cleavage angular.

Figs 4.23 and 4.24 show the general features of the air-cleaved surface. The features are revealed by decoration (see section 4.5) by iron nuclei. Usually these cleavage lines are curved but they flow in parallel directions and form channels. In Fig 4.24 the cleavage is concentrated in a bunch and from it the other cleavage lines spread over the surface.

iii) Vacuum-cleaved and exposed-to-air surfaces.

The KI crystal is fixed in the holder in the vacuum chamber, its temperature is raised to the required value and, when the pressure of the chamber is 10^{-5} m.m. Hg., then the crystal is cleaved. After the crystal has cooled down to room temperature, it is then exposed to atmosphere by letting air into the chamber. It is then pumped down to 10^{-5} m.m. Hg. The iron film and a carbon film are then deposited on the cleaved surface.

Fig 4.25 shows the surface features of a KI crystal which was heated to $70^{\circ}C$. The cleavage lines are parallel to each other. In the middle of the figure, the structure gives a general impression of

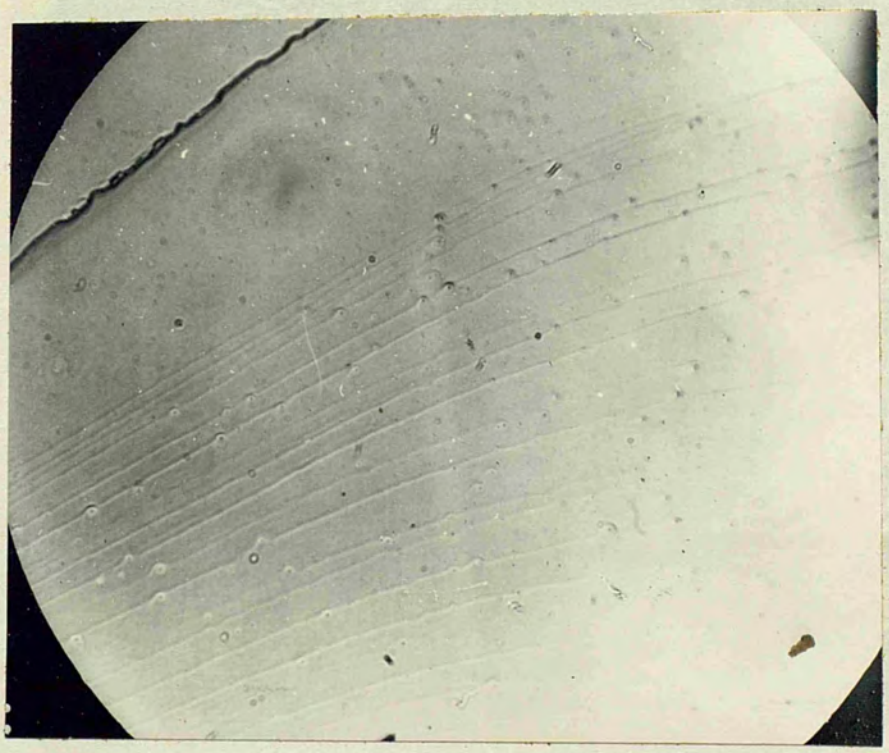

Fig 4.22
X300

Phase-contrast micrograph of (001) KI air-cleaved surface.

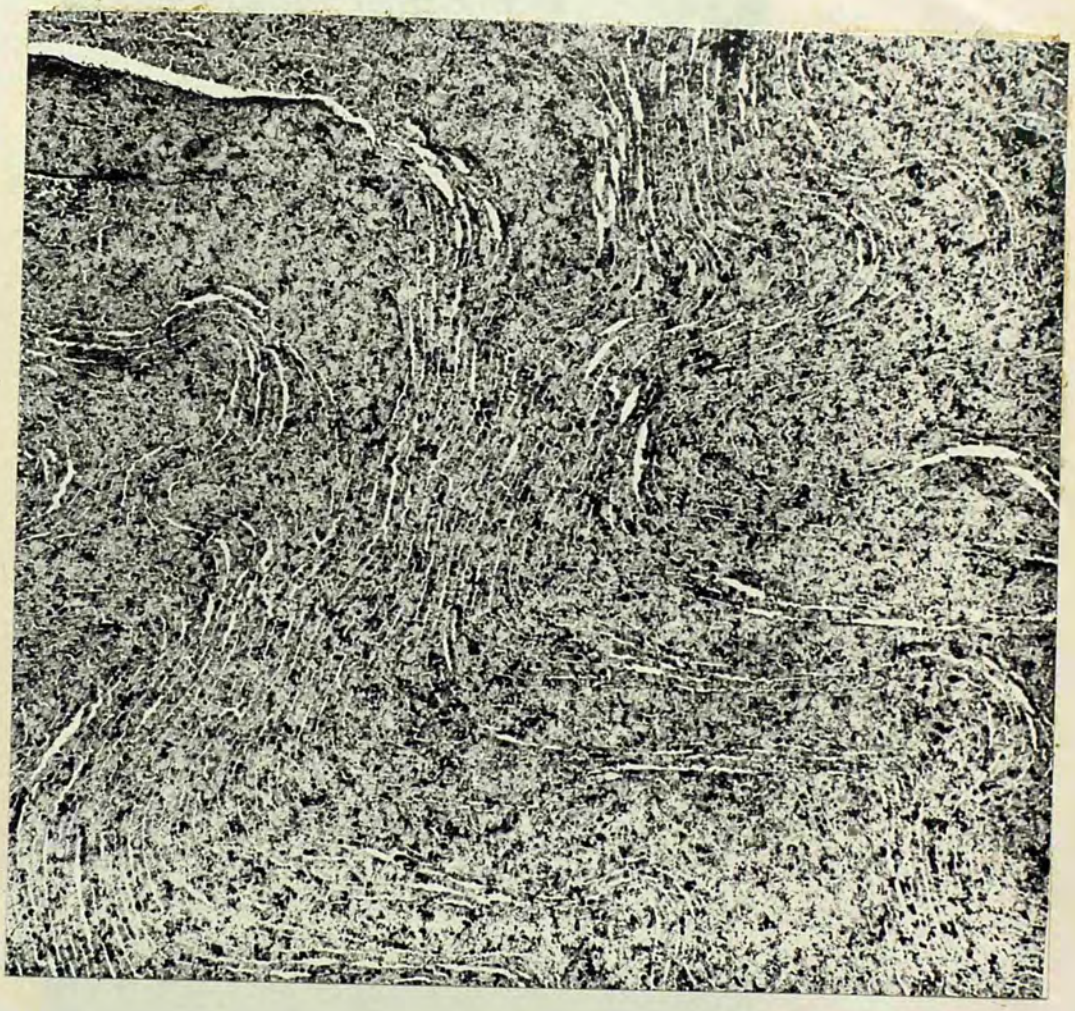

Fig. 4.23
X10,000

Decoration of (001)KI air cleaved surface at 250°C.

Fig 4.24
X9,000

Decoration features on KI (001) air cleaved surface at 70°C.

Fig. 4.25
X8,000

Surface features of KI at 70°C.

parallel lines and the distance between them is about 1μ. On closer examination, the cleavage lines do not appear continuous but are seen to consist of zig zag and rectangular features which have two sides parallel to each other.

Fig 4.26 shows the surface features of a crystal under the same conditions. The cleavages follow the same direction but sometimes turn through a right angle. After a further distance of about 1μ they again turn at right angles and thus follow the original direction.

As the temperature of the surface is raised above 70°C, the general features of the surface remains the same. At about 100°C the surface generally shows linear features (Fig. 4.27) but here and there etch features appear. The etching is quite pronounced along the steps. Due to shadowing by carbon, these steps are well revealed. The height of the steps is about 400 A° and the maximum length about 5,000 A°. In between the steps, there appear etch figures which are of square and rectangular in shape. They join together and form lines parallel to the prominent cleavage lines.

The temperature of the crystal surface is raised to 120°C. Here, as is evident from Fig. 4.28, the surface is slightly etched along the cleavage line, thus showing the micro-features along the edges. There is also some evidence of the rough surface covered with micro-etch figures. Fig. 4.29, 4.30, show some etch figures which are

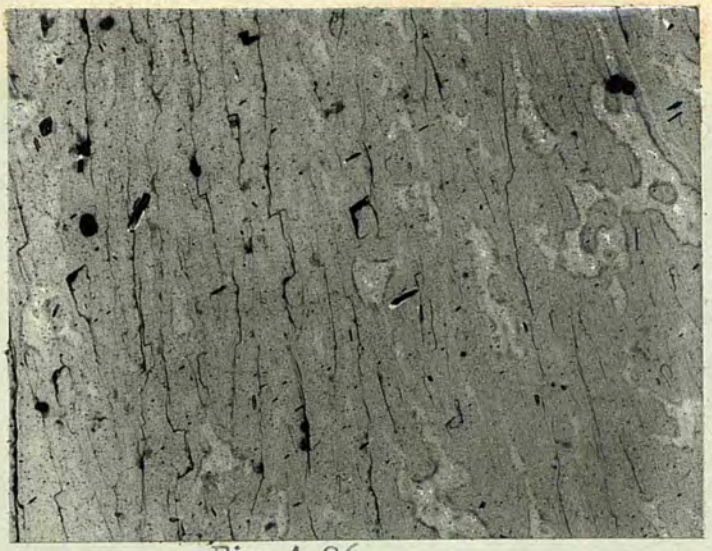

Fig 4.26
X5,300

Cleavage lines twining at right angles.

Fig 4.27 (a)

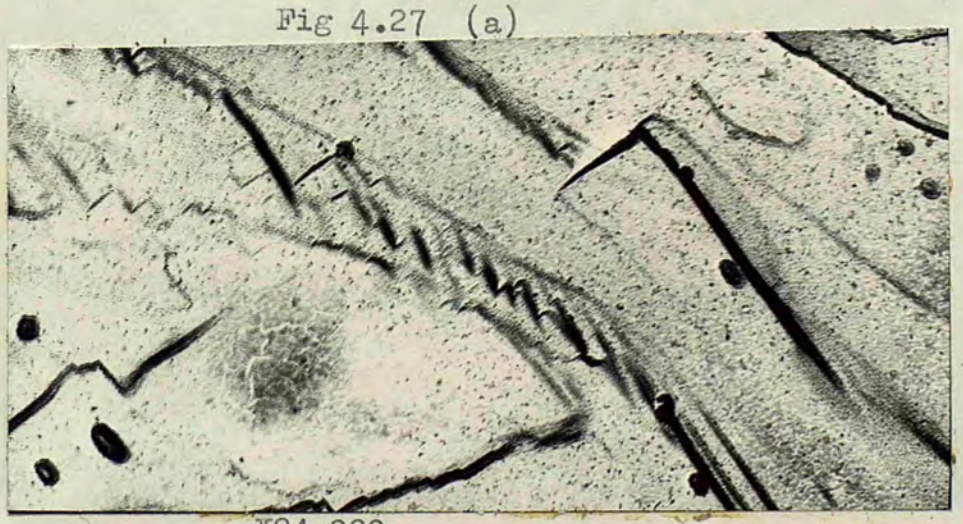

X24,000

Start of etch figures at 100°C on (100) KI.

Fig 4.28
X24,000

Etching along cleavage lines

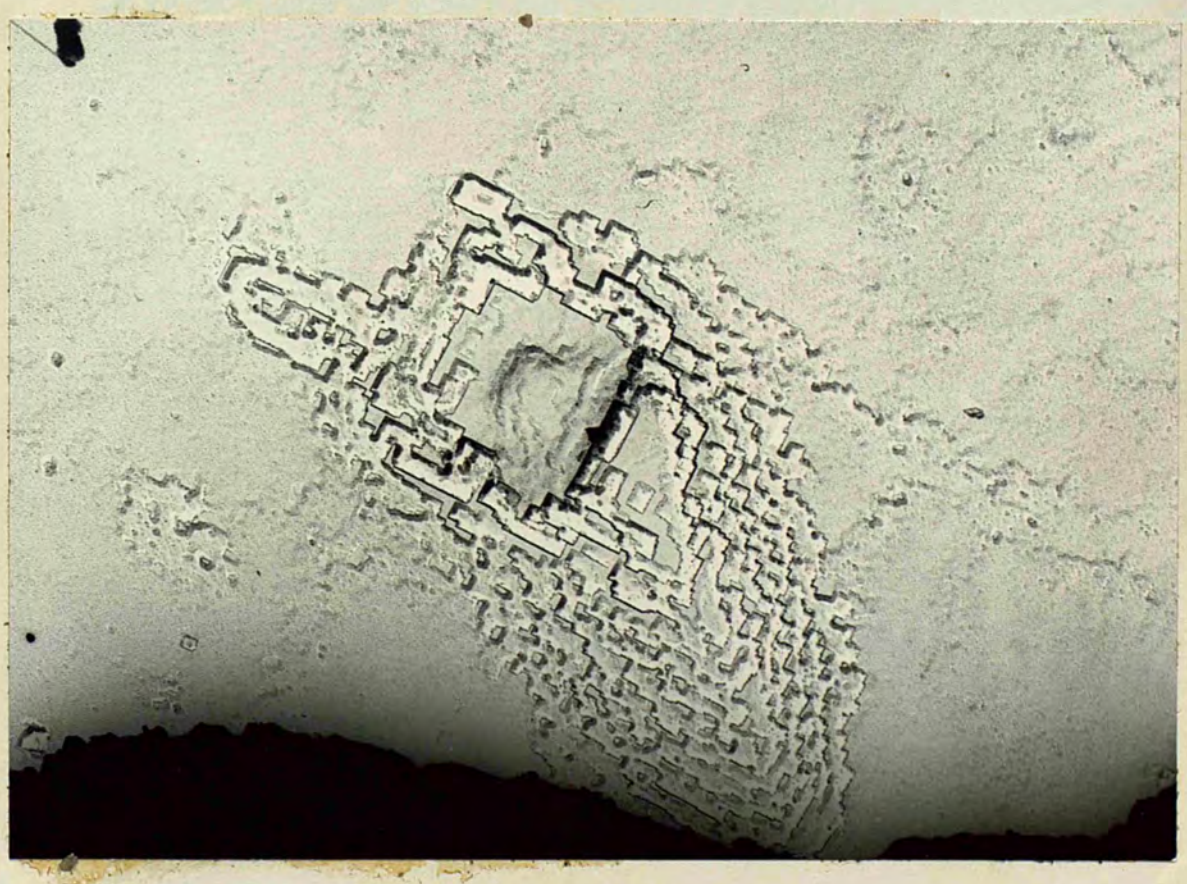

Fig 4.29
X3,000

Etch Pyramids.

Fig 4.30
X10,600

Etch figure.

not formed at the cleavage edges but are on the plane in between the cleavages, showing that etch figures may be formed on the so called atomically flat surfaces due either to impurities in the crystal or to dislocations which act as nuclei for etching. Fig 4.31 shows an etched cleavage line. On the junction of the cleavage line, there is a square etch figure of 1 square micron in area. This is a pyramid with the steps rising and in the middle, the surface appears to be at the same height as the plane away from the steps. It seems also that etching is more prominent along one cleavage line than perpendicular to it. This is probably due to the fact that the cleavage line in one direction is more marked than that in the other. This study of the surfaces of the substrate cleaved in vacuum and exposed to atmosphere shows that the surfaces are rather rough than is generally thought to be the case.

iv) Vacuum-cleaved Surfaces.

Since the features of a surface are dependent on the way the crystal is cleaved, two pieces of KI crystal, from the same crystal are cut, and cleaved at the same time. While on one, iron is deposited during cleaving, the other is kept covered and subsequently exposed to atmosphere.

Fig. 4.32 represents a vacuum cleaved surface at room temperature. The cleavage lines are formed by small steps. The dimensions of

Fig 4.31
X10600

Etching along the cleavage lines.

Fig 4.32
X32,000

Vacuum cleaved (001) KI surface.

these steps are very small compared either to an air-cleaved surface or to one vacuum cleaved and exposed to atmosphere. From these small steps, curved stairs come out. These seem to be the result of conchoidal fracture. These are usually either on the left or right of the cleavage line but never on both sides. As indicated by the shadowing effect, these rise step by step until a plateau is formed and then again these stairs start decreasing in height. This sequence takes place if one is scanning the figure from top to bottom. The big black crystallites may be the result of sudden arcing of carbon or be due to small KI crystallites left on the surface after cleaving.

Fig 4.33 shows a film prepared under the same conditions except that it was deposited at 120°C. The general features of the surface remain unchanged. The blotches on the surface indicate that the crystallites have failed to float off from the substrate. There is also no evidence of etching at this temperature. KI crystals are hygroscopic. It is possible that when they are cleaved in vacuum and the film is deposited, etching by water vapour is prevented.

v) Conclusion.

The vacuum-cleaved surface of KI is featureless as compared to the air-cleaved surface or that vacuum-cleaved and exposed to air. The vacuum cleaved surfaces are more resistant to etching than the other surfaces.

Fig 4.33
X14,500

Vacuum cleaved surface at 120°C.

4.5. Decoration features of air- and vacuum-cleaved crystals.

i) Decoration by gold.

Effects similar to the decoration of steps and slip plane edges on cleavage faces of crystals with thin deposits of gold reported by Bassett[1] 1958 and Sella[7] etal 1958, have also been observed with iron films vacuum evaporated on (100) cleavage faces of KI (Figs. 4,23,24). Before it could be decided whether this is a decoration feature or due to magnetic effect, it was felt to be advisable to examine some gold films.

The pattern of the steps on cleaved KI surface are revealed only when the mean thickness of the gold film is less than 30 A°. At this stage, the size of the crystallites increases, their density decreases and thus they fail to show up the features of the surface. Fig 4.34 shows the decoration features of the (100) KI surface. The mean thickness of the film is about 10 A°. The crystallite size is 60 A° but at certain points the crystallite size is far greater i.e. 500 A°. These sites are point defects which are scattered all over the surface but they appear to be more pronounced along the cleavage lines which are made up of small stairs.

As it is evident from Fig 4.34 the steps act, in general, as preferred nucleation sites and a greater density of nuclei on these regions is to be expected. The spacing between the nuclei is also smaller. The increasein size of the nuclei can be affected both

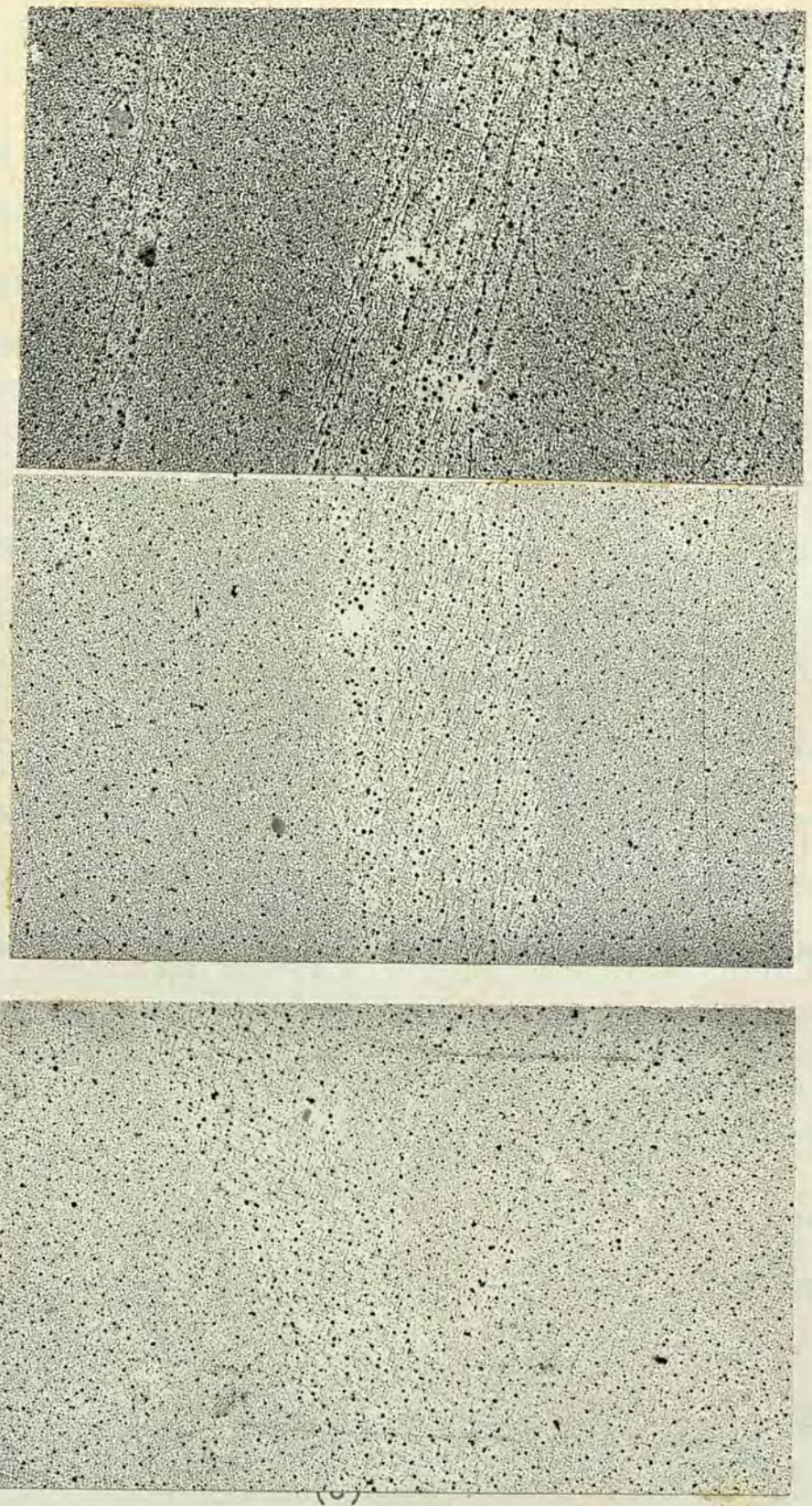

a

b

c

Fig 4.34
X15,000
Decoration of (001) KI surface by gold nuclei.

by the receipt of new deposit atoms, and by receipt from neighbouring nuclei which eventually disappear. It seems that in the very beginning both processes may occur but as the thickness increases, one process may dominate.

In the case of gold, Bassett[1] (1958) has shown that the nuclei formed along the terminal step of a cleavage 'stair-case', i.e. the step adjoining a flat region of a crystal, are intermediate in size between nuclei formed on the flat crystal and in the centre of the cleavage step. This is because the mobility of the gold on the crystal surface permits this terminal step to draw upon mobile material on the flat surface on one side of the step.

Bassett has calculated the critical distance gold nuclei can migrate by considering the distance between the wandering steps and the size of the nuclei in between them. When two such steps are at a greater distance than 200 A°, nuclei form with a density and size corresponding to the flat regions of the crystal. As the steps get closer together than about 200 A°, all arriving gold is able to migrate to the nucleating sites along the step edges. This effect is not well marked in Fig 4.34. The reason is that the distance between micro-steps on the stair case is greater than 1000 A°. Hence the crystallite size is the same as that on the flat surface of the crystal. As is shown above, the increase in the size of the nuclei is due to the

migration of the small nuclei to the larger ones, the size of the nuclei increasing and the number of nuclei decreasing as the thickness of the film increases. This results in a lack of resolution of the decoration patterns at low coverage.

ii) Decoration by iron.

To study the decoration of the KI cleaved crystal by iron, several specimens of various thicknesses were prepared. Surprisingly enough no decoration features were observed in vacuum cleaved and vacuum deposited crystals nor in the case where the thickness of the film was greater than 100 A^{o}.

Fig 4.35 shows the general features of an iron film of thickness 20 A^{o} at 250^{o}C on KI air-cleaved surface. Heavily decorated parallel cleavage lines are 3000 A^{o} apart but there are lightly decorated features in between. From the general impression of this figure it appears that the cleavage lines are curved. In fact, they are formed by micro-angular cleavage lines which are usually at right angles to each other as shown in three dimensional Fig 4.36. Heavy black lines indicate the accumulation of crystallites along the edges of the steps.

Fig. 4.37 a,b,c show the micro-cleavage lines perpendicular to each other. Fig 4.37 a, shows a small shell shaped feature, made up of minute perpendicular cleavage lines. In Fig 4.37 b,c, this feature

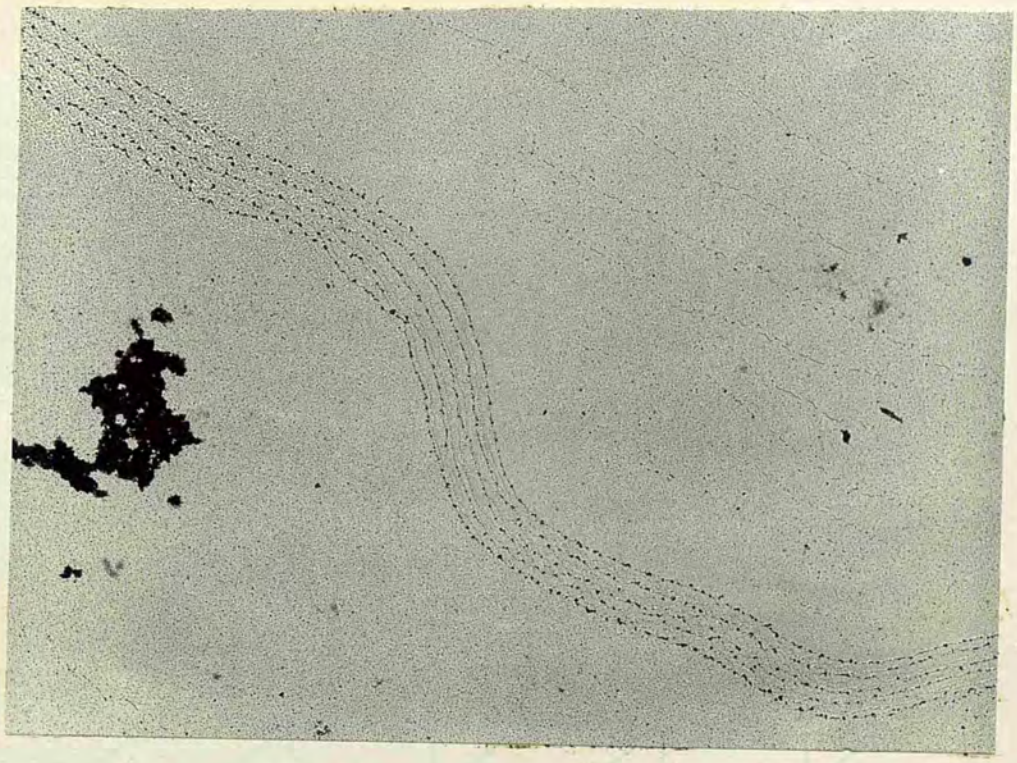

X10,000

(a)

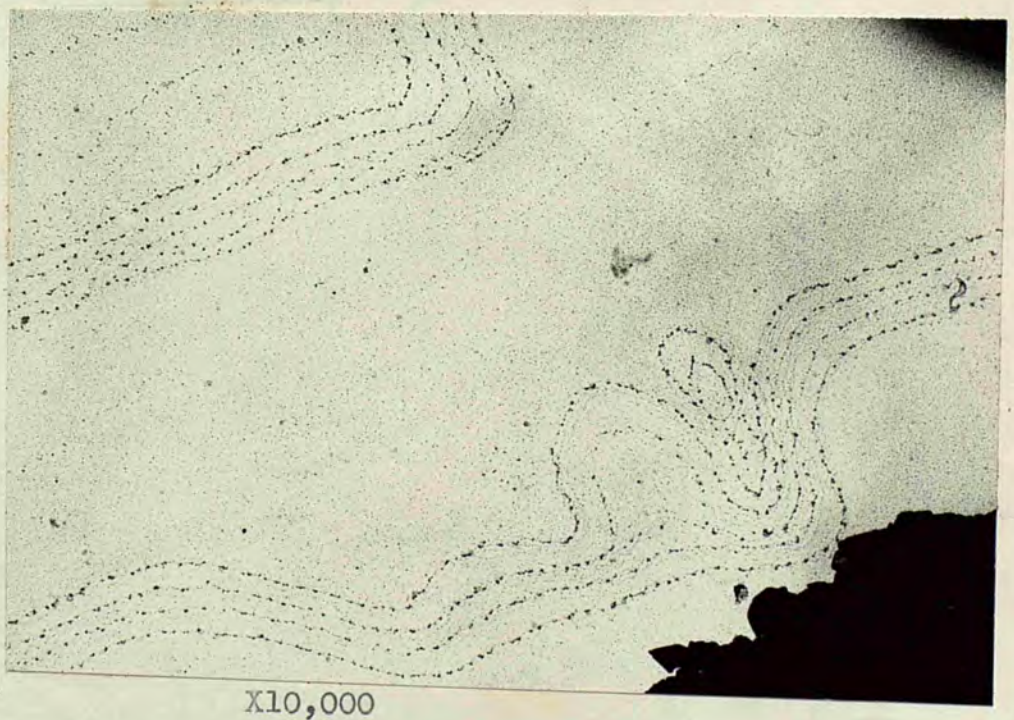

X10,000

(b)

Fig 4.35

Decoration features on air cleaved surface.

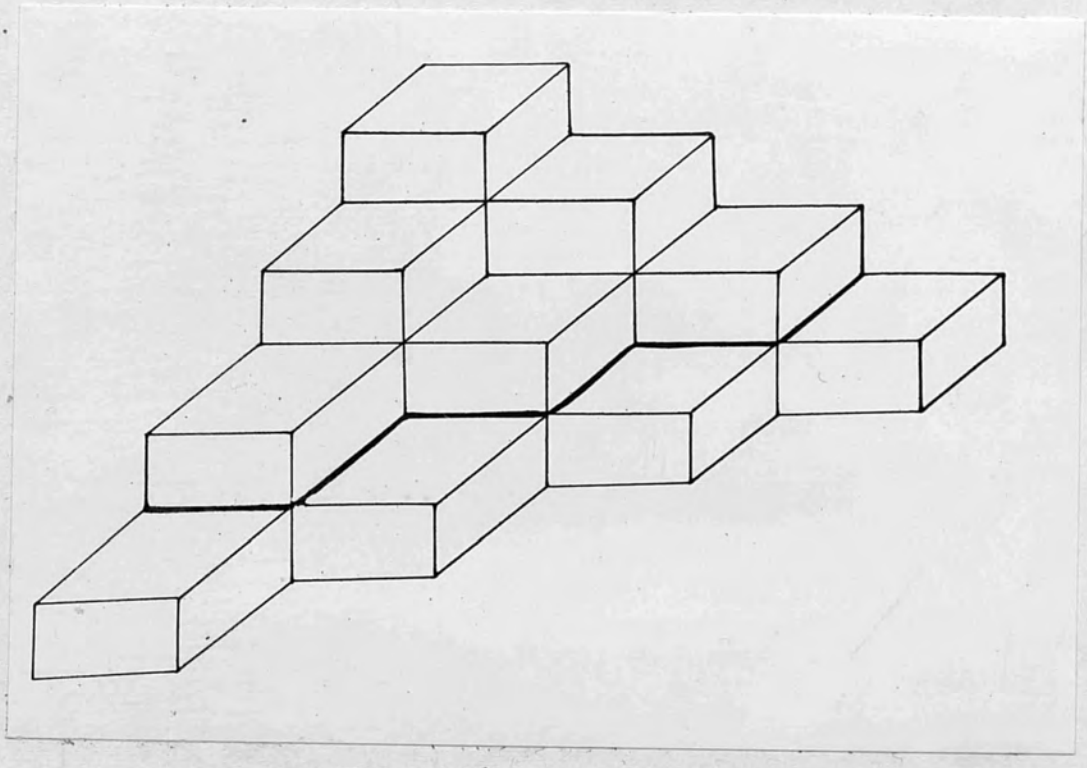

Fig 4.36

Steps on (100) surface.

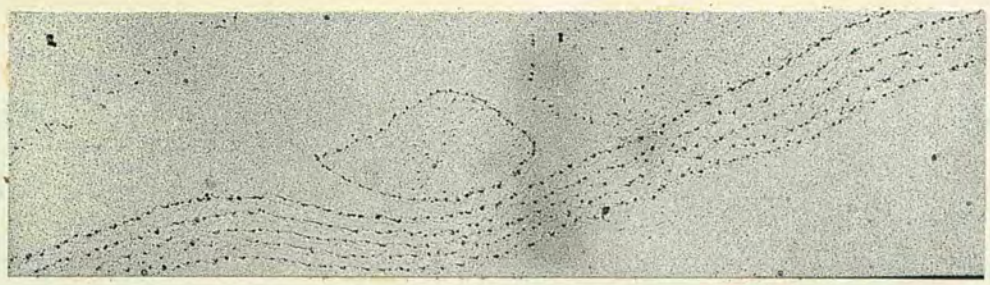

(a)

(b)

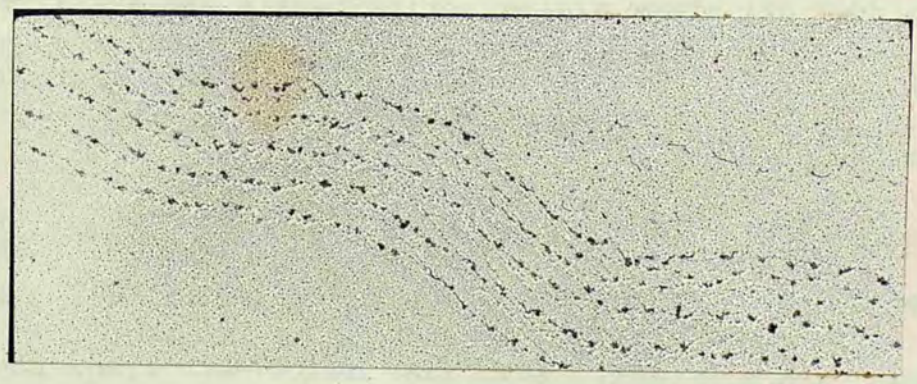

(c)

X24,000

Fig 4.37

Micro-cleavage lines are perpendicular to each other.

is obvious on the cleavage lines. There seem to be two kinds of crystallite accumulation - in one case all the crystallites align together at the edge of the cleavage line and in the other, the crystallites form a bunch. In front of the first kind of accumulation, there is space devoid of crystallites. At the most, this space is 200 A° in width. This, most probably, arises from the large mobility of the iron crystallites at 250°C. Presumably, they obtain energy from the substrate to travel such a long distance. The crystallite size is large as compared to that on the plane surface.

Fig 4.38 a,b,c represents the clustering phenomenon of the iron nuclei. The crystallites join together in a haphazard way. It is likely that these are either at the points where the etching has just started or at point defects, which due to the large mobility of iron nuclei at this temperature are able to attract a large number of nuclei. The points, which are indicated by letter A, are the part of the film where there is a lot of clustering. These are circular in shape and their dimensions vary from 0.5 μ to 1 μ. In Fig 4.38c the crystallites join together and form a chain. These features do not show up at all in films which are deposited at lower temperatures. Most probably, the mobility of the iron crystallites is very small and they thus fail to cluster together in this fashion.

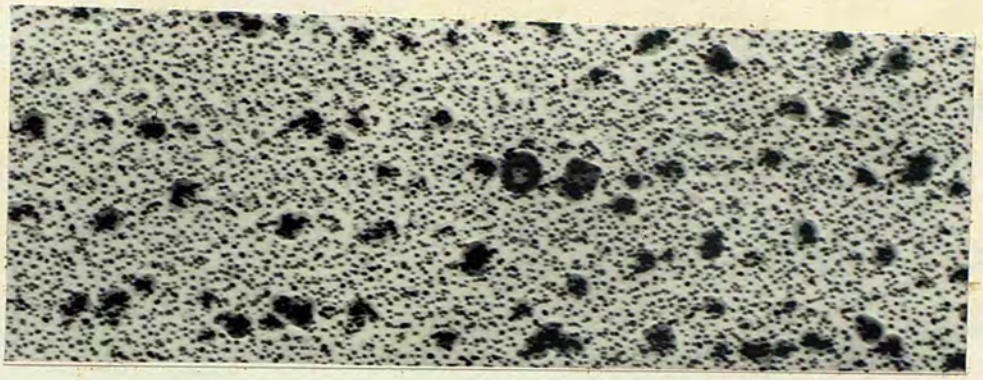

(a)

(b)

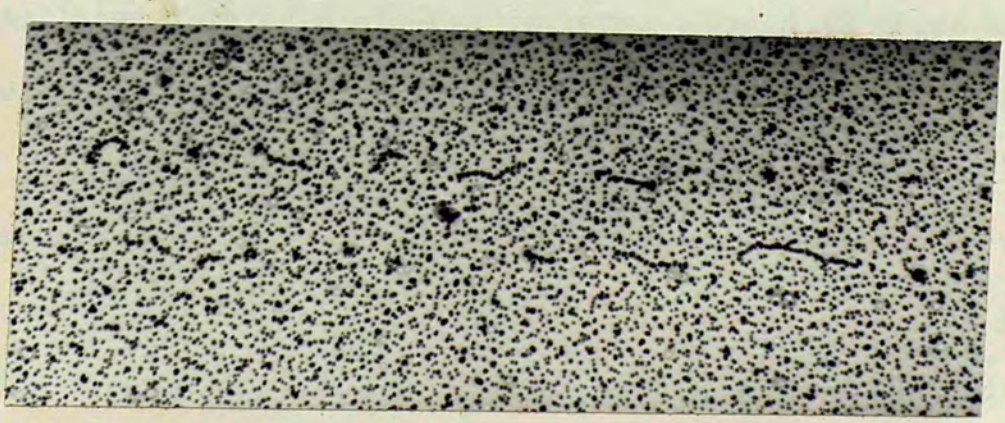

(c)

X32,000

Fig 4.38

Clustering of iron nuclei.

Figs. 4.24, 39 show the general features of a film deposited on an air-cleaved surface at 70°C. The thickness of the film is 90 A°. This is really an extreme case where the surface is heavily and wildly decorated by iron. Bassett (L.C.) studied the decoration patterns close to a scratch made on NaCl crystal surface. There the surface is covered with curved parallel cleavage lines and also by zig-zag cleavage lines which are normally absent from a strain-free surface. From this it appears that the crystal is deformed plastically and on cleaving, instead of producing parallel steps, it has produced edges which intersect the cleavage lines.

Fig 4.40 shows another part of the surface of KI crystal. It consists of bunches of parallel cleavage line. Between four and six cleavage lines cover a space of 0.1 μ to 0.2 μ. In between these cleavage bands there is a space of 0.05 μ left which is covered by crystallites forming a zig-zag pattern. Fig 4.42 shows besides the above mentioned features, a well defined series of concentric circles with ordered and disordered crystallites in alternate bands. It's maximum diameter is 1 μ. Such well defined circles are not seen on any other part of this film or on any other film. This, probably, might be the result of some foreign body included in the crystal which is accidently exposed by cleaving.

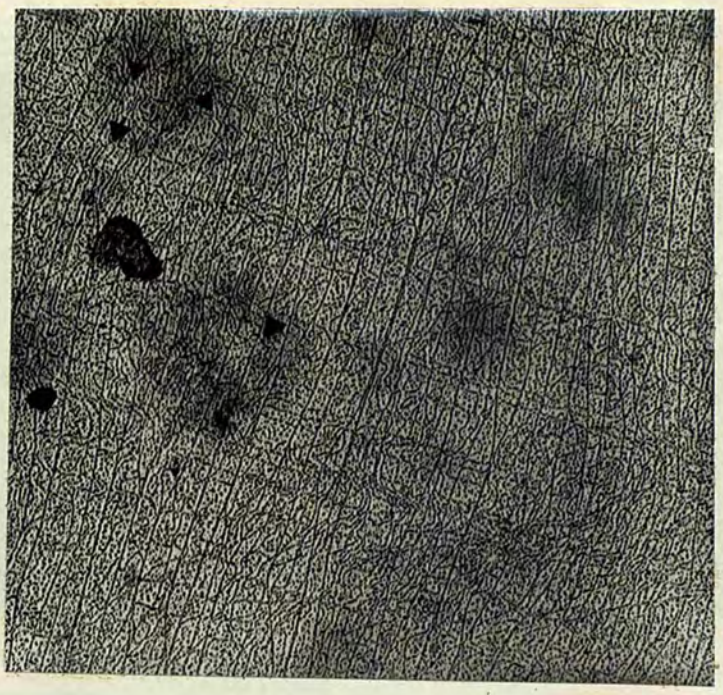

Fig 4.39
X16,000

Decoration of a KI (100) face at 70°C.

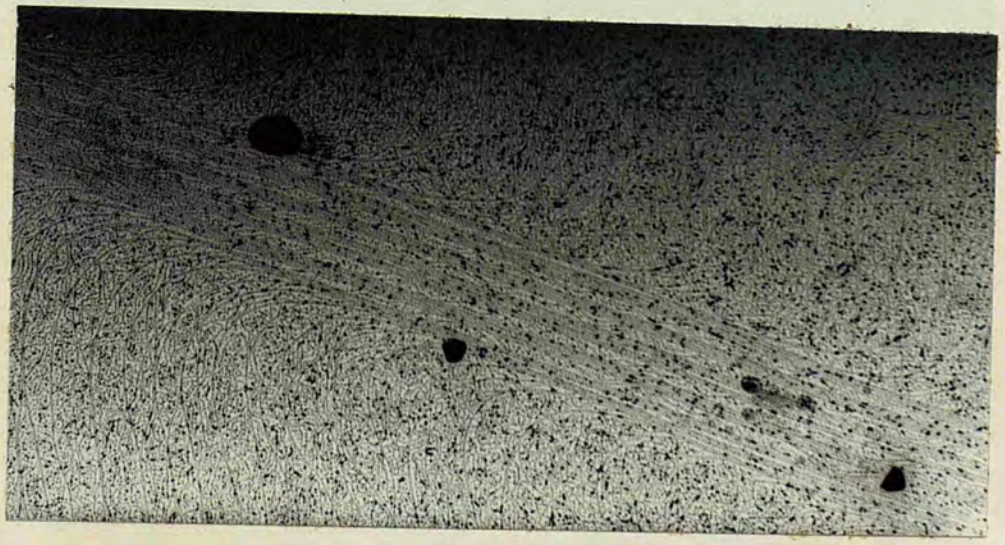

Fig 4.40
X14,500

Parallel cleavage line bunches.

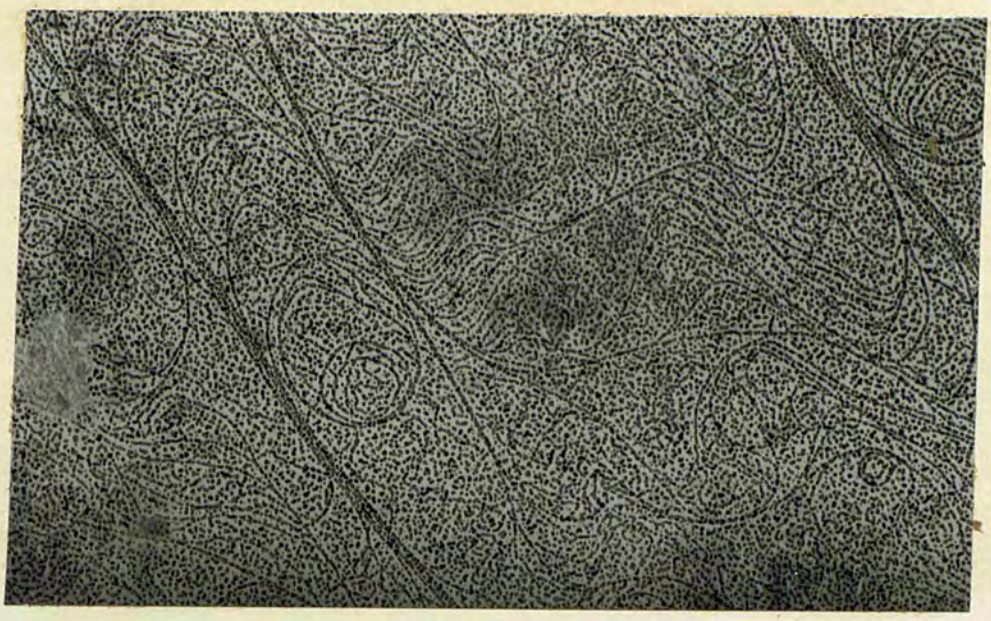

X26,000
(a)

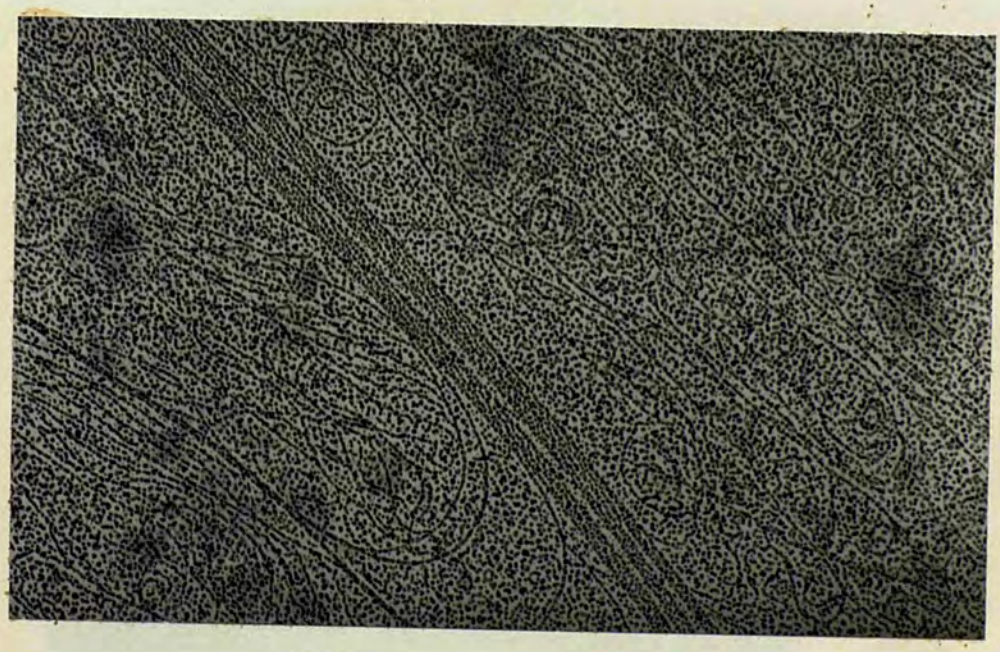

X26,000
(b)

Fig 4.41
Abundance of circular features.

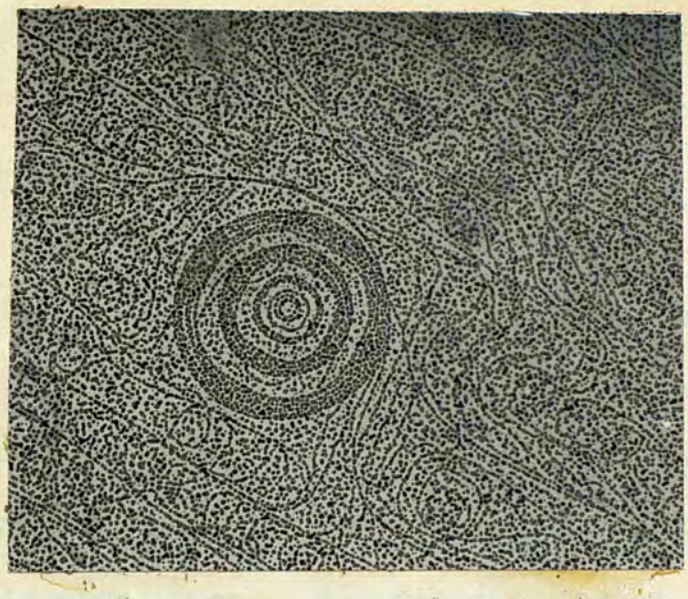

X26,000

Fig 4.42

A unique circular feature.

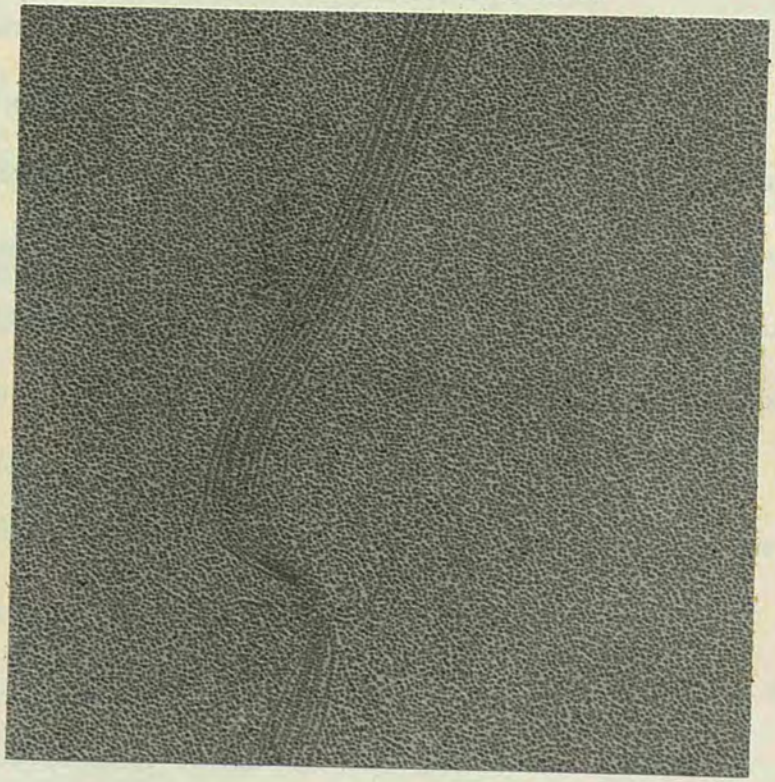

Fig 4.43

Decoration feature on vacuum cleaved and exposed to air surface.

Fig 4.43 shows the decoration features on a vacuum cleaved and exposed to air surface. The film thickness is 80 A^{o} and is deposited at 80°C. The decoration features consist of parallel cleavage lines which bend at right angles and converge on a point and then diverge into a parallel cleavage line following the original direction. At the point of convergence, there are circles tangential to the decorated cleavage lines. Besides this slight decoration, the whole surface appears featureless. Similarly, other crystals surfaces were devoid of decoration except those which had become etched. Here the iron crystallites accumulate at the edges of the cleavage as shown in Fig 4.44.

Similarly, the surface decoration of vacuum cleaved KI crystals was studied. In all the specimens which were prepared under identical conditions as those on air-cleaved and vacuum cleaved exposed to air surfaces, there did not seem to be any indication of decoration.

iii) Theory of decoration.

From the study of decoration of KI by iron crystallites, the following conclusions can be drawn.

i) the density of the crystallites along the cleavage edges is greater than those on the plane surface.

ii) when the temperature of the surface is below 100°C, the size of the crystallites along the cleavage edges is the same as that on the plane surface, but with rise in temperature, it increases along the edges.

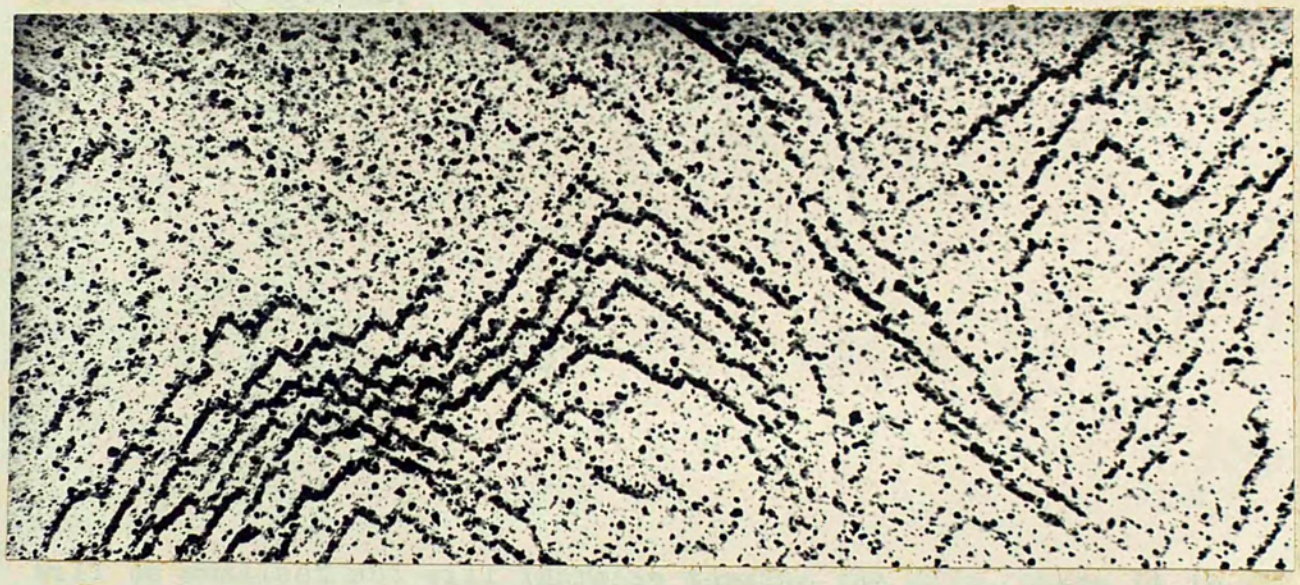

X32,000

Fig 4.44
Decoration of etched surface.

iii) the decoration by iron crystallites persists to greater thickness, i.e. upto 100 A^{0}, as compared to gold which is discernable only at thicknesses below 20 $A.^{0}$

It is an established fact that the initial nucleation of the crystallites occurs at cleavage lines and point defects. Afterwards, the increase in the size of the crystallite can take place by the following processes.

i) the loss of atoms from the smaller nuclei to the larger.

ii) migration of the atoms across the substrate.

iii) accretion by the newly arrived atoms.

The difference in the gold and the iron decoration can be explained by basing the argument on the crystallite growth. In the case of gold, the crystallite size increases by merging of small nuclei with the bigger. So in the middle of a 'stair' pattern, the size of nuclei will be smallest and will increase towards the edge, where it is intermediate, and is largest on the plane between the cleavage lines. Now as the thickness increases, the smaller nuclei will merge with the bigger nuclei and also smaller ones will join together. Hence the resolution of decoration vanishes at small coverage. On the other hand, the mobility of the iron crystallites is small at low temperature and their size does not increase at the expense of the smaller crystallites. Their size actually increases by accretion of

the arriving atoms. This leads to the conclusion that the crystallite will be of uniform size on the plane as well as on the cleavage stair case, since the probability of receiving iron from the source is the same at all points on the surface. With higher surface temperature, the surface mobility of the iron crystallites increases, resulting in the accumulation of crystallites along the edges and leaving the surface infront sometimes completely devoid of crystallites. This lower mobility of the iron crystallites on KI substrate compared with gold explains the persistence of the decoration patterns at higher thicknesses as compared to gold.

iv) Conclusion.

To study the surface features, by decoration techniques, it seems essential that metals of small mobility for the corresponding surface should be used, as under this condition thickness control is not very critical. Hence iron, nickel, iron-nickel alloy are preferred for the study of halide surfaces.

4.6. Comparison of Epitaxy on air- and vacuum cleaved crystals.

i) Introduction.

Sella etal [8] (1963), studied the growth of metallic films on the vacuum cleaved crystals, and concluded that the epitaxial temperature is systematically lower than that on the air-cleaved crystals. A study of the epitaxial growth of iron on the air- and vacuum-cleaved

crystals was made, more emphasis being laid on the structure, crystal size, the mechanism of nucleation and growth of the film.

ii) Study of Diffraction patterns on the air- and vacuum cleaved surfaces.

Fig 4.45 shows the diffraction pattern of a 40 A^{o} thick film at room temperature grown on air-cleaved surface. It is completely polycrystalline. The rings are diffused showing that the crystallite size is quite small. Fig. 4.46 shows the diffraction pattern of a similar film grown on vacuum cleaved crystal. The rings are sharper and more intense than that of the film on air-cleaved surface, indicating that the crystallite size is larger than the previous one. There is also a slight indication of double orientation.

As the temperature of the substrate is raised, the crystallites also tend to orient themselves. Fig 4.47, 48 show the difference in orientation at 70°C when the thickness of the film is about 75 A^{o}. There is a marked orientation of the crystallites on the vacuum cleaved crystals as compared to the air cleaved crystals. Because of the limitation of the heater, the temperature of the substrate surface is not raised above 120°C. Although the orientation of the crystallites on vacuum cleaved surface improves, the hazard of etching of the surface arises with rise in temperature, causing the surface to become very irregular. It is clear that a very inhomogeneous nucleation and a very high micro-relief will lead to iron films of

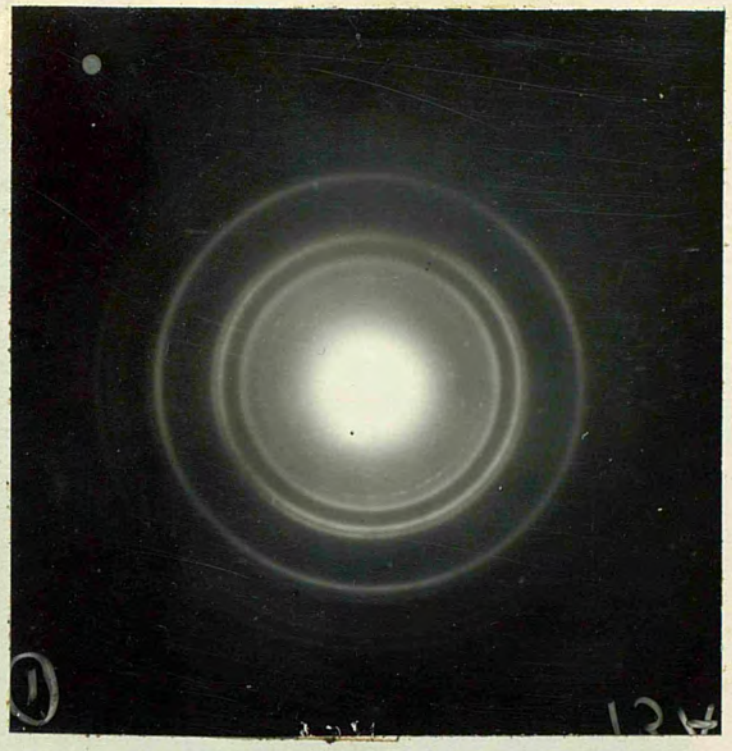

Fig 4.45

Diffraction pattern of 40 A° thick iron film deposited at 20°C on air cleaved substrate.

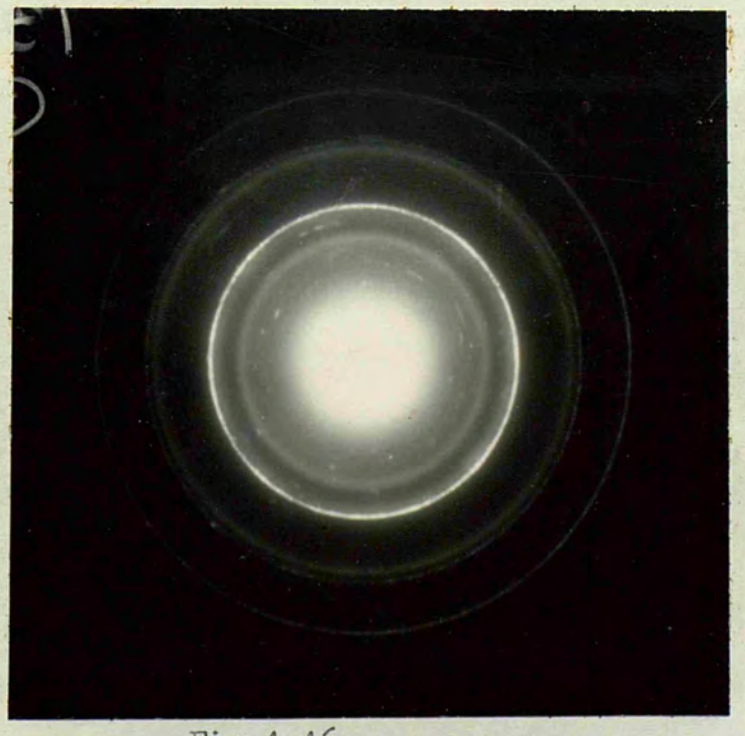

Fig 4.46

Diffraction pattern of 40A° thick iron film deposited at 20°C on vacuum cleaved substrate.

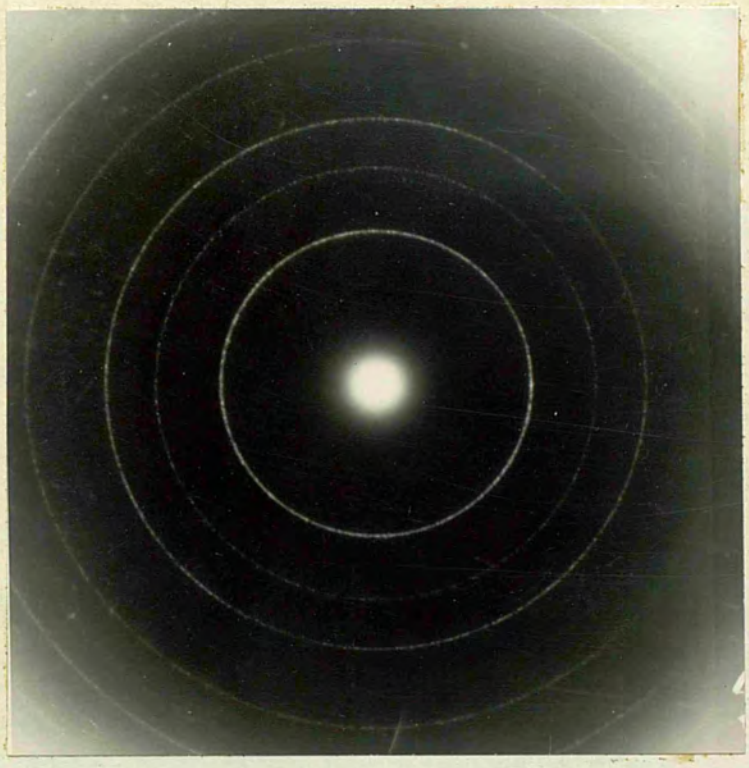

Fig 4.47
Diffraction pattern of 75 Å° thick iron film deposited on air-cleaved substrate at 70°C.

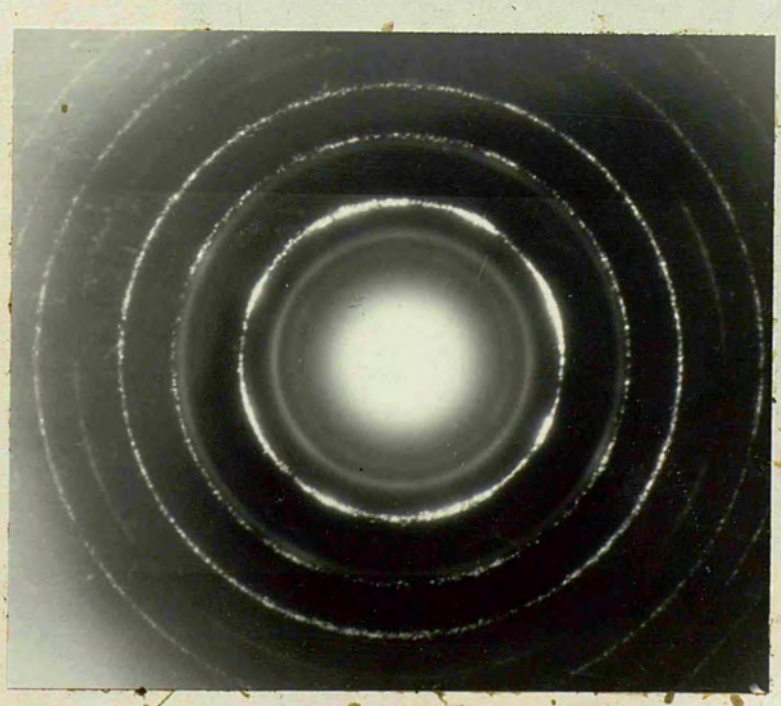

Fig 4.48
Diffraction patternof 75 Å° thick iron film deposited on vacuum cleaved substrate at 70°C.

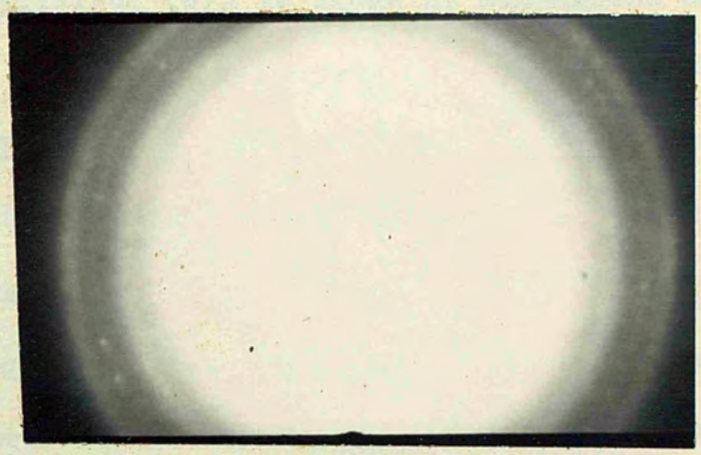

Fig 4.49

Iron film on an air cleaved surface at 120°C.

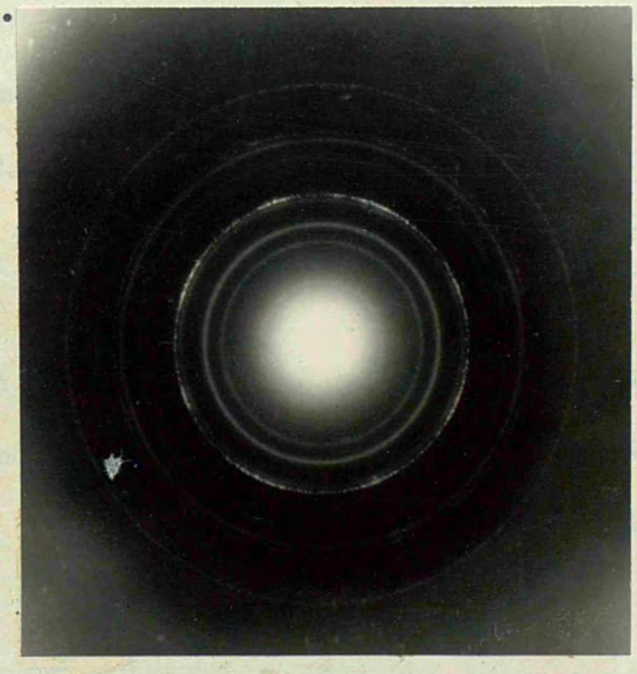

Fig 4.50

Iron film on a vacuum cleaved surface at 120°C.

inhomogeneous structure and orientation. As regards the orientation of the crystallites, this is shown by comparison of Fig 4.49 (air-cleaved) and Fig 4.50 (vacuum cleaved). The thickness of the film is 30 A^{o}. The reason for such a high degree of polycrystalline material is the substantial micro-relief of the surface.

iii) Conclusion.

It is quite a common practice to eliminate partially the absorbed gases from air-cleaved or polished surfaces, by etching at a certain temperature. The above discussion shows that the films so produced show little homogeneity of orientation as well as many deformations. Hence it seems reasonable to cleave the crystal in vacuum and deposit the film at once to eliminate the thermal etching of the substrate and to reduce the irregularity in this way.

4.7. Comparison of the crystallite size on air- and vacuum-cleaved crystals.

Figs. 4.51 and 52 are the micrographs of 100 A^{o} thick films deposited on air- and vacuum cleaved surfaces simultaneously at a 70°C. This shows a marked change in the size of the crystallites on differently cleaved substrates.

On vacuum cleaved substrates, another interesting phenomenon was observed, the existence of the different size of the crystallite in the same film, Fig. 4.53. Considering the crystallites to consist of

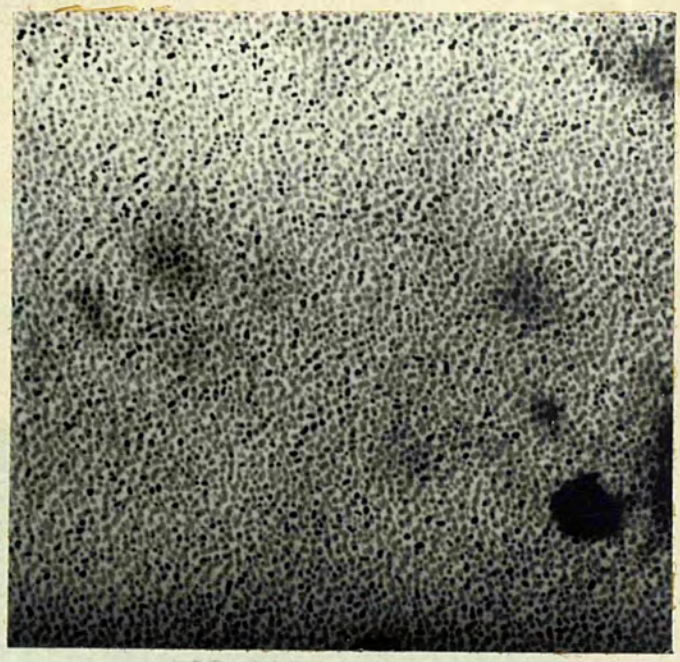

X32,000

Fig 4.51

Electron-micrograph of a film on air-cleaved surface.

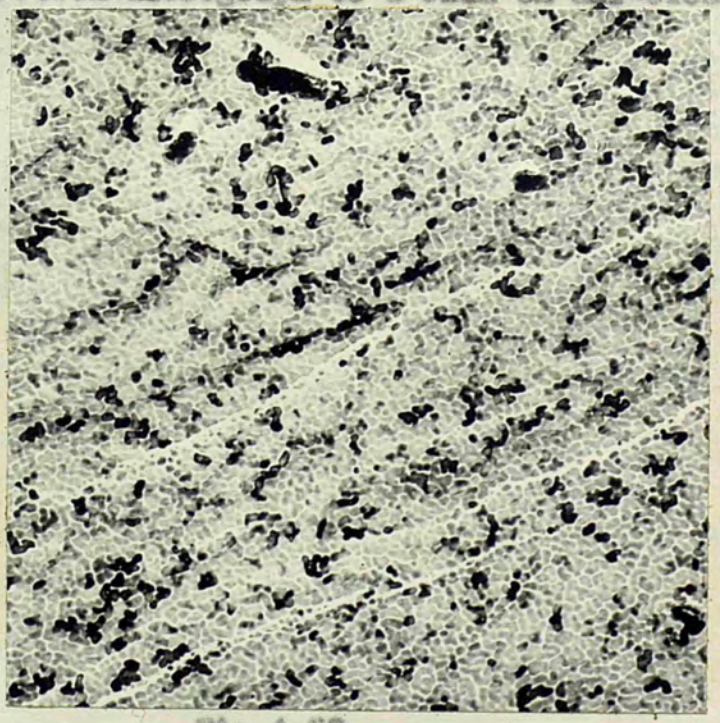

Fig 4.52

Electron-micrograph of a film on vacuum cleaved surface.

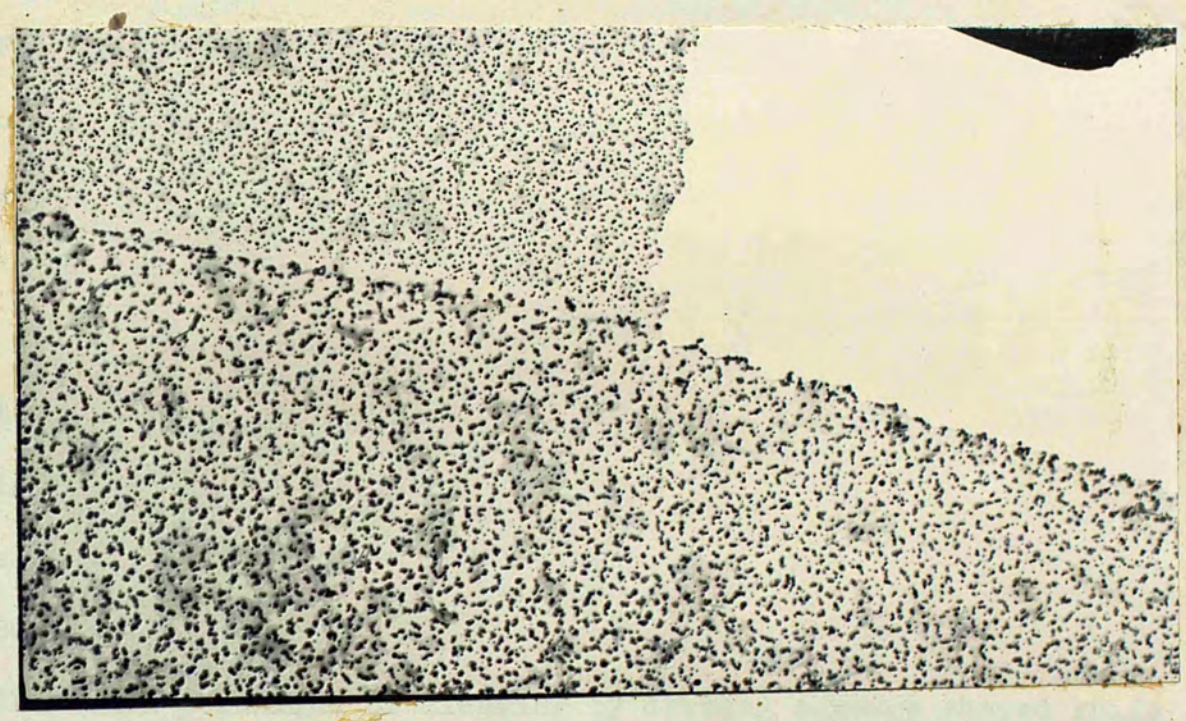

X26,000

Fig 4.53

Different size crystallites on the same film.

circular patches of constant height, the difference in the mass per unit area, on the two sides was found to vary by 50% indicating that there is difference in the coefficient of condensation on the two part. It is possible that these are the two different faces of the substrate where the condensation coefficient may vary.

Fig 4.54 shows an air cleaved surface where the crystallites have condensed along the sides of a shell shaped feature. Figs. 4.55, 56 show the grain boundaries on the substrate. These grain boundaries may be the result of straining the surface while clamping the crystal with a greater force than usual. At some grain boundaries the direction of the iron crystallites is quite different as marked A and B in Fig 4.55 and shown magnified in Fig 4.56. This could have happened in a vacuum cleaved surface, if the crystal is strained.

4.8. Surface of L-shaped crystal.

The usual technique of cleaving by driving a wedge shaped knife parallel to the (100) plane of a halide crystal produces a visibly rough surface. The major imperfections of the face are tear marks, i.e. very large fracture steps, radiating from a point where the blow of the knife falls.

Gobeli[5] etal (1960) succeeded in avoiding such tear marks by using a shadowing technique for silicon and germanium. Using an L-shaped crystal of KI as shown in Fig 4.57, surfaces, A,B and C are clamped firmly and a slight blow with a sharp knife-edge is given.

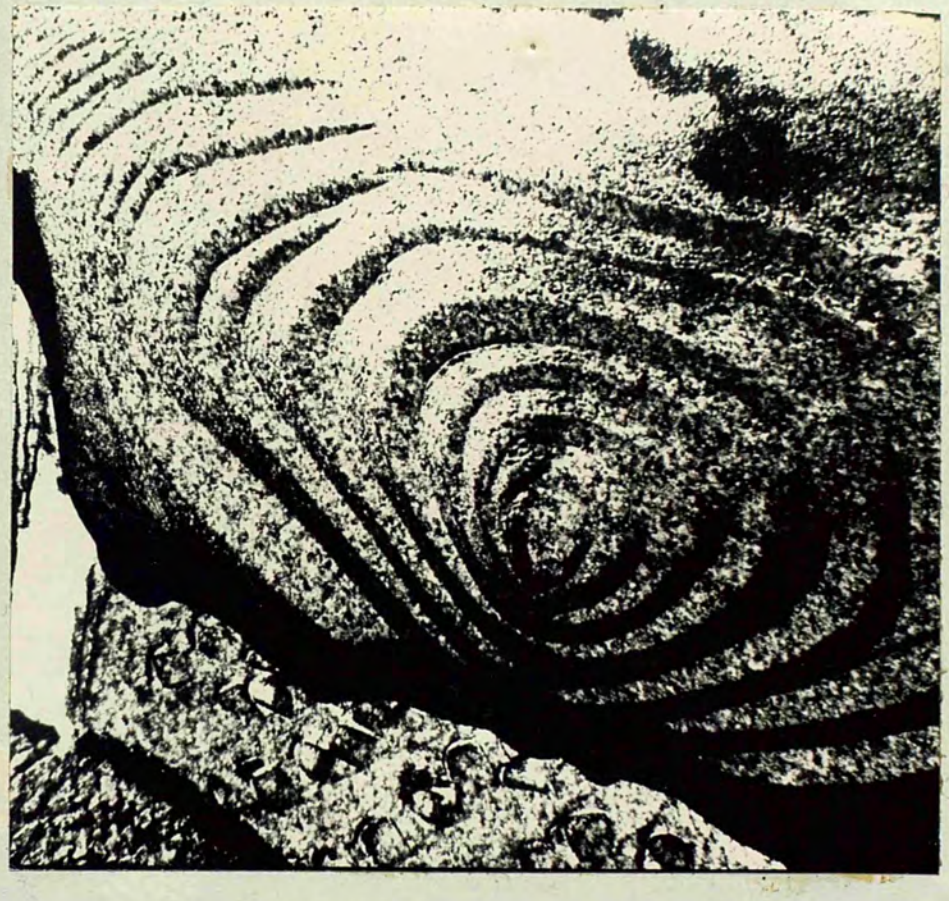

X5,000

Fig 4.54

Shell shaped feature on a strained substrate.

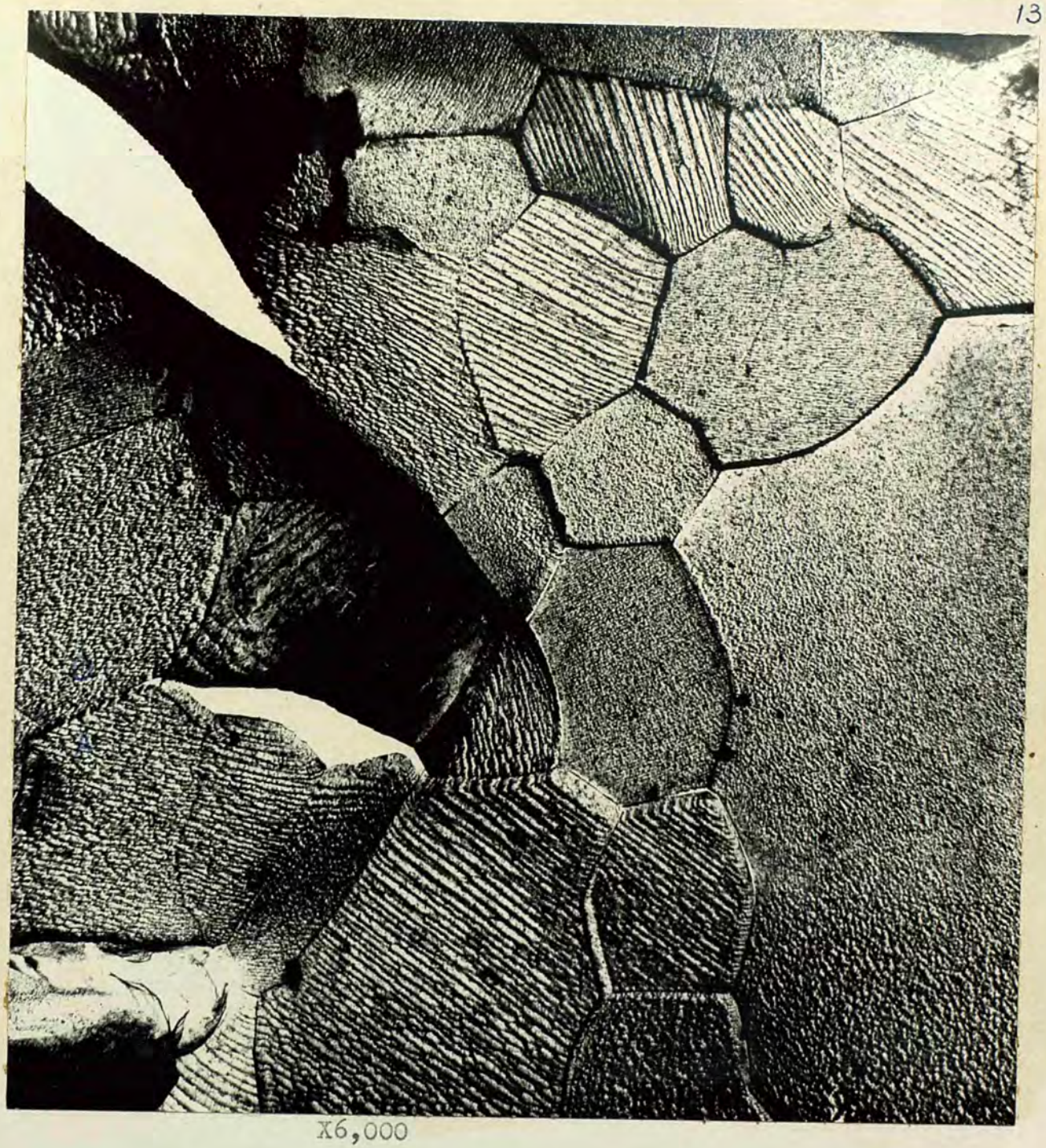

X6,000

Fig 4.55

Grain boundaries on a strained crystal.

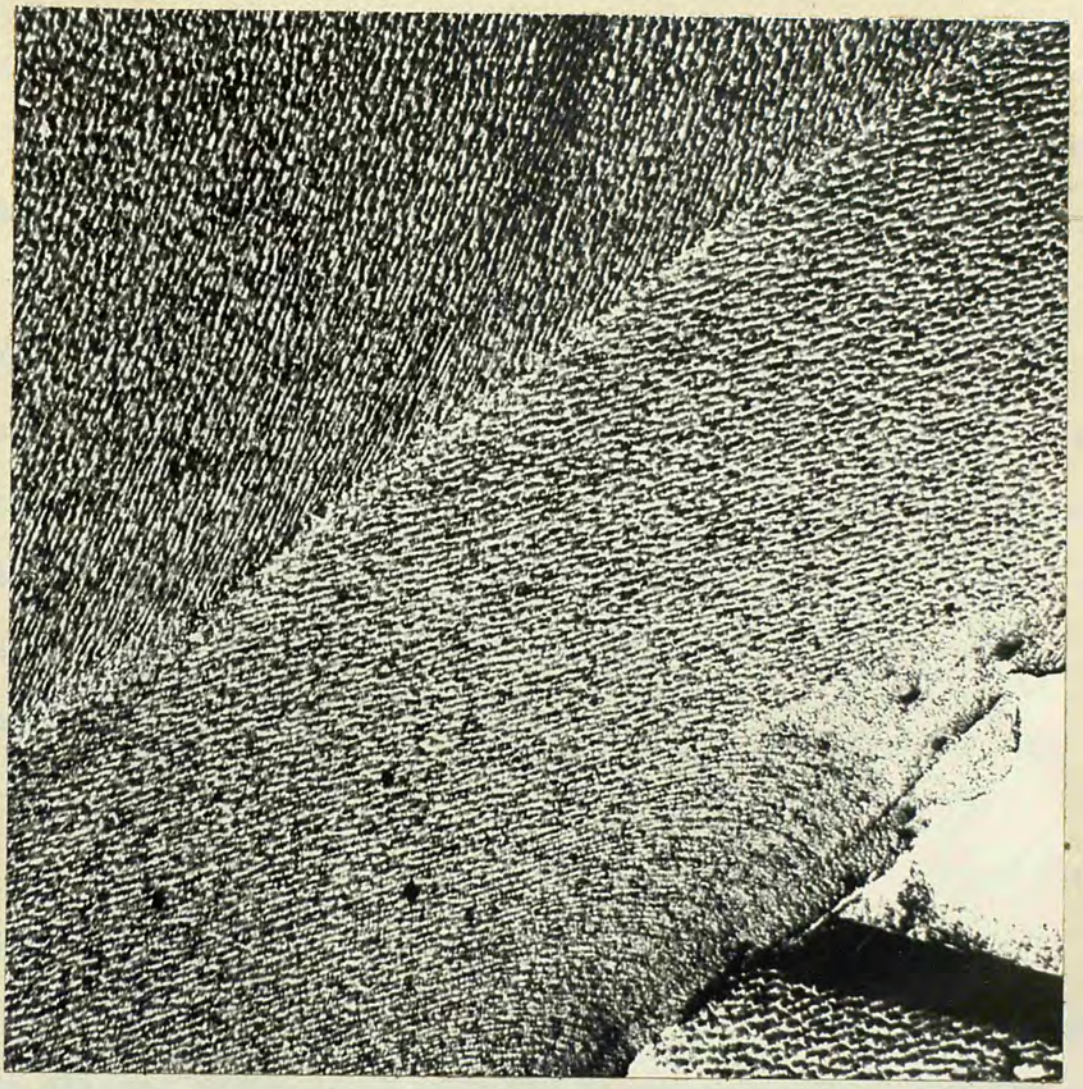

X24,000

Fig 4.56

Magnified view of the grain boundaries and the direction of crystallites.

Fig 4.58 shows the photo-micrograph of the cleaved surface, showing that in this case tear marks are diffracted from the inner corner of L and spread all over the crystal face. The spacing between the tear marks increases with distance from the corner. From Fig 4.58, it is also clear that a large part of the surface is not (100) type, indicating that the crystal itself is not perfect, hence resulting in this kind of tear pattern. An iron film was deposited on the crystal and then a carbon film to study the topography. Over most of the crystal, the surface in between the tear lines is plane and featureless as in Fig 4.59.

4.9. Conclusion.

Single crystal iron films can be produced on NaCl and KCl crystals at 330°C. The films become continuous at 400 A° thickness.

Films can be grown epitaxially easily at lower temperature on vacuum cleaved surfaces as compared to air-cleaved. The crystallite size is greater in vacuum cleaved surfaces as compared to air-cleaved. Decoration features can be studied in a better way by using iron rather than gold.

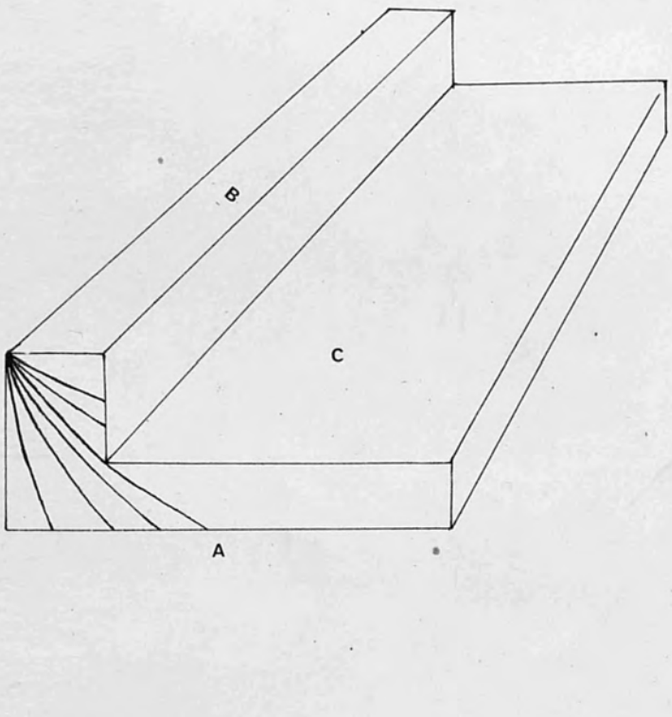

Fig 4.57
L-Shaped crystal.

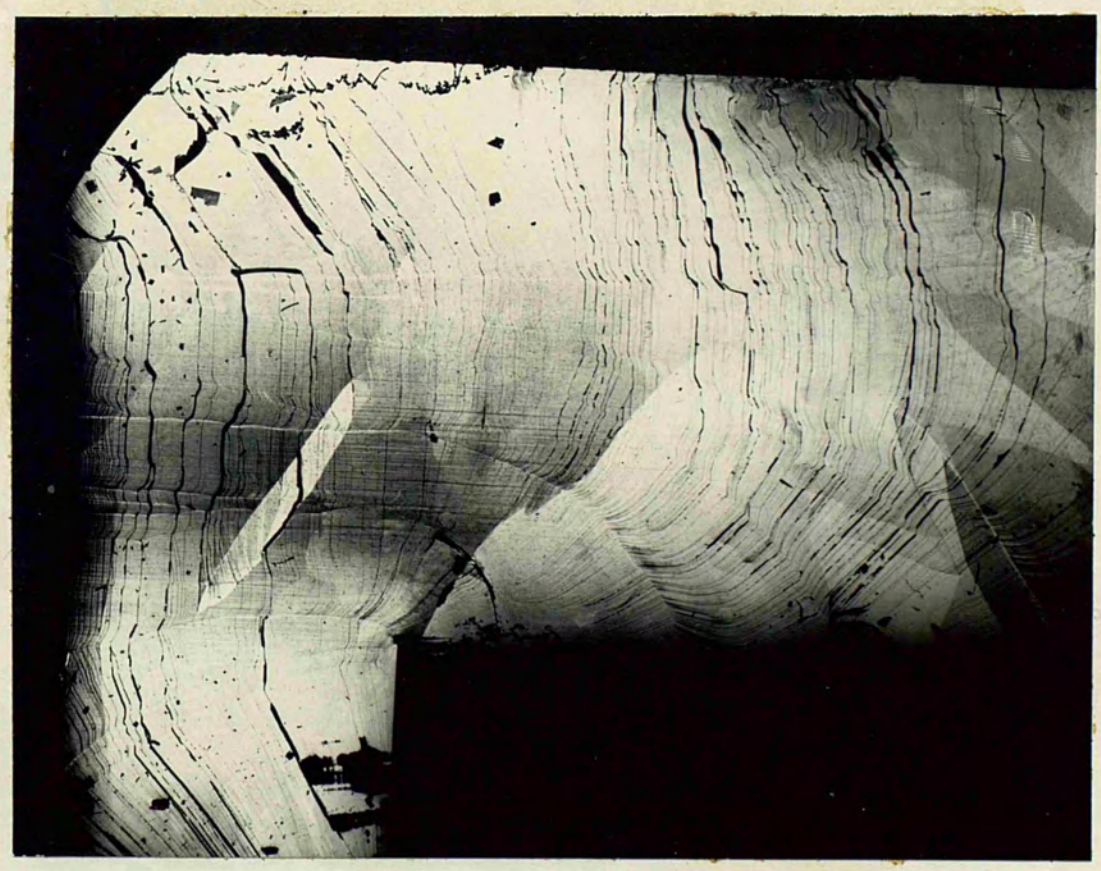

X10

Fig 4.58

Surface of cleaved
L-Shaped crystal.

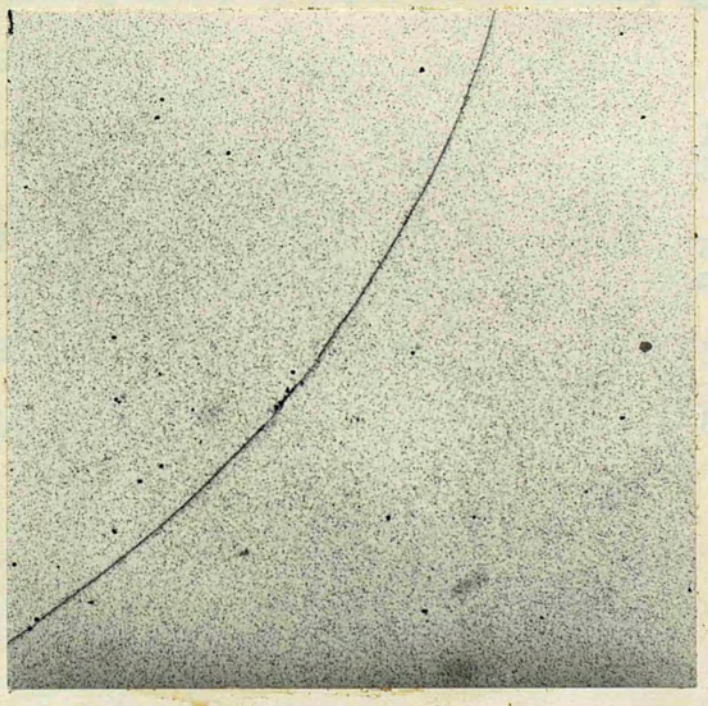

X5,300

Fig 4.59.

Surface between tear marks.

REFERENCES

1. Bassett, 1958, Proc. Fourth Internat. Conference on Electron Microscopy, Berlin, 1,512.

2. Brück, 1936, Ann. Phys., 418, 233.

3. Collins and Heavens, 1957, Proc. Phys. Soc. B, 70,265.

4. Germer, Macrae and Hartman, 1961, J. Appl. Phys., 32, 2432.

5. Gobeli and Allen, 1960, J. Phys. Chem. Solids, 14, 23.

6. Miller, 1962, Ph.D. Thesis. London University.

7. Sella, Conjeaud and Trillat, 1958, Proc. Fourth Internat. Conference on Electron Microscopy, Berlin, 1, 508.

8. Sella and Trillat, 1963, Conference on single crystal films at the Philco Scientific Laboratory, Blue Bell - Pennsylvania.

9. Shirai, 1937, Proc. Phys.-Math. Soc. Japan, 19, 937.

10. Shirai, 1938, Proc. Phys.-Math. Soc. Japan, 20, 855.

CHAPTER 5

Epitaxial Growth of Nickel on Copper.

5.1. Introduction.

Heavens etal 1961 showed that nickel and nickel-iron films can be grown epitaxially on the principal planes of copper. Following their technique, continuous nickel films were grown on (001) and (011) faces of copper.

5.2. Copper films on NaCl.

Copper was evaporated on polished (001) and (011) faces of rock salt, maintained at 330°C in vacuo. The deposition rate was 1000Å/mt. The thickness of copper films were 1500Å°. Fig 5.1 and 5.2 shows the diffraction patterns of (001) and (011) copper films. These grow in parallel orientation with the sodium chloride substrate. Fig. 5.3 and 5.4 show the micrographs of such films. Copper films become continuous at about 1000Å° thickness and thus give nickel a continuous, smooth and fresh substrates for its subsequent deposition.

5.3. Nickel film on Copper.

The mode of growth of nickel films is quite different from that on sodium chloride. The crystallites are irregularly shaped which readily join together, and eventually form a substantially flat continuous layer at about 100 Å° thickness. These films showed considerably less twinning as compared to the nickel films grown on

Fig 5.1.

Diffraction pattern of Copper on polished (001) face of rocksalt.

Fig 5.2.

Diffraction pattern of Copper on polished (011) face of rocksalt.

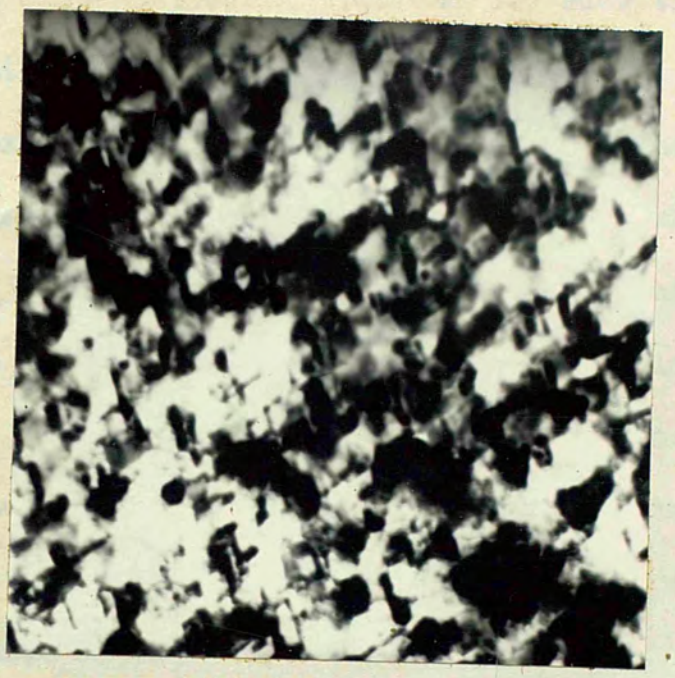

Fig 5.3.

Micrograph of (001) oriented
Copper film.

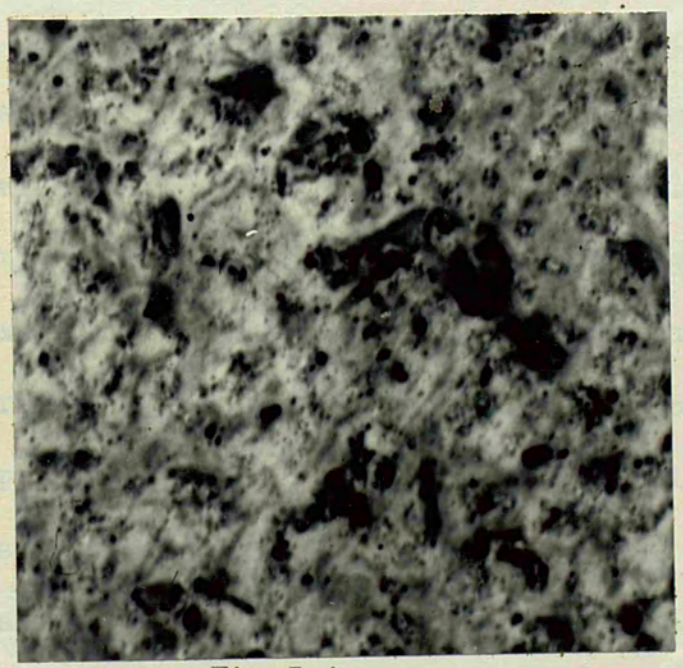

Fig 5.4.

Micrograph of (011) oriented
Copper film.

sodium chloride crystals, Figs. 5.5. and 5.6 show the nickel films on (001) and (011) faces.

Careful examination of the micrographs of continuous films revealed the presence of small, dot-like features which might be dislocations. It is difficult to be certain of this in view of the relatively high resolution limit of the electron-microscope used (about 100 A°). The larger opaque regions often seen on these films are probably due to small deposits of some insoluble material on the film. The most likely substance is insoluble copper chloride.

5.4. Conclusion.

Nickel has been epitaxially grown in parallel orientation on copper, so as to produce thin monocrystalline films in (011) and (001) orientations. These films are continuous for thickness 100 A° and are good approximation to the ideal parallel-sided single crystals, having relatively few structural faults compared with films on rock-salt.

A better method could be desired of removing the nickel from the copper substrate since contact with water must enhance oxidation. A non-aqueous organic solvent would be ideal. Also, the possibility of traces of copper-chloride, or indeed, copper metal, remaining on the nickel surface present presents a serious risk of contamination, should annealing be attempted. However, for the purposes of the present measurements, the films prepared by the above technique provided the best specimens available.

Fig 5.5.

Diffraction pattern of
Nickel film. (001).

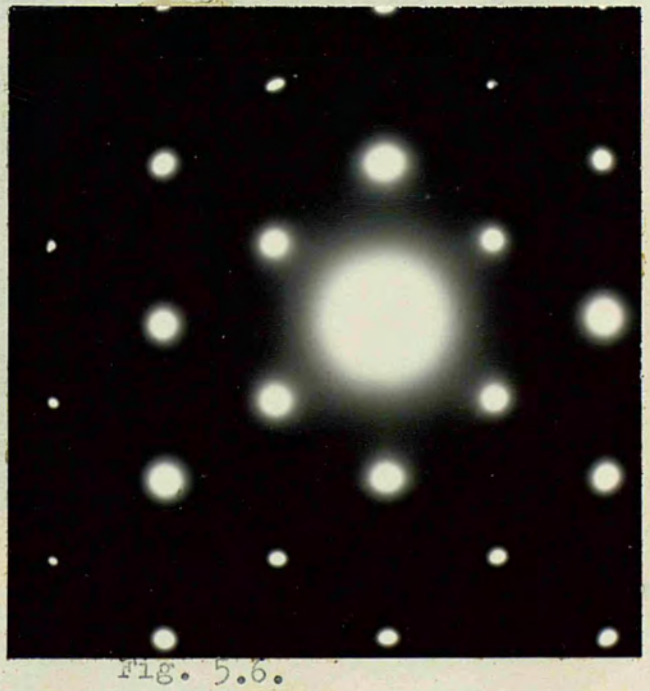

Fig. 5.6.

Diffraction pattern of
Nickel film. (011).

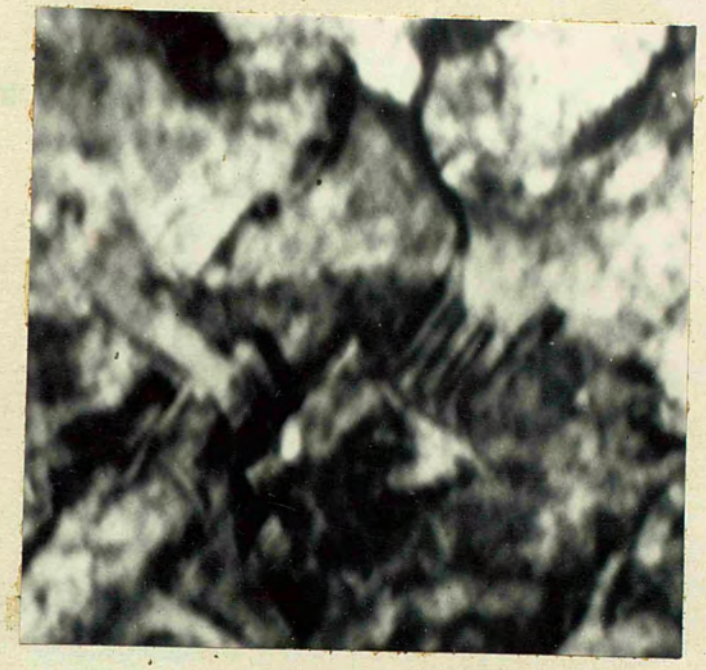

Fig 5.5a

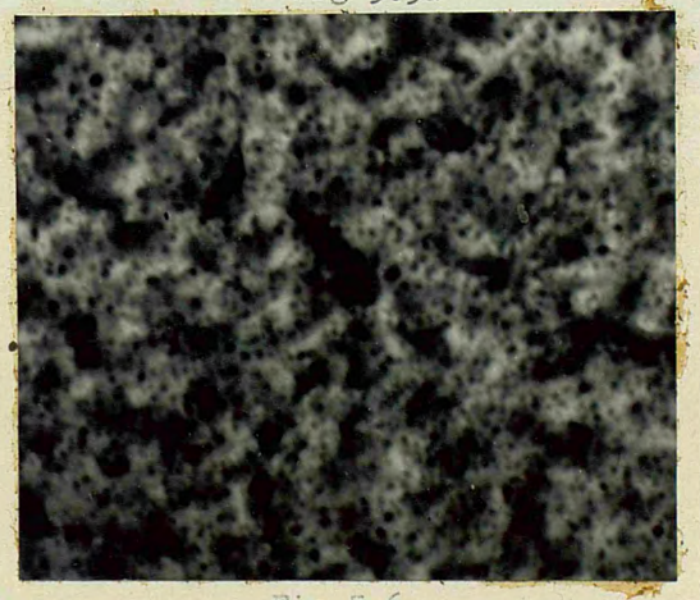

Fig 5.6a.
X 32000
Micrograph of (001) and (011) face of Ni (X20,000).

REFERENCE

Heavens, Miller, Moss and Anderson, 1961, Proc. Phys.Soc., 78,33.

CHAPTER 6

Measurement of Faraday Effect.

6.1. Introduction and State of Problem.

The magnetic rotation of the plane of polarization of light, which Faraday discovered, is a property of all matter. A great deal of work has been done on the measurement of Faraday rotation in solids, liquids and gases, but there have benn very few accurate measurements on ferromagnetic materials at optical frequencies. The variations between different observer's results are considerable because of inaccuracies in the measurement of thickness of the film and difference in their structure. Heavens and Miller[1] (1962), by growing continuous parallel-sided epitaxial nickel films in vacuum and measuring the Faraday rotation in (001), (011) and(111) films, opened a new avenue for research. This gives a method for measurement of Faraday rotation in specific directions in the crystal. Their work is extended to measure anistropy in the Faraday rotation with respect to the direction of electric vector of plane polarized light and that of the crystal lattice. A brief review of the theoretical work on Faraday Rotation is given by Miller[3] (1962).

6.2. The Principle of Polarimeter.

The technical details of polarimeter used to measure the Faraday rotation in nickel films are described by Miller (1962).

The accuracy of measurement of this instrument is ± 3%. This is obtained by employing the principle of Ingersoll[2]'s a.c. photo-electric polarimeter (1953). If the light transmitted by a polariser is polarised in a plane which is at 45° to each of the principal planes of a double image prism, then the two beams produced by the prism are of equal intensity. If the plane of polarisation incident on the double image prism is rotated, e.g. by a specimen placed after the polariser, this results in an increase in intensity of one beam and reduction of the other. If X is the angle (normally 45°) between the incident plane of polarisation and the principal planes of the double image prism, we have, for the intensity of either beam.

$$I = \text{const.}\ I_o \cos^2 X$$

where I_o is the intensity of the incident beam

$$\frac{dI}{I} = -2 \tan x\, dx.$$

where $x = 45°$

$$\frac{dI}{I} = -2\, dx$$

since dI is positive for one beam and negative for the other, so the relative change

$$\delta I = 2\, dI$$

$$\text{or } dx = \frac{\frac{1}{4}\delta I}{I} \text{ radians}$$

$$= \frac{45}{\pi} \frac{\delta I}{I} \text{ degrees}$$

For a rotation of 1', it is necessary to be able to detect a relative change in the two beams of 1 in 859.

The most sensitive means of detecting small changes in the intensity of light is photomultiplier tube, but with it is associated noise due to shot effect. This is avoided by using the coherent rectifier system. In this method, the signal is amplified, and then rectified synchronously. The signal appears as unidirectional after rectification but noise components whose frequencies differ from that of the commutators appear as alternating. The output from the rectifier is smoothed by a filter circuit with an appropriately long time constant, and measured by a d.c. instrument. The optical rotation produced by the specimen is measured directly by measuring the rotation of polariser which is necessary to restore balance.

6.3. The method of Measurement.

The polarimeter is aligned with all its components perpendicular to the axis of the optical bench. The mercury lamp, the rotor and all the electrical supplies are switched on. The specimen is demagnetised by an alternating current and then a predetermined current is passed through the magnetic coil to give a required magnetic field. The polariser is rotated until a balance is reached and this rotation is observed by an optical lever. After this, the specimen is demagnetised and again the rotation is observed for a reversed magnetic field. The difference in the position of the optical lever gives the double rotation produced by the specimen for the reversal of the known magnetic field. This method is repeated for a range of magnetic field from 0 to 8K0e, the readings are tabulated as in the table 6.1.

TABLE 6.1.

Rotation result for a Ni-film epitaxially grown on a (001) face of Cu.

Coil Current I	Applied magnetic field H KOes.	Scale reading of optical lever in m.m. a H	b -H	minutes double rotation $\frac{b-a}{3}$
0.25	0.72	225.0	238.0	4.3
0.50	1.64	232.0	260.0	9.3
0.75	2.48	239.0	281.0	14.0
1.00	3.32	244.0	295.0	17.0
1.25	4.04	248.5	308.5	20.0
1.50	4.84	251.5	318.0	22.2
1.75	5.24	253.0	322.5	23.2
2.00	6.04	256.0	331.5	25.2
2.50	6.72	257.0	335.0	26.0
3.00	7.24	258.5	338.0	26.5
4.00	7.96	257.5	339.0	27.2
5.00	8.40	257.0	339.5	27.5
6.00	8.76	256	340.0	28.0

Since we are interested in the variation of the rotation for different orientations of the electric vector relative to the crystal arcs, the quartz cover slips, on which the films are supported, are examined in crossed nicols to see whether there is any birefrengence in them to eliminate the possible strained substrates.

While depositing the film, the line giving a direction on the mask, should be parallel to <100> direction in (001) and (011) films. This film is mounted on a quartz slip so that this mark is parallel to any side of the slip. After seeing this film on a bench microscopy of magnification X50, the area is selected where there are no holes.

A series of circular apertures of various sizes from 1 m.m. to 3 m.m. diameter were punched in pieces of black adhesive P.V.C. tape 2.5 c.m. square. The area where there are less than three or four holes, of about 10 μ size is selected otherwise it is rejected. This is due to the fact that local distortions in the magnetic field might be quite significant and might be difficult to estimate. The masked specimen is placed between the electromagnet, so that <100> is vertical. The polariser is so arranged that the electric vector of the plane polarized light is at 45° to the vertical under ordinary circumstances. In the case of (001) film, the observations so obtained are for the case when the electric vector is parallel to <110> direction.

After taking the observations with the electric vector parallel to $\langle 110 \rangle$ direction, the polariser is rotated through 90°. This brings the electric vector parallel to $\langle \bar{1}10 \rangle$ direction, fig 6.1. Now to bring electric vector parallel to $\langle 010 \rangle$ direction, the polariser is rotated through 45° in the opposite direction and a 45° wedge is inserted beneath the Wollaston prism to keep its principal planes at 45° to the plane of polarisation. Now if the polariser is rotated by 90° in the same direction, then the electric vector will be parallel to $\langle 100 \rangle$ direction. In this way measurements are made on (001) films to find out whether there is any variation in rotation due to the variation of the direction of the electric vector. The results are shown in the Fig. 6.3, indicating that at least with this accuracy of the instrument there is no variation in the Faraday Rotation due to different direction of $\underline{E}$.

Consider the film (011) and its principal directions shown in the Fig 6.2. Under the normal condition of the polariser the electric vector of the polarised light makes an angle of 45° with $\langle 001 \rangle$. By rotating the polariser by 45° and putting the 45° wedge below the wollaston, the electric vector is parallel to $\langle 110 \rangle$ of the film and the plane of polarisation make an angle of 45° with the principal planes of the prism. If now the polariser is rotated by 90° in the opposite direction, the electric vector is parallel to $\langle 001 \rangle$. Then the polariser is brought to the normal position and the 45° wedge is removed from under the Wollaston prism. The polariser is then rotated by $9^{\circ}44'$

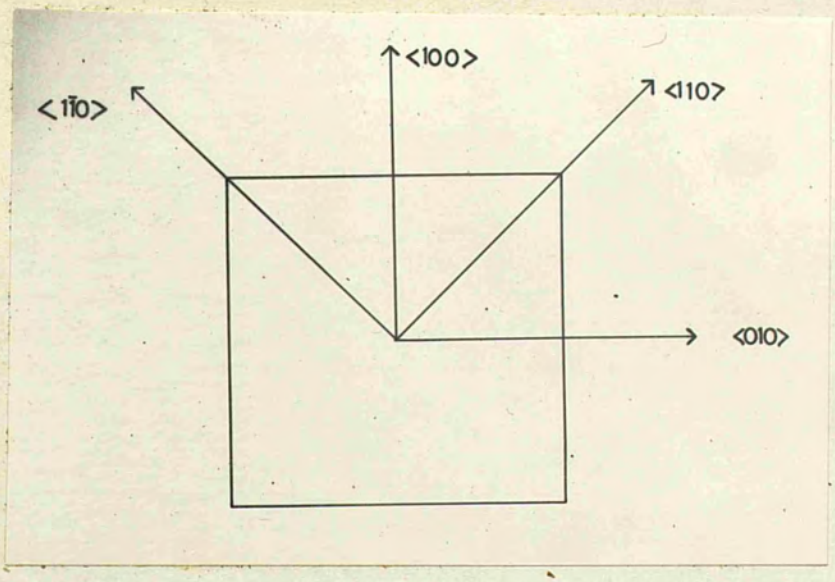

Fig 6.1.

Principal directions of
(001) plane.

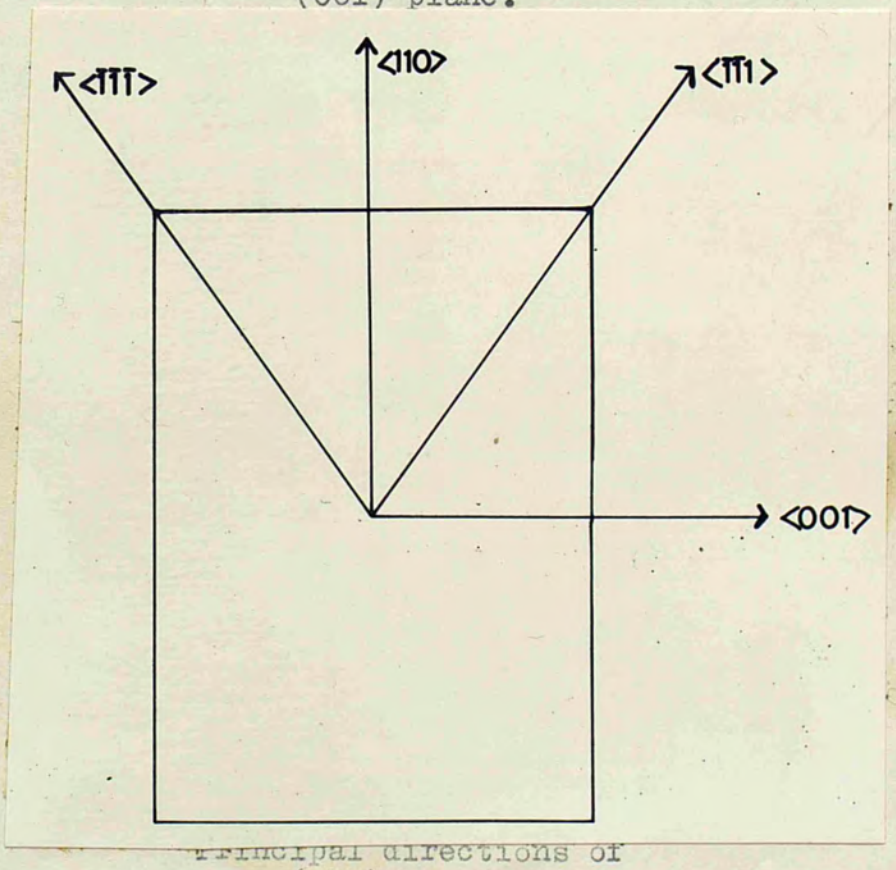

Principal directions of
(011) plane.

Fig 6.3

Faraday Rotation Measurements
on (001) nickel films.

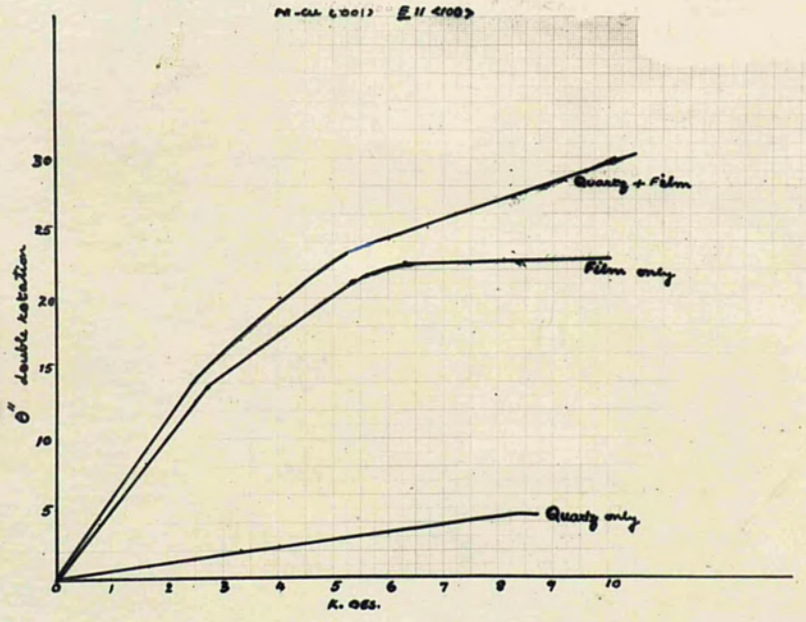
Ni-Cu (001) E ∥ <100>
θ" double rotation
30
25
20
15
10
5
0
1
2
3
4
5
6
7
8
9
10
K. OES.
Quartz + Film
Film only
Quartz only

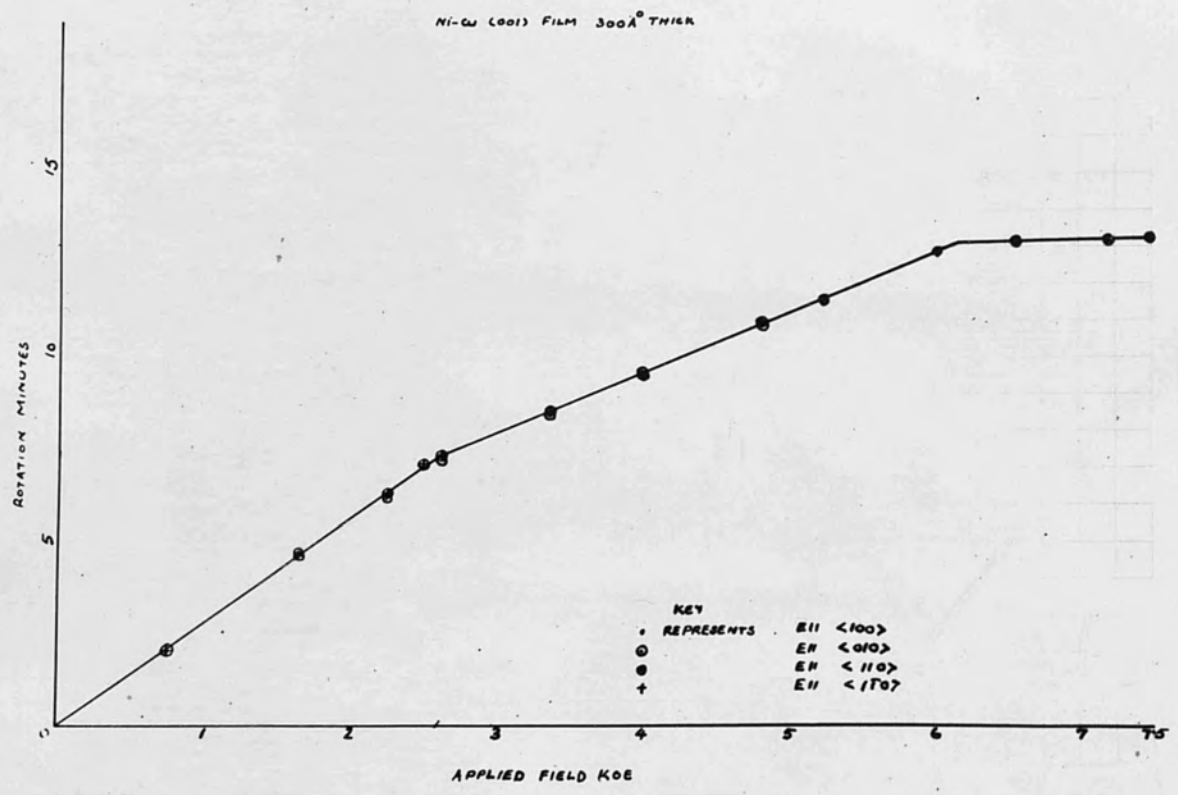
Ni-Cu (001) FILM 300Å° THICK
ROTATION MINUTES
5
10
15
0
1
2
3
4
5
6
7
7.5
APPLIED FIELD KOE
KEY
• REPRESENTS
E11 <100>
E⊥ <010>
E⊥ <110>
E11 <1T0>

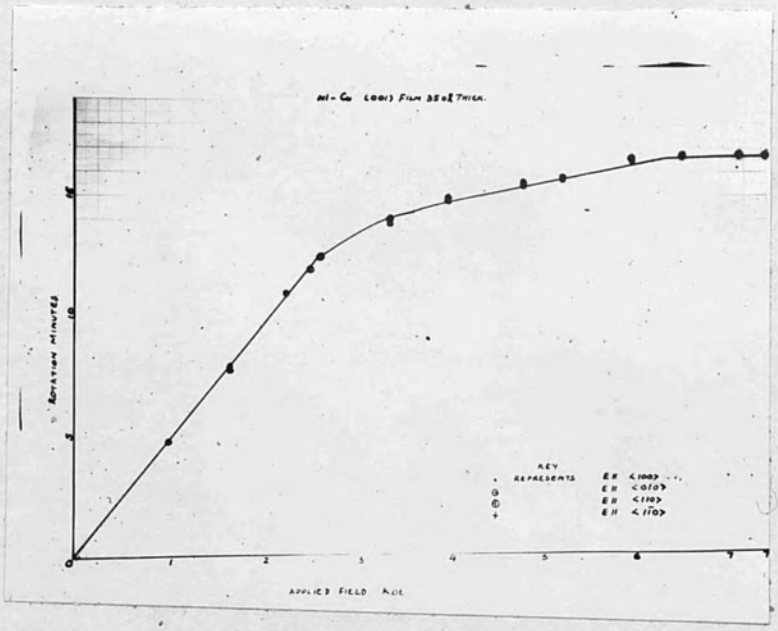
Ni-Cu (001) Film 350Å Thick.
ROTATION MINUTES
APPLIED FIELD KOE
KEY
REPRESENTS E ∥ <100>
E ∥ <010>
E ∥ <110>
E ∥ <1̄10>

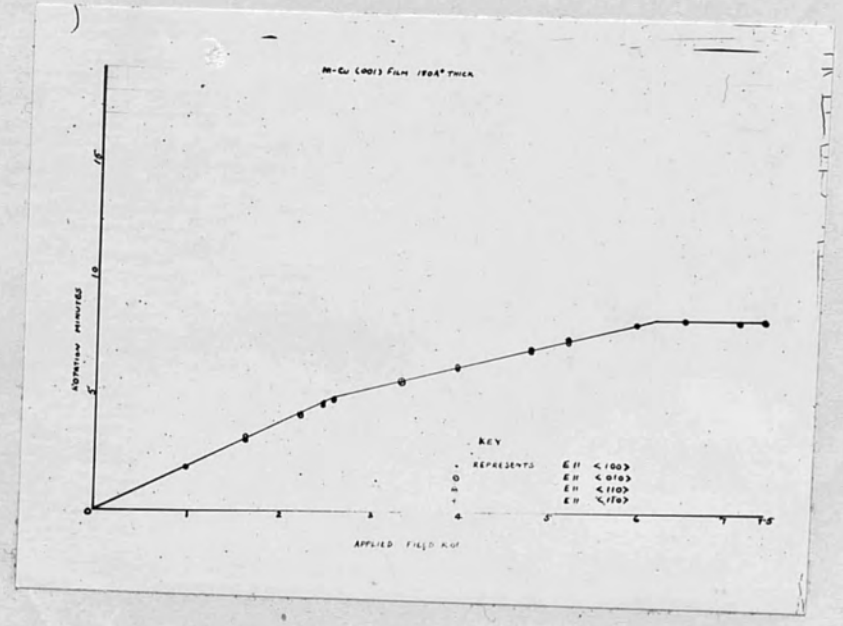
Ni-Cu (001) Film 180Å Thick
ROTATION MINUTES
APPLIED FIELD KOE
KEY
REPRESENTS E ∥ <100>
E ∥ <010>
E ∥ <110>
E ∥ <1̄10>

Fig 6.4.

Faraday Rotation Measurements
on (011) nickel films.

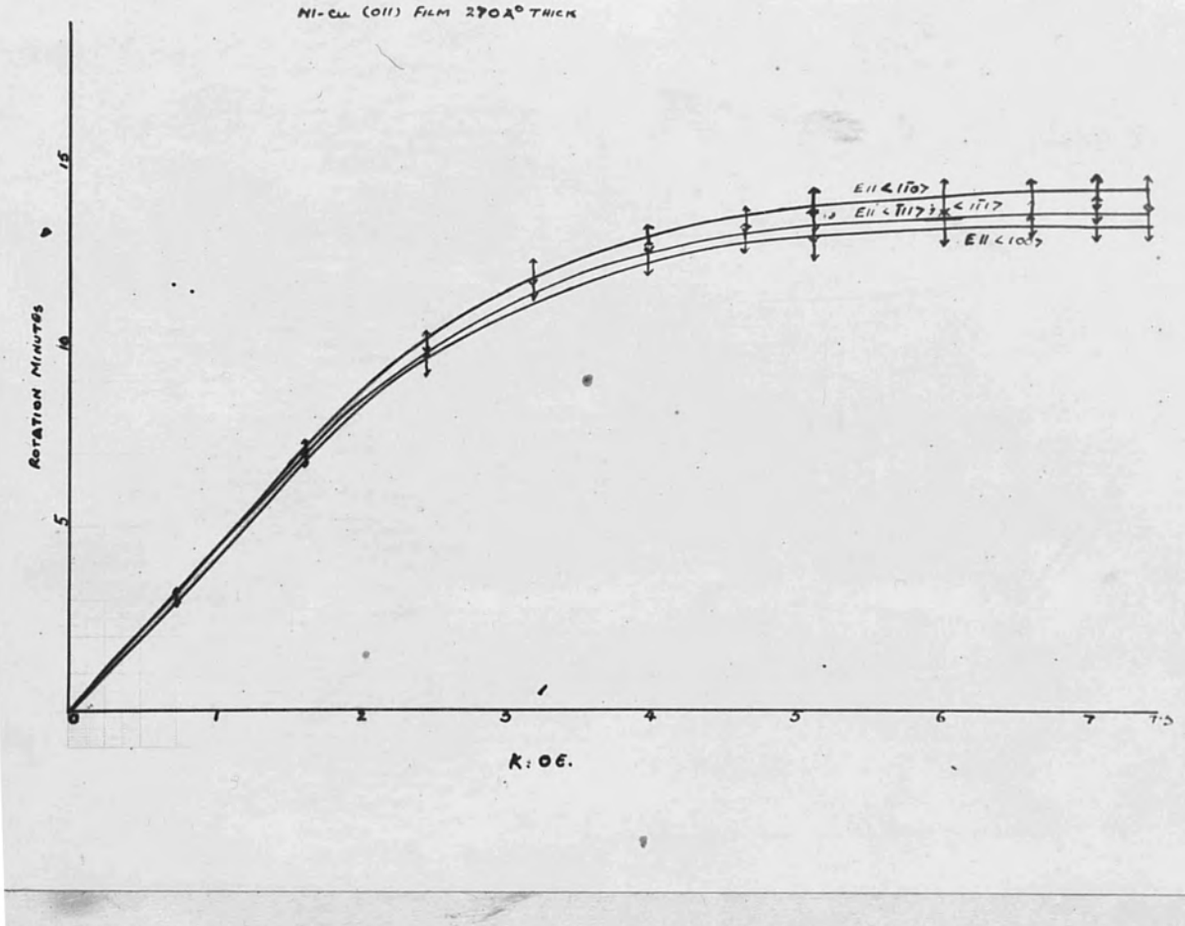
Ni-Cu (011) Film 270A° thick
Rotation Minutes
E ⊥ <1$\bar{1}$0>
E ⊥ <$\bar{1}$11> & <11$\bar{1}$>
E ⊥ <100>
0
1
2
3
4
5
6
7
7.5
5
10
15

K:06.

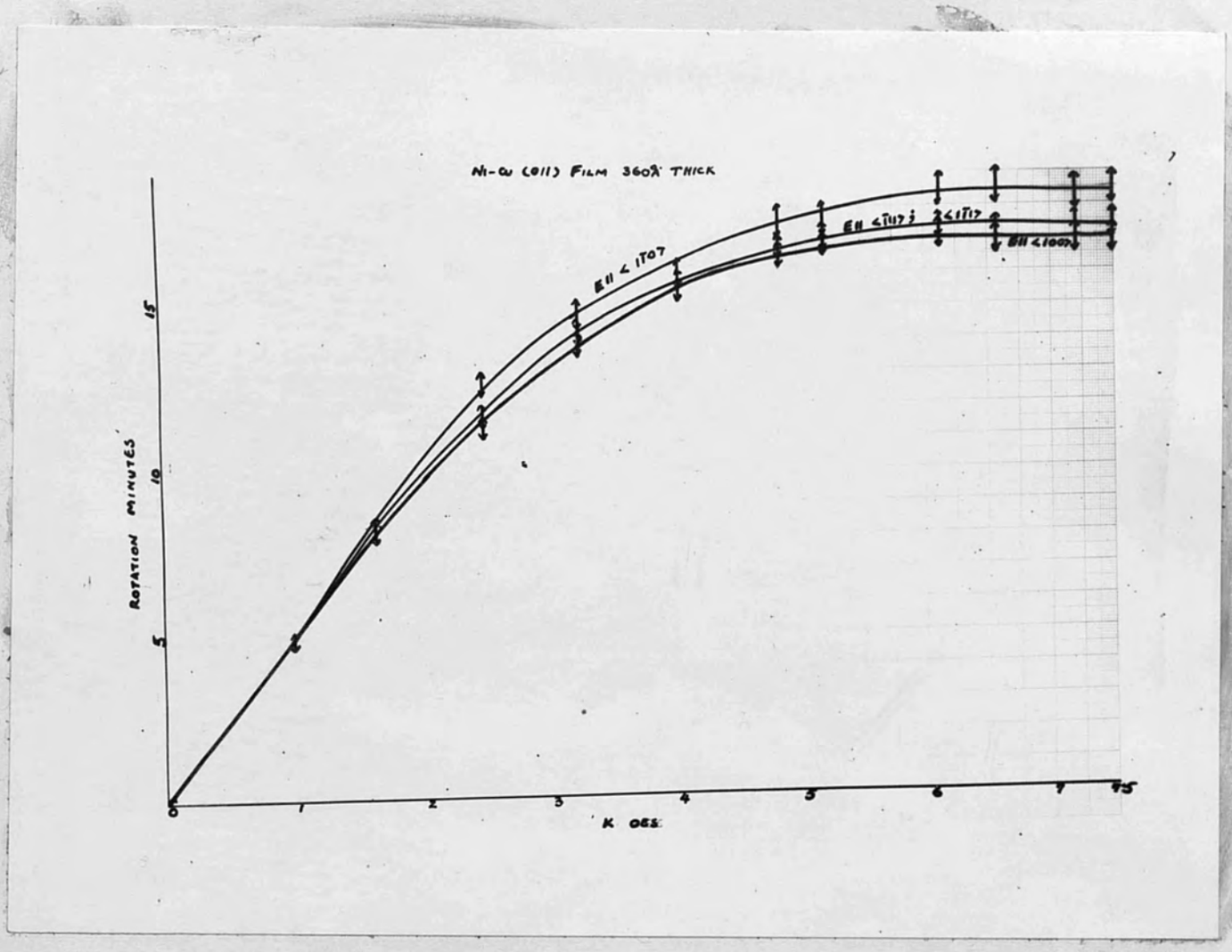
Ni-Cu (011) Film 360Å Thick
E ∥ ⟨111⟩
E ∥ ⟨110⟩
E ∥ ⟨100⟩
Rotation Minutes
15
10
5
0
1
2
3
4
5
6
7
8
K oes.

towards the $\langle 110 \rangle$ direction, so that the electric vector lies parallel to $\langle 111 \rangle$ of the film. Below the Wollaston prism a 35° 46' wedge is introduced to keep the principal planes of the prism at 45° with the plane of polarisation. Now if the polariser is rotated by 90° towards the $\langle \bar{1}\bar{1}0 \rangle$, the electric vector will be parallel to $\langle \bar{1}\bar{1}1 \rangle$. Fig 6.4 shows the result of this measurement on 270 Å and 360 A° thick films. This definitely shows that there is a variation of rotation due to the variation of the electric vector with respect to the different crystallographic direction in the (110) Ni film. The rotation is maximum when $\underline{E}$ is parallel to $\langle 1\bar{1}0 \rangle$ direction and minimum when E is parallel to $\langle 100 \rangle$. The change in rotation is about 6%.

REFERENCES

1. Heavens and Miller, 1962, Proc. Roy.Soc., A 2 66, 547.

2. Ingersoll, 1953, J. Sci. Instr., 24, 23.

3. Miller, 1962, Ph.D. Thesis, London University.

Chapter 7.

Future Work.

The experiments, which have been described here, have been done at a pressure of 10^{-5} m.m. Hg. Since specimen structure is sensitive to purity of specimen, the thermal evaporation should have been carried out in a vacuum of the order of 10^{-10} m.m. Hg. The vacuum system described in Chapter 3 could be improved by the addition of a liquid nitrogen trap, to reduce the back-streaming of pump fluid molecules.

The method of electron bombardment evaporation is regarded as satisfactory, as a means of producing a pure vapour stream, but the use of vacuum pumps which do not employ oil or mercury would reduce any risk of contamination due to cracked or oxidised material formed by the action of the incandescent filament.

The cleanliness of the surface of the substrate is quite important in the epitaxial growth of the film. Hence, vacuum cleaving of the halide crystals should be performed under ultra-high vacuum conditions. This can be achieved either by using an electromagnet hammer or by thrusting a fine knife edge in the crystal with the help of metallic bellows sealed to the system. In any case care should be taken, first to select vacuum-grown halide crystals and secondly since even these crystals release some gas on cleavage, to delay deposition of the film until a low ambient pressure is reached. This is, to ensure the pumping out of all gas, mainly water and carbon

monoxide bursts released from the cleaved surface (Vanderslice and Whetten[1] 1962).

A comparison of the condensation coefficient on air- and vacuum cleaved surfaces should be made at different temperatures. This will help in understanding how the growth of the film is affected by the cleanliness of the surface.

If alkali-halides are cleaved rapidly and with a single blow, there is no likelihood of introducing dislocations. (Vanderslice and Whetten L.C.) Hence, if the halide is subsequently strained, dislocations will be introduced, and a comparison can then be made of the dislocation densities on the surface of the halide and that introduced in the film as well as the mode of growth of the film on the strained surface.

An electron microscope capable of about 10A^{o} resolution is an essential piece of apparatus for learning more about the structure of the film deposited and the surface of the substrate. Only then will it be possible to learn something of the nature of the small scale imperfections in relation to the surface features.

In the work described here, the thickness measurements were carried out by multiple-beam interferometry. This method renders the film unsuitable for subsequent use. Instead, the X-ray method described by Neugebauer[2] (1959) which does not affect the film, is accurate and speedy, may possess advantages.

REFERENCES

1. Vanderslice and Whetten, 1962, J. Chem. Phys., 37, 535.

2. Neugebaur, 1959, Structure and Properties of Thin Films (Wiley),358.